

**Eco-Informatics Summer Institute 2007
H.J. Andrews Experimental Forest**

Methods in Environmental Monitoring

**Information Packet to Accompany Lecture Topic:
“Debris Flow Disturbance in Stream Networks”**

Compiled By

**¹Steve Taylor, Ph.D.
Earth and Physical Science Department
Western Oregon University
Monmouth, OR 97361
taylors@wou.edu**

July 3, 2007

(¹On research leave at H.J. Andrews Experimental Forest, in collaboration with Frederick J. Swanson, Research Geologist, Pacific Northwest Research Station, U.S. Forest Service, Corvallis, Oregon 97331; fred.swanson@orst.edu)

Table of Contents

Topic	Page(s)
Mass Wasting Basics	1
Process Defined	2-3
Varnes Classification	4-5
Slope Hazards	6-7
Fundamentals of Landscape Analysis	8
Taylor Surficial Mapping Protocol	9-13
Physical Geomorphology of Debris Flows	14
Key Terms	15
Costa, 1984 Review Notes on Debris Flow	16-22
Physical Properties of Debris Flow	23-24
Topographic Occurrence of Debris Flow	25-27
Super Elevation and Runout Rheology	28-29
Geomorphic Evidence for Debris Flow	30
Recurrence Intervals	31
Material Transfer Processes in Forested Watersheds	32
Transport Processes and Routing Mechanisms	33-34
Debris Flow Transport and Channel Networks	35-39
1996-1997 Oregon Storm Event (Robison et al., 1999)	40
Map of 1996-97 Landslide Occurrence	41
Precipitation	42
Historic Landslide Inventories – Western Oregon	42A-42B
1996-97 Landslide Inventory	42C-42E
96-97 Landslide Occurrence vs. Stand Age Class	43
Rainfall-Debris Flow Threshold Map – Western Oregon	44
Landslide and Debris Flow Occurrence at HJ Andrews	45
Geologic Map of Western Cascades (Swanson and Swanston, 1977)	46
HJA Landslide Data	47-48
Map of 1996 Debris Flow Paths, Blue River Basin	49
Effects of 1996 Debris Flow on Channel Systems	50
HJA Debris Flow Inventory (Snyder, 2000 Thesis)	51-56
Watershed 10 Transport Processes	57
Debris Flow and Stream-Channel Impacts: Oregon Coast Range	58
May and Gresswell (2003) Post-Debris Flow Wood and Sediment Study	59-63
Forest Road Processes at HJ Andrews	64
Conceptual Models of Roads on Landscape	65-68
Hydrogeomorphic Impacts of Road Construction at HJ Andrews	69-74
Geologic Time Scales	75-76
References Cited – This Document	77-78
Review of Debris Flow Literature	79-85

Mass Wasting Basics

MASS WASTING BASICS

2. Mass Movement Types

a. **FALL** - free vertical drop of material

(1) Subclass

- (a) rock fall
- (b) debris fall
- (c) earth fall

(2) Other Terms

- (a) Talus = cone-like accumulations of rock debris at the base of bedrock cliffs, generally a temporary accumulation of rock fall debris.
 - i) landform, or alternately block apron
- (b) Scree = deposit (= sediment) alternately block mantle

b. **Topple** - block rotation / tipping

(1) Subclass

- (a) rock topple
- (b) debris topple
- (c) earth topple

c. **SLIDE**: mass sliding along well-defined failure surface

(1) Subtypes

(a) Translational / Planar Slide

- i) rock slide
- ii) rock-block slide
- iii) debris slide
- iv) earth slide

(b) Rotational Slide (Slump)

i) Characteristics

- a) slope collapse along a basal,
- b) concave upward rupture surface, with subsequent downslope movement and backward rotation of the slump block.
- c) The nose of the slump commonly experiences flow conditions resulting in a lobate form to the debris.

ii) Subtypes

- a) rock slump
- b) debris slump
- c) earth slump

(2) Landform Products:

- (a) Landslide scar on upslope portion where slide originated
- (b) Lobate/hummocky pile of debris at downslope resting point.
- (c) A possible damming of lower valley drainage and subsequent

lake development.

d. **Lateral Spread:**

- (1) rock spread
- (2) debris spread
- (3) earth spread

e. **FLOW:** - intermixing of material within mass (confined to channel or hollow)

(1) Subtypes

- (a) rock flow
- (b) debris flow
- (c) earth flow

(2) Special Considerations

- (a) **CREEP:** very slow, imperceptible, movement of slope materials. Gradual downslope creeping of soil and regolith (partially weathered rock). Involves the entire area of the hillslope under the force of gravity.

i) creep is enhanced by water saturated conditions, and freeze/thaw process with the upheaving and compressing of materials on a slope, slowly pushing material down slope.

ii) Factors influencing creep process:

- a) > slope > creep rate;
- b) > vegetative cover/rooting < creep rate;
- c) > moisture content > creep rate.

(b) **SOLIFLUCTION** - special case of creep in cold climate areas. Involves the downslope movement (at slow rates) of partially thawed/water saturated soil and regolith over an impermeable "permafrost" layer.

i) permafrost- permanently frozen subsoil in cold climate areas. Forms an impermeable layer relative to the overlying "active layer" of soil which experiences thawing during the warm weather/summer season. soil flow

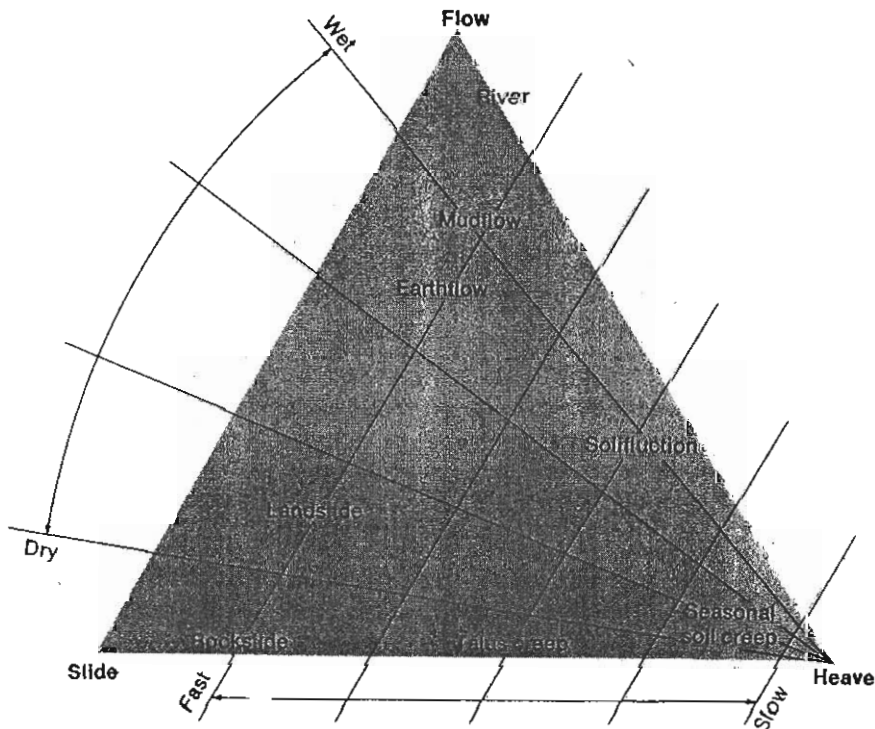
(c) **AVALANCHE:** trapped basal cushion of air and/or water

- i) snow avalanche
- ii) debris avalanche:
 - a) rapidly "sliding" debris - (typically originates from a debris slide)

TABLE 4.6 Classification of mass movement types in different parent materials.

Type of Movement		Type of Material			
		Bedrock	Engineering Soils		
			Predominantly coarse	Predominantly fine	
Falls		Rockfall	Debris fall	Earth fall	
Topples		Rock topple	Debris topple	Earth topple	
Slides	Rotational	Few units	Rock slump	Debris slump	Earth slump
	Translational		Rock block slide	Debris block slide	Earth block slide
		Many units	Rockslide	Debris slide	Earth slide
Lateral Spreads		Rock spread	Debris spread	Earth spread	
Flows		Rock flow (deep creep)	Debris flow	Earthflow (soil creep)	
Complex		Combination of two or more principal types of movement			

From D. J. Varnes, 1978, "Landslides: Analysis and Control," *TRB Special Reports 176: Landslides*, Transportation Research Board, National Research Council, Washington, D.C. Used by permission.



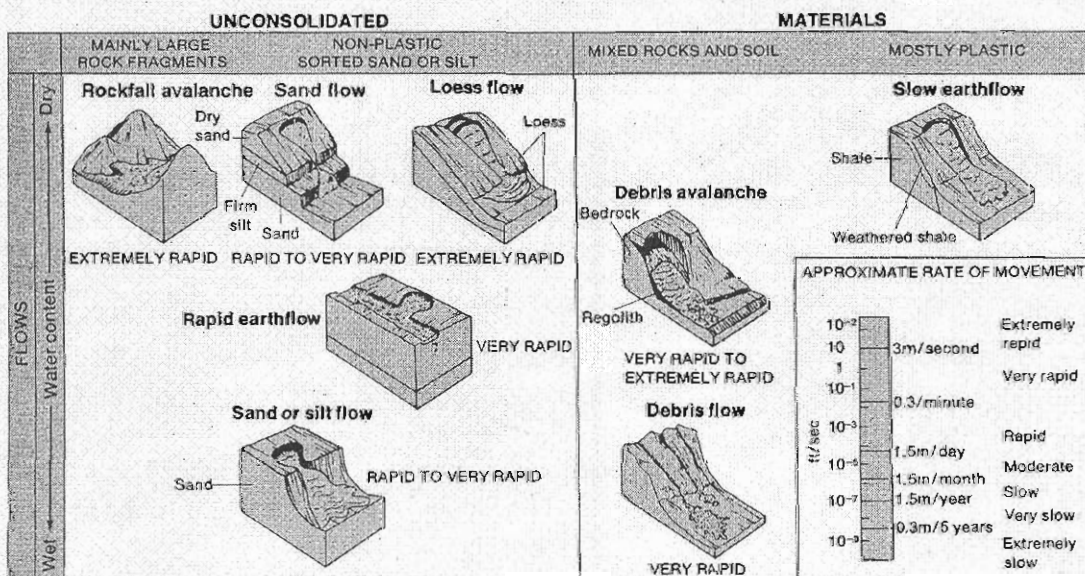
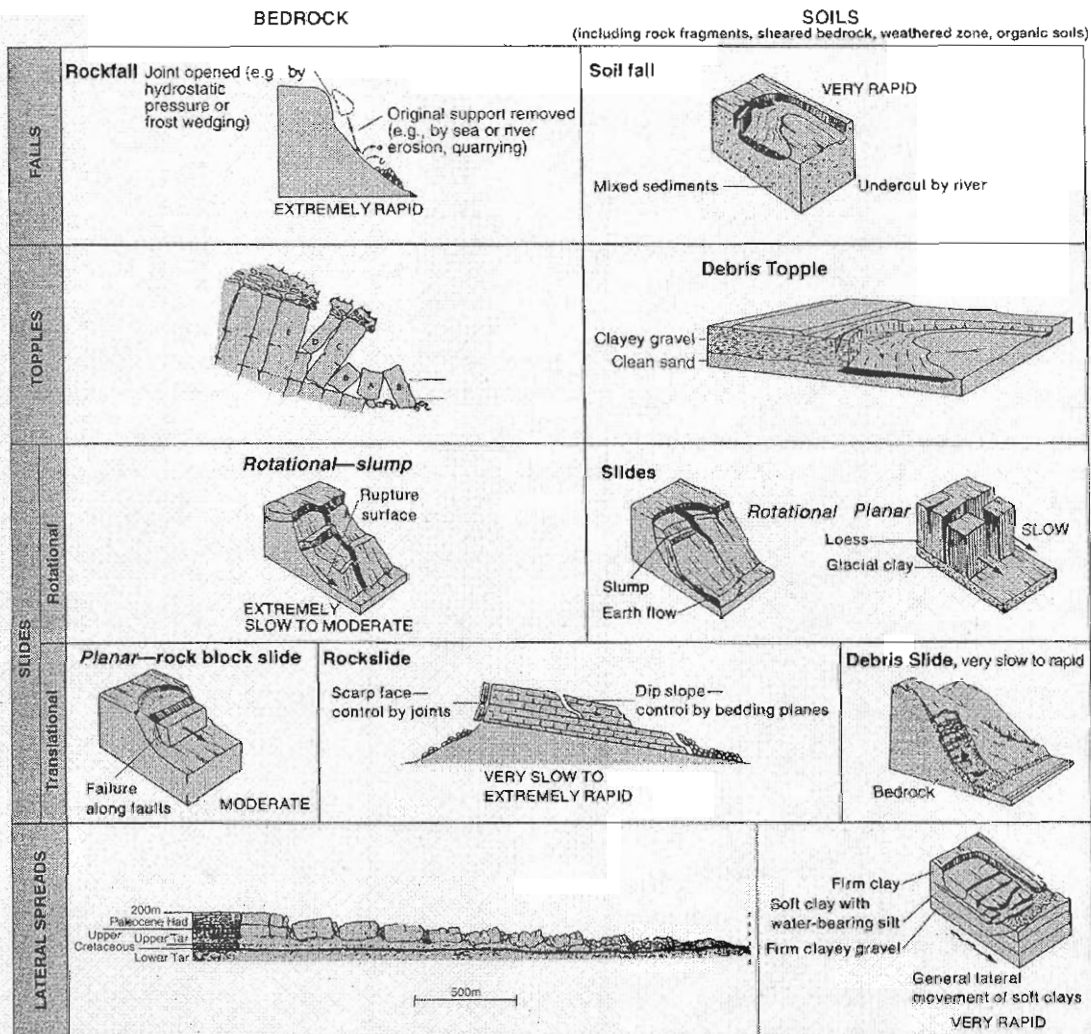


Figure 3. Landslide types. (From Ritter and others, 1995)

5

strength of slopes and the flow of water can adversely affect slope stability. Construction of roads, buildings, dams, and other infrastructure typically involves earth movement and redirection of water. For example, surface paving that redirects water to hazardous areas, excavations that remove materials from the base of marginally stable slopes, and removal of vegetation on marginally stable slopes are a few of the more common factors that can increase the likelihood of slope failures.

In forested terrain, logging activities can also have a negative impact (Swanson and Dyrness, 1975; Sidle and others, 1985). Vegetation can stabilize slopes by binding soil masses together with roots and by affecting the distribution and rate of water flow through the system. It is difficult to quantify the effects of vegetation on the stability of a particular slope, but removing vegetation increases susceptibility for slide initiation in most cases (Burroughs and Thomas, 1977; Sidle and others, 1985; Robison and others, 1999). In addition, logging practices that leave loose material in debris flow paths can significantly increase the size and downslope impact of flows.

Redirecting water, excavations, and vegetation removal are only a few of the many actions that can adversely affect the stability of slopes in steep terrain. Other common human actions that can cause or exacerbate slope instability may be loading slopes (e.g., with buildings or equipment), replacing natural materials with lower strength materials (e.g., nonengineered fill), and removing soil reinforcement.²

Debris Flow Initiation

The factors mentioned in this section are interrelated. Although other factors can also

² More information and detailed descriptions of human effects, triggering mechanisms, and slope stability factors can be found in Turner and Schuster, 1996.

be critical in evaluating the stability of particular sites, the factors listed below are the most commonly used in landslide hazard modeling efforts. Based on research into these factors, regional and site-specific models have been developed to address potential landslide initiation (e.g., Ward and others, 1978; Burroughs, 1984; Hammond and others, 1992; Montgomery and Dietrich, 1994; Carrara and others, 1997; Fannin and others, 1997; Rollerson and others, 1997; Wilkinson and Fannin, 1997; Pack and others, 1998; Vaugeois and Shaw, 2000; Wu and Abdel-Latif, 2000). Reviews of the various types of initiation hazard modeling approaches are included in Swanson and Dyrness (1975), Sidle and others, 1985, Montgomery and Dietrich (1994), Carrara and others (1997), May (1998), Montgomery and others (2000), and Vaugeois and Shaw (2000).

In addition to triggering mechanisms, a number of related factors must be considered in assessing the potential for debris flow initiation. For regional hazard evaluations in particular, topography and other inherent physical parameters are often the focus, such as slope steepness, landform (concave, convex, planar), rock and soil properties, hydrol-

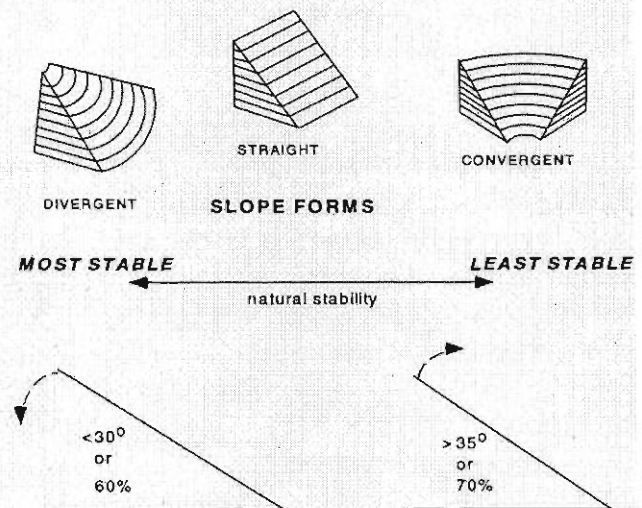


Figure 13. Schematic of divergent, straight, and convergent topography. (From Benda and others, 2000)

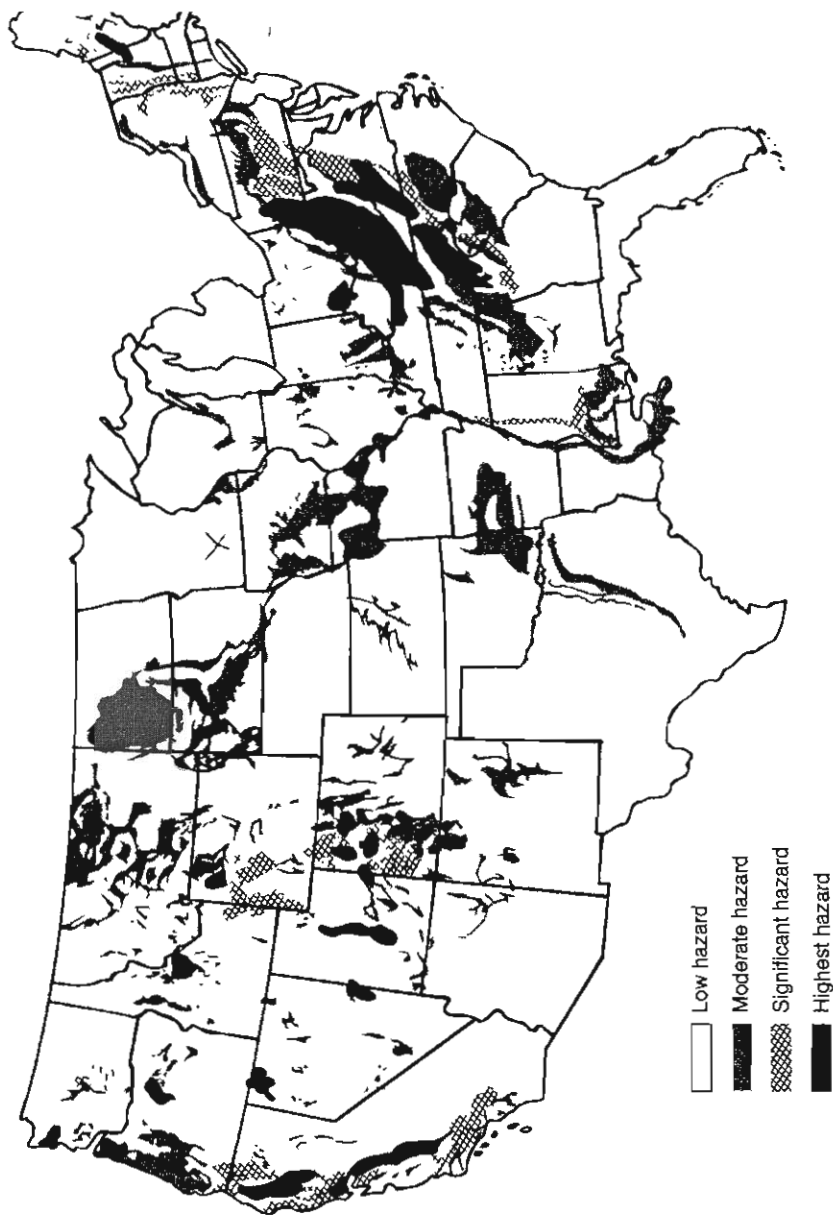


FIGURE 4.38

Major slope hazard regions in the United States. Darkest areas represent greatest severity. Details can be found in U.S. Geological Survey Professional Paper 1188.

(Hayes 1981)

Fundamentals of Landscape Analysis

FUNDAMENTALS OF LANDSCAPE ANALYSIS

- I. Landscape Analysis
 - a. Landforms and Topography – shape of the Earth’s surface
 1. Constructional landforms – created by deposition and accumulation of rock material or sediment
 2. Destructional Landforms – created by erosion or removal of rock material or sediment
 3. Erosional vs. depositional topographic surfaces
 - b. Material – the earth materials that comprise and underlie the landform
 - i. Bedrock – solid rock connected to the Earth’s interior
 - ii. Regolith – loose, weathered and broken rock material (e.g. “sediment”, or “soil”)
 - c. Processes – source(s) of force used to create the landforms via deposition or erosion
 - i. Surface Agents
 1. Wind – force exerted by flowing atmospheric gas (i.e. wind)
 2. Water – force exerted by flowing water (e.g. rivers, ocean currents, waves)
 3. Ice – force exerted by flowing glacial ice
 4. Gravity – force exerted by pulling to center of earth, e.g. landslides or rockfall on highway
 5. Biologic / Humans – force exerted by digging gophers or bull dozers
 - ii. Regolith / Process Terminology
 1. Alluvium – river-processed deposits
 2. Colluvium – gravity-processed deposits
 3. Residuum – in-situ weathered regolith (little to no transport)
 4. Aeolian – wind-processed deposits
 5. Till and outwash – glacier-processed deposits
 6. Volcaniclastics – primary eruptive products deposited by atmospheric, fluvial, and mass wasting processes.
 - d. Age – time required for processes to occur, time since surface process transported the mass or sculpted erosional landforms
 - i. Age of Rocks – time since rock became lithified in Earth’s crust
 - ii. Age of surface deposits – time since regolith was processed and deposited at current location
 - iii. Age of surface topography – time since erosion/deposition surfaces were formed

A. Type I Criteria: Age, Origin, Landform, Material.

- 1. Age of Surficial Material**
 H = Holocene (< 10,000 years old)
 W = Wisconsin (ca. 89 to 10 ka)
 I = Illinoian
 P = Pleistocene Undifferentiated
 EP = Early Pleistocene
 MPI = Middle Pleistocene
 LP = Late Pleistocene
 Q = Quaternary Undifferentiated
 CZ = Cenozoic Undifferentiated

B. Type II Criteria: 2-D Surface Features

- 3. Landform Units (Cont.)**
B. Valley Bottom
 ch = channel
 fp = floodplain (RI <= 2-3 yr)
 t = terrace (t1, t2 ...; height AMRL)
 f = fan
 f-l = fan terrace (f1, f2 ...; height AMRL)
 a = apron (footslope deposit)
 lo = lobe
 lv = levee
 ox = oxbow, abandoned channel
C. Other
 ft = flow track (debris flows)
 hm = hummocky topography
 rb = rock-block slide deposits
 x = excavated, fill, disturbed ground
 d = della
 du = dune

C. Type III Criteria: - Data Reference Points

- Sandwich symbols showing stratigraphy
 Depth to bedrock (drilling or seismic data)
 Minimum depth to bedrock (log data)
 Test hole / boring
 Well
 RE = refusal (in test boring)
 Hand-auger hole, shovei hole,
 Fossil locality
 Paleocurrent direction
 Observation Point

2. Origin / Surficial Process

- A. Hillslope**
 r = residuum (in situ regolith)
 c = colluvium (mass wasting)
 ds = debris slide
 rt = rock fall or topple
B. Valley Bottom
 a = stream alluvium (normal flow)
 hcf = hyperconcentrated flow
 df = debris flow
 sw = slackwater deposition
C. Lacustrine
 l = lacustrine deposit, undiff
 lb = lake-bottom deposit
 ld = lacustrine deltaic
D. Other
 g = glaciofluvial, undifferentiated
 go = glacial outwash
 e = eolian
 co = collapse (solution)
 cr = cryoturbation
 x = anthropogenic disturbance
 f = artificial fill
 rk = bedrock (process n/a)

4. Material (Composition and Texture)

- b = boulders (>256 mm; clast supported)
 c = cobbles (64-256 mm; clast supported)
 p = pebbles (4-64 mm; clast supported)
 g = gravel (>2 mm; clast supported)
 sg = mixed sand and gravel
 s = sand (0.05-2.0 mm)
 st = silt (0.002-0.05 mm)
 cy = clay (<0.002 mm)
 l = loam (mix of sand, silt, clay)
 d = diamiction undifferentiated
 bbd = very bouldery diamiction
 bd = bouldery diamiction
 cd = cobbly diamiction
 pd = pebbly diamiction
 ds = sandy matrix diamiction
 dt = silty matrix diamiction
 dy = clayey-matrix diamiction
 rk = bedrock (modify with lithology)
 rs = rotten stone, saprolite
 tr = travertine
 tu = tufa
 ma = marl
 og = organic-rich sediment
 w = water
 u = unknown

3. Landform Units

- A. Hillslope**
 n = nose
 sl = side slope
 h = hollow
 veneer = < 2m of regolith
 blanket = > 2 m of regolith
 bf = boulder field
 bs = boulder stream
 pg = patterned ground
 lls = talus deposits

Hillslope Units after Hack and Goodlett (1960)

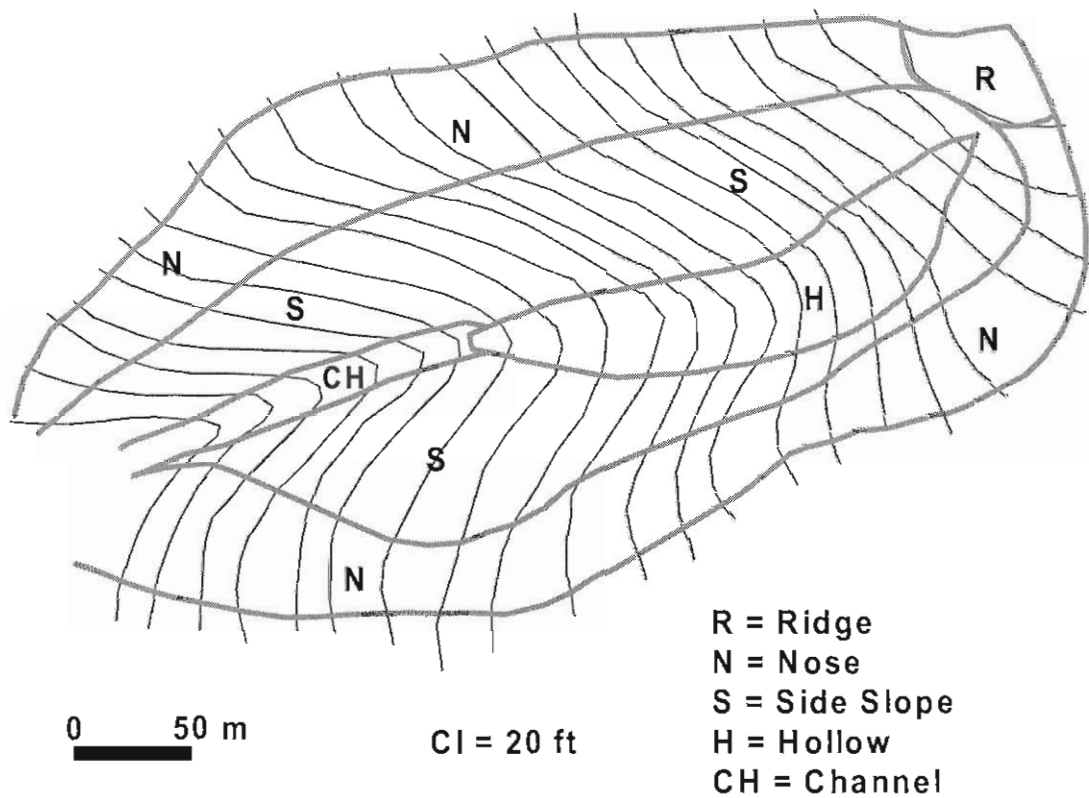
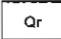
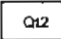
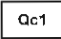
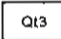
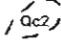


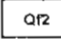

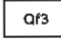
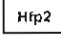
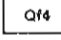
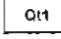
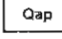


Figure 5-1. Hillslope landform elements after Hack and Goodlett (1960). Net transport flow paths are divergent on nose, convergent in hollows, and parallel on side slopes (Reneau and others, 1989). Noses represent drainage divides between zero- to first-order tributaries. Ridge crests serve as drainage divides between higher-order watersheds.

 Qr Quaternary Residium	 Qt2 Quaternary Terrace Alluvium (2-4 m)
 Qc1 Quaternary Colluvium - Side slopes/noses	 Qt3 Quaternary Terrace Alluvium (4-6 m)
 Qc2 Quaternary Colluvium - Hollows	 Hf Historic Fan Deposits (at present grade)
 Holocene Channel Alluvium	 Qt2 Quaternary Fan-Terrace Deposits (4-6 m)
 Historic Debris Slide / Flow Scar	 Qt3 Quaternary Fan-Terrace Deposits (6-8 m)
 Hfp2 Holocene Floodplain Alluvium (1-2 m)	 Qt4 Quaternary Fan-Terrace Depsots (8-10 m)
 Qt1 Quaternary Terrace Alluvium (2 m)	 Qap Quaternary Apron Deposits

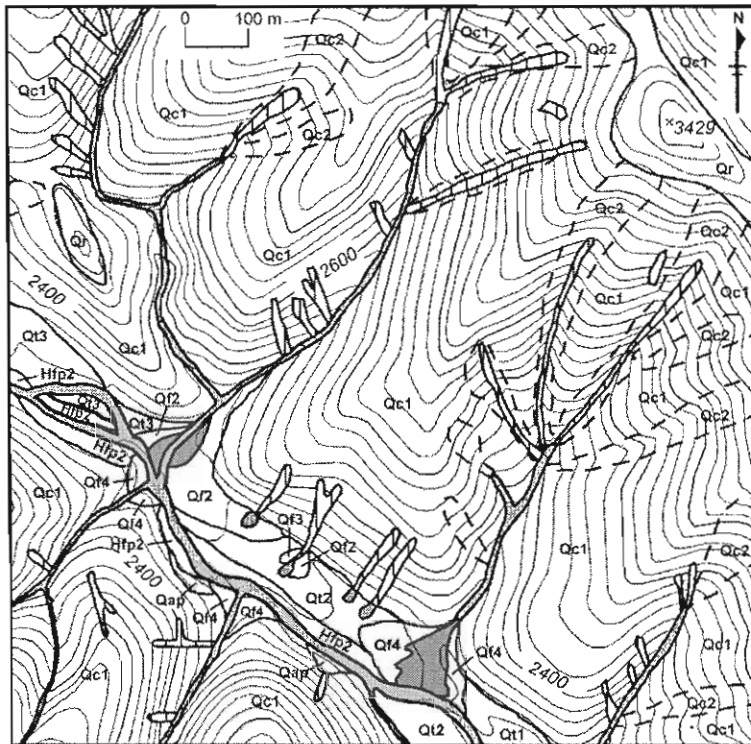


Fig. 3. Portion of the surficial geology map for the Little River area, Augusta County, Virginia. Features were originally mapped at a scale of 1:9600 (Taylor and Kite, 1998). Refer to Table 1 for an expanded explanation of map units. The contour interval is 40 ft.

include simple and compound forms, the latter of which are associated with complex map patterns and inset fan terrace relationships (Taylor, 1998; 1999). Fan terraces are preserved segments that have been otherwise dissected by tributary channels following deposition. Debris fans are preserved at select tributary junctions, with greater than 75% occurring at the intersections of first- or second-order channels with higher-order trunk streams (Fig. 7). Critical quantitative parameters, derived from systematic fan mapping, are listed in Table 3.

Mapping and morphometric data (Tables 2 and 3; Figs. 4 and 7) indicate that compared to the other two areas, Little River is a steep, rugged watershed with significantly higher drainage density and higher percentage area of valley bottom. Accordingly, Little River also has the highest volume of fan deposits in storage. Comparatively, the Little River consistently shows greater values in the categories of valley-bottom area, number of fans and total fan area.

These results suggest that compared to the other areas, geomorphic conditions at the Little River are more

Table 1
Principal surficial map units recognized at Fernow, North Fork and Little River study areas

Map unit	Map unit description	Age	Origin (process)	Landform	Material (texture)
Qr	Quaternary residuum	Quaternary (undiff.)	Residuum	Ridge-veneer	Cobble- to boulder-diamicton with silty loam matrix
Qc1	Quaternary colluvium (side slopes)	Quaternary (undiff.)	Colluvium	Nose-side slope veneer	Cobble- to boulder-diamicton with silty loam matrix
Qc2	Quaternary colluvium (hollows)	Quaternary (undiff.)	Colluvium	Hollow veneer	Cobble- to boulder-diamicton with silty loam matrix
Hch	Holocene channel alluvium	Holocene	Alluvium	Channel and narrow floodplain	Cobbles, boulders and pebbly loam (rounded to subrounded)
Hfp1	Holocene floodplain alluvium (0.5 to 1.0 m surface)	Holocene	Alluvium	Floodplain	Cobbles, boulders and pebbly loam (rounded to subrounded)
Hfp2	Holocene floodplain alluvium (1.0 to 2.0 m surface)	Holocene	Alluvium	Floodplain	Cobbles, boulders and pebbly loam (rounded to subrounded)
Hfp2A	Holocene floodplain alluvium (1.0 to 2.0 m surface)	Holocene	Alluvium	Floodplain	Sandy loam
Hfp2B	Holocene floodplain alluvium (1.0 to 2.0 m surface)	Holocene	Alluvium	Floodplain	Clayey loam
Qt1	Quaternary low-terrace alluvium (2.0 m surface)	Quaternary (undiff.)	Alluvium	Terrace (floodplain?)	Cobbles, boulders and pebbly loam (rounded to subrounded)
Qt2	Quaternary terrace alluvium (2.0 to 4.0 m surface)	Quaternary (undiff.)	Alluvium	Terrace	Cobbles, boulders and pebbly loam (rounded to subrounded)
Qt3	Quaternary terrace alluvium (4.0 to 6.0 m surface)	Quaternary (undiff.)	Alluvium	Terrace	Cobbles, boulder, and pebbly loam (rounded to subrounded)
Qt4	Quaternary terrace alluvium (6.0 to 8.0 m surface)	Quaternary (undiff.)	Alluvium	Terrace	Cobbles, boulder, and pebbly loam (rounded to subrounded)
Hf	Holocene (historic) fan deposits (undissected)	Holocene	Alluvium-debris flow (?)	Fan	Cobbles, boulders and gravel diamicton
Qf	Quaternary fan deposits (undissected)	Quaternary (undiff.)	Alluvium-debris flow (?)	Fan	Cobble- to boulder-diamicton with silty loam matrix (subangular to rounded)
Qf1	Quaternary fan-terrace deposits (2.0 to 6.0 m surface)	Quaternary (undiff.)	Alluvium-debris flow (?)	Fan	Cobble- to boulder-diamicton with silty loam matrix (subangular to rounded)
Qf2	Quaternary fan-terrace deposits (4.0 to 6.0 m surface)	Quaternary (undiff.)	Alluvium-debris flow (?)	Fan	Cobble- to boulder-diamicton with silty loam matrix (subangular to rounded)
Qf3	Quaternary fan-terrace deposits (6.0 to 8.0 m surface)	Quaternary (undiff.)	Alluvium-debris flow (?)	Fan	Cobble- to boulder-diamicton with silty loam matrix (subangular to rounded)
Qf4	Quaternary fan-terrace deposits (8.0 to 10.0 m surface)	Quaternary (undiff.)	Alluvium-debris flow (?)	Fan	Cobble- to boulder-diamicton with silty loam matrix (subangular to rounded)
Qf5	Quaternary fan-terrace deposits (>10.0 m surface)	Quaternary (undiff.)	Alluvium-debris flow (?)	Fan	Cobble- to boulder-diamicton with silty loam matrix (subangular to rounded)
Qap	Quaternary apron deposits	Quaternary (undiff.)	Colluvium	Apron	Cobble- to boulder-diamicton with silty loam matrix

characterized by V-shaped valleys with exposure of bedrock channels throughout the drainage network (Fig. 6A). In contrast, the Little River valley is notably wider and gravelly alluvial fill is abundant in fourth-order and higher tributaries (Fig. 6B). Reaches floored by bedrock are limited to lower-order channels in the steepest headwater zones (Fig. 5). Drilling logs were obtained for the southeastern corner of the Little River area, near the mouth of the watershed (unpublished

data, Headwaters Conservation District, Verona, Virginia). Drilling data support the map observations and document 5 to 10 m of alluvium in the lower channel reaches (Fig. 5).

4.3.2. Distribution of debris fans

Fan map units are delineated according to fan-surface morphology and height above channel grade (Table 1). Debris fans mapped in the study areas

Physical Geomorphology of Debris Flows

Key Words for Debris Flow Hazards and Processes

(i.e. check the notes, book, and readings to make sure you know the significance of these terms)

Landforms

hillslope
hollow
debris fan
hillslope gradient
channels

Process

weathering
mass wasting
 slide
 flow
 creep
 slump
debris flow
flow processes
 normal water flood
 hyperconcentrated flow
 debris flow
lahar

Material

weathered mantle
 regolith
 colluvium
sediment texture
 clay
 silt
 sand
 gravel
volcaniclastic
diamicton
matrix
woody debris

Physics Principles

velocity
density
granular solids
viscous fluids
buoyancy
shear strength
dispersive pressure

pore pressure
sediment porosity
pore fluids
atmospheric pressure
positive pore pressure
negative pore pressure
dilation
liquefaction
shear strength
cohesive
non-cohesive
soil strength
root strength

Debris Flow Features

snout
high friction gravel rind
lobe
superelevation
levee
sediment bulking
rapidly moving landslides
channel erosion
channel deposition
stream alteration
head scar
transport zone
runout zone
woody debris dam

Debris Flow Occurrence

rate of colluviation
hollow filling
recurrence interval
clear cutting
triggers
 meteorologic
 seismic
 anthropogenic
 road cut
 loading
rainfall intensity
hazard - likelihood of occurrence

Costa, John E. 1984. Physical geomorphology of debris flows: in Costa, J. E., and Fleisher, P. J., eds., *Developments and Applications of Geomorphology*, Berlin, Springer-Verlag, p. 268-317.

I. Introduction

A. Debris Flows and Damage

1. dollars and death yearly
2. Japan, Peru, Indonesia, Africa, China Russia.... death and destruction everywhere
 - a. it's a crying shame
 - b. send more tax dollars immediately!!!

B. Debris Flows

1. gravity-induced mass movement
2. transitional between flooding and landsliding with different mechanical characteristics than each
3. rapid flow of granular solids, water and air (solids 65-80% observed)
4. viscosity variable according to mixture
5. variations
 - a. mudflows: sand, silt and clay
 - b. lahars: volcanic mudflows
 - c. tillflows
 - d. debris avalanches

II. Origins and Types of Debris Flows

A. genesis

1. poorly sorted rock and soil debris mobilized on hillslopes and channels
 - a. gravity
 - b. moisture increase (rain, snowmelt, glacial outburst)
 - c. sparse vegetation
 - d. unconsolidated materials
2. Most prone areas: small, steep drainage basins... why?
 - a. rain drop > proportion of water to small basins
 - b. high elevations, steep slopes (> 30 degrees)
 - c. moisture >, > pore pressure
3. Threshold relations
 - a. $I = 14.82 D^{-0.39}$ where I = rainfall intensity (mm/hr), D = duration in hours

B. Lahars

1. volcanic debris flows, may be hot or cold in origin
 - a. rainfall
 - b. rapid eruption melt of snow caps, glaciers
 - c. rapid drainage of crater lakes
 - d. pyroclastic flows that bulk up in water from mixing and melting of eroded snow
 - e. seismic-induced instability

- f. failure of landslide-dammed lakes

C. Tillflows

- 1. glacial debris flows at ice front during melting
 - a. slumping of sed. over ice
 - b. backwasting of sed. laden slopes of stagnant ice
 - c. ablation of debris-laden ice

III. Failure Mechanisms

A. conditions

- 1. steep slopes > 15-20 degrees
- 2. large influx of water
 - a. saturation of pore space
 - b. pore pressure increases
 - (1) rate of deep percolation < rate of surface infiltration
 - (2) decreases shear strength, failure
 - (3) spontaneous liquefaction and flow
 - c. shear strength decreases
- 3. originate in head-of-hollows commonly
 - a. initial failure: slide, slump or topple
 - b. transformation downslope to debris flow
 - (1) via dilatancy- increase in bulk volume of soil mass, > pore volume, > failure
 - (2) incorporation of additional water
 - (3) liquefaction
 - c. change in resisting force from sliding friction to internal viscosity of flow
 - (1) allows rapid velocity > down slope

IV. Characteristics of Flowing Debris

A. General

- 1. relatively few direct observations, but some exist and are summarized in a table

B. Character

- 1. commonly use preexisting drainage ways, although can use open slopes
 - a. levees form to contain flow
 - b. "surging wet concrete moving down valley"
 - (1) surges: temporary damming and breaching of channels by debris
 - (2) surges commonly carry largest boulders
 - (3) surges followed by more fluid, watery slurries
- 2. Vel. observed 0.5-20 m/sec
- 3. Texture of flow
 - a. 10-20% silt and clay
- 4. Non-newtonian rheology: viscosity up to 8000 poises

5. water content: 10-30%
6. capacity to carry large boulders many miles
7. High erosive capacity on channel sides
 - a. up to 6 times the shear stress on channel beds compared to flood flow
 - (1) bedrock scour observed: 4 m in less than 24 hours
8. Mobility of debris flows over gentle slopes
 - a. function of clay content
 - (1) 1-2% clay, < permeability, > pore pressure in fluid, > mobility
9. other
 - a. ground shaking, loud rumbles/sound

V. Physics of Debris Flows

A. Impact Force

1. very high impact force
 - a. tree uprooting
 - b. houses removed etc.

B. Shear Strength

1. > sediment concentration, > viscosity, > shear strength to flow
 - a. shear strength K - internal strength of mass that must be overcome by critical shear stress before motion takes place
 - (1) source: fine matrix, cohesive
 - (2) coarse clasts = friction internally (interlocking)

C. Viscosity

1. Debris flows: are they Newtonian or Bingham fluids??

D. Coulomb-viscous Model

1. plastico-viscous bingham fluid models

E. Dilatant Model

F. Boulder Transport and Suspension of Solids

1. General
 - a. boulders commonly transported
 - b. "float" or weakly tumble in flow
 - c. commonly deposit as diamicts
 - d. what keeps these big boys floating at top of flow???
2. mechanisms of boulder support and transport
 - a. Cohesion: clay -water slurries as support medium
 - (1) > density, increased internal strength to support
 - b. Buoyancy: density differences

- c. Dispersive Pressure
 - (1) Bagnold concept from 50's
 - (a) during shear flow, largest clasts drift towards free surface
 - (b) commonly find boulders at top and front of flow
- d. Turbulence
- e. Structural Support: grain to grain contact and support

VI. Deposition of Debris Flows

- A. conditions of deposition
 - 1. low gradient areas of decreased confinement
 - a. e.g. fans at trib. mouth, spreading, thinning, deposition
 - b. < fluids, > internal friction... deposition
 - 2. debris flow generation: complex between precip. and sed. supply
- B. Alluvial fans and debris flows; d.f. common on fans in west
 - 1. pretty good fan discussion on facies and deposition

VII. Differentiation of Water Floods and Debris Flows

- A. Introduction
 - 1. continuum: water floods to debris flows
 - 2. floods
 - a. mud floods vs. clear water floods
 - (1) clear water floods: solids separate from liquids during deposition
 - (2) debris flow: en masse deposition with little phase separation
 - 3. Waterfloods
 - a. turbulent water flows with small amount of seds.
 - b. deposits: stratified, sorted to poorly sorted
 - 4. Mudfloods = hyperconcentrated flows
 - a. stream flows enriched in sediment (40-70% seds)
 - (1) e.g. Rio Puerco, NM

summary comparison

Flow	sed. load	bulk density	fluid type	deposits
water flood	1-40%	1-1.3 g/cu. cm	Newtonian	stratified
hyperconc. flow	40-70%	1.3-1.8 g/cu. cm	Newtonian?	poorly sorted weak strat.
debris	70-90%	1.8-2.6 g/cu. cm	Visco-plastic	diamict,

** all three flow types may exist at any given time during a given event

B. Field Evidence

1. field data, land forms, sedimentology
 - a. presence or absence of bouldery levees and fans
 - b. sed. of deposits
 - c. extent of veg. damage
 - d. extent of ground litter disruption below high water marks
 - e. gaging station records

2. Levees and terminal lobes
 - a. common in debris flows

3. boulder berms
 - a. open framework gravels and boulders adjacent to drainage ways
 - (1) large boulders at top of berms
 - (2) no matrix
 - (3) localized or short occurrence along channels

 - b. origin? a mystery:
 - (1) slip faces of boulder dunes/deltas?
 - (2) macroturbulence features?
 - (3) kolk vortex action?

C. Sedimentologic Evidence

1. diamict common in debris flows
 - a. matrix supported boulders
 - (1) matrix washing may result in clast supported
 - b. woody debris, organics
 - (1) commonly floats
 - c. bedding and sorting poor

2. water-laid seds.
 - a. sharp bedding contacts
 - b. stratification
 - c. cut and fill
 - d. imbrication of clasts
 - e. percussion marks from turbulence on clasts
 - f. open-framework gravels

3. examples of textural analysis for use in i.d. process
 - a. trask sorting factor
 - b. grain plots, etc.

D. Vegetation Damage

1. water floods turbulent
 - a. scar and destroy veg. in path of flood
2. debris flows
 - a. complete removal of all veg. and trees
 - b. sheared trees suggesting lift off of channel bottom

E. Gaging Station Records

1. examples of gage records, case studies

F. Estimating the Discharge of Sediment Bearing Flows

1. paleohydraulic methods will be screwed up if applying water flood techniques to debris flow
 - a. will greatly over estimate flood discharge
 - b. diff. rheology than water, e.g. Mannings eq. would not work

G. Empirical Formulas

1. gives e.g. of formulas that have been modified for use with debris flows to determine vel., Q, etc.

H. Bulking Factors

I. Superelevation of Flows around channel bends and Runup

1. Tendency for fluid flows to reach higher elevations around outside of channel bends than on inside
 - a. superelevation common in debris flows
 - b. centrifugal force and radial acceleration around bend
 - (1) may be used to determine flow velocity, e.g. given using Newtonian physics

J. Photographic Techniques

1. on site radar guns, videos etc. used to reconstruct flows and velocities

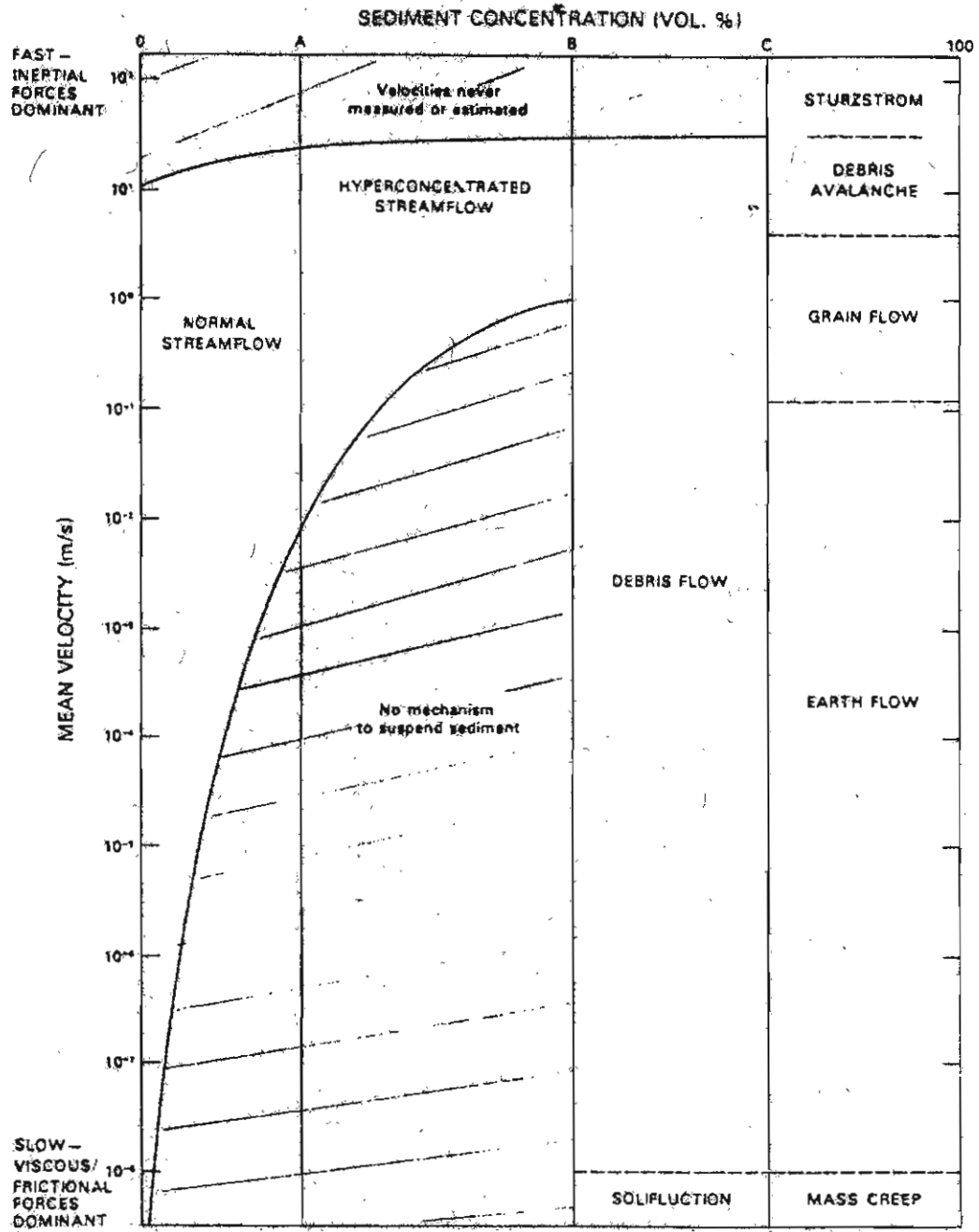
VIII. Mitigation of Debris-Flow Hazards

- A. Avoidance of Hazardous Areas
- B. Control of Grading, clearing and drainage
- C. protective structures
- D. warning and evacuation

IX. Further Research

- A. Cause, moisture conditions, ppt
- B. field identification
- C. mechanisms
- D. characteristics
- E. flow parameters and paleohydraulics of debris flows?
- F. Occurrence and risk analysis, recurrence estimates.

P. Pearson & Costa, 1987



FLUID TYPE	NEWTONIAN	NON-NEWTONIAN	
INTERSTITIAL FLUID	WATER	WATER + FINES	WATER + AIR + FINES
FLOW CATEGORY	"	STREAMFLOW	SLURRY FLOW GRANULAR FLOW
FLOW BEHAVIOR	LIQUID	PLASTIC	

Figure 4. Fitting appropriate existing flow nomenclature into proposed rheologic classification.

COSTA, 1984

Table 1. Physical properties of sampled debris flows

Location	Velocity (m/s)	Slope (%)	Bulk density (g/cm ³)	Newtonian viscosity (Poise)	%Clay	Depth (m)	Solids (% Wt.)	Shear strength (dn/cm ²)	Reference
Rio Reventado, Costa Rica	2.9-10	4.6-17.4	1.13-1.98	-	1-10	8-12	20-79	-	Waldron 1967
Hunshui Gully, China	10-13	-	2.0-2.3	15-20	3.6 (<0.005 mm)	3-5	80-85	294-490	Li and Luo 1981
Bullock Creek, New Zealand	2.5-5.0	10.5	1.95-2.13	2,100-8,100	4	1.0	77-84	-	Pierson 1981
Pine Creek, Mt. St. Helens, Wa.	10-31.1	7-32	1.97-2.03	200-3,200	-	0.13-1.5	-	3,900-11,300	Fink et al., 1981
Wrightwood Canyon, Ca. (1969 flow)	0.6-3.8	9-31	1.62-2.13	100-60,000	-	1.0	59-86	-	Morton and Campbell 1974
Wrightwood Canyon, Ca. (1941 flow)	1.2-4.4	9-31	2.4	2,100-6,000	<5	1.2	79-85	-	Sharp and Nobles, 1953
Lesser Almatinka River, U.S.S.R	4.3-11.1	10-18	2.0	-	-	2-10.4	58	-	Niyazov and Degovets 1975
Matanuska Glacier, Alaska	0.001-1.3	2-47	1.8-2.6	-	≈ 3	0.01-2.0	67-89	$<0.4 \times 10^4$ to 1.5×10^4	Lawson 1982
Nojiri River, Japan	12.7-13.0	5.8-9.2	1.81-1.95	-	-	2.3-2.4	-	-	Watanabe and Ikeya 1981
Mayflower Gulch, Colorado	2.5	27	2.53	30,000	1.1 (<0.004 mm)	1.5	91	-	Curry 1966
Dragon Creek, Arizona	7.0	5.9	2.0	27,800	-	5.8	80	221	Cooley, et al. 1977

* Calculated values from deposits
 * Type I, II, III flows only

24

CHARACTERISTICS OF DEBRIS FLOWS

Debris flows, shown schematically in Figure 5 and by example in Figure 6, consist of water-charged soil, rock, colluvium, and organic material traveling rapidly down steep topography (Johnson, 1984). Debris flows are often triggered by small landslides (Figure 7) that then mobilize and grow to be large flows, entering and scouring stream channels downslope (Figure 8). When momentum is eventually lost, the scoured debris is often deposited as a tangled mass of boulders and woody debris in a matrix of finer sediments and organic material (Figure 9).

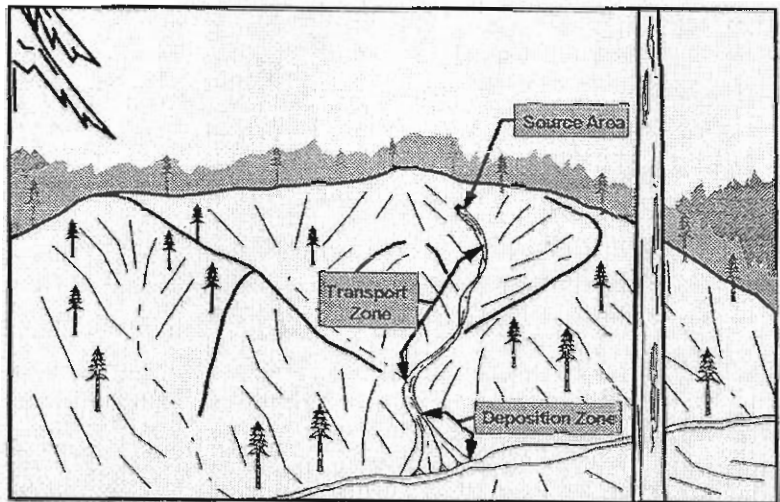


Figure 5. Diagram of a debris flow showing zones of initiation (source areas), transport, and deposition. (From Pyles and others, 1998)

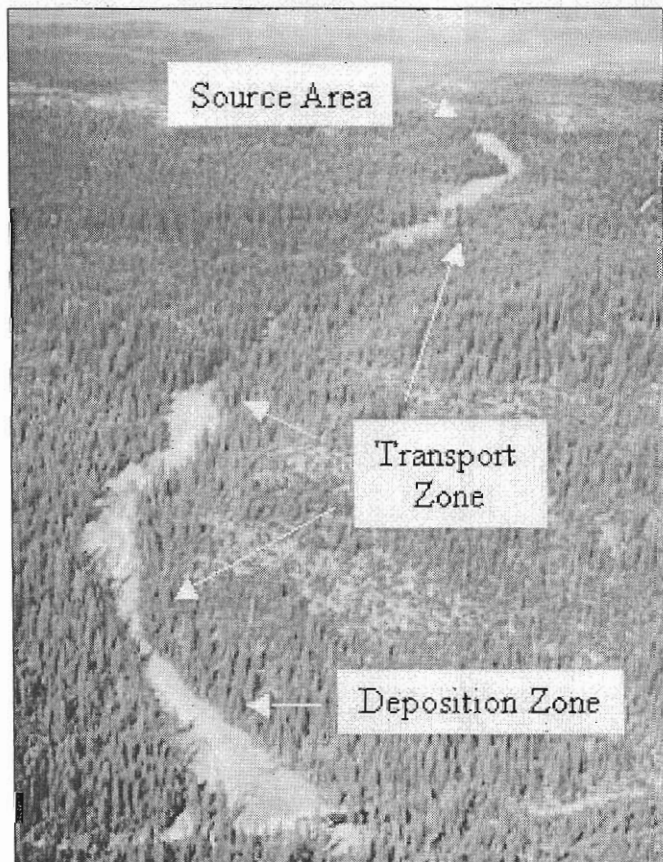


Figure 6. Photo of a debris flow showing zones of initiation, transport, and deposition. (Photo courtesy of U.S. Geological Survey)

Although debris flows can be extremely variable and chaotic, they have some common characteristics. These characteristics form the basis of much of our scientific understanding and provide the keys to identifying and modeling potentially hazardous locations. Before describing the development of the hazard map, therefore, useful background on factors that affect debris flow potential is provided.

For descriptive purposes, it is helpful to segment debris flow paths into areas of initiation, transport, and deposition as shown generally in Figures 5 and 6. Some of the common debris flow causes (termed trigger mechanisms) are outlined below, followed by some of the significant factors affecting debris flow initiation, transport, and deposition. This section provides only a brief overview of the subject.

Trigger Mechanisms

Debris flows can be initiated in marginally stable slopes by a number of natural and unnatural disturbances. Because most steep slopes are near their point

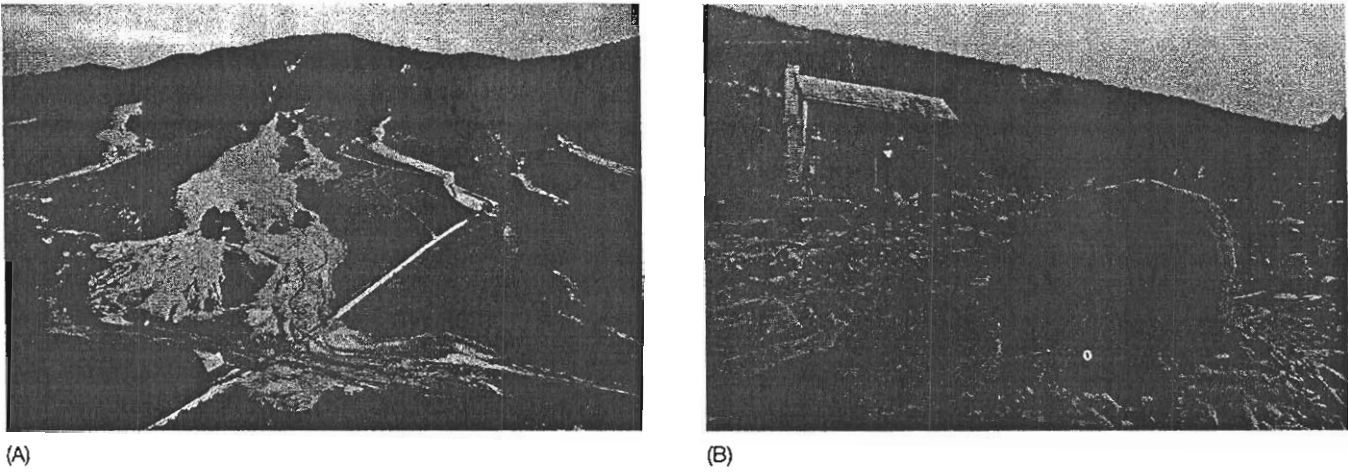


FIGURE 4.39

Debris flow and avalanches in Nelson County, Va., during 1969. (A) Flows deposited debris on small fans at the base of first-order hillslope channels (near Lovington). (B) Catastrophic erosion and impact forces from these flows removed some structures and devastated others (view from Davis Creek).

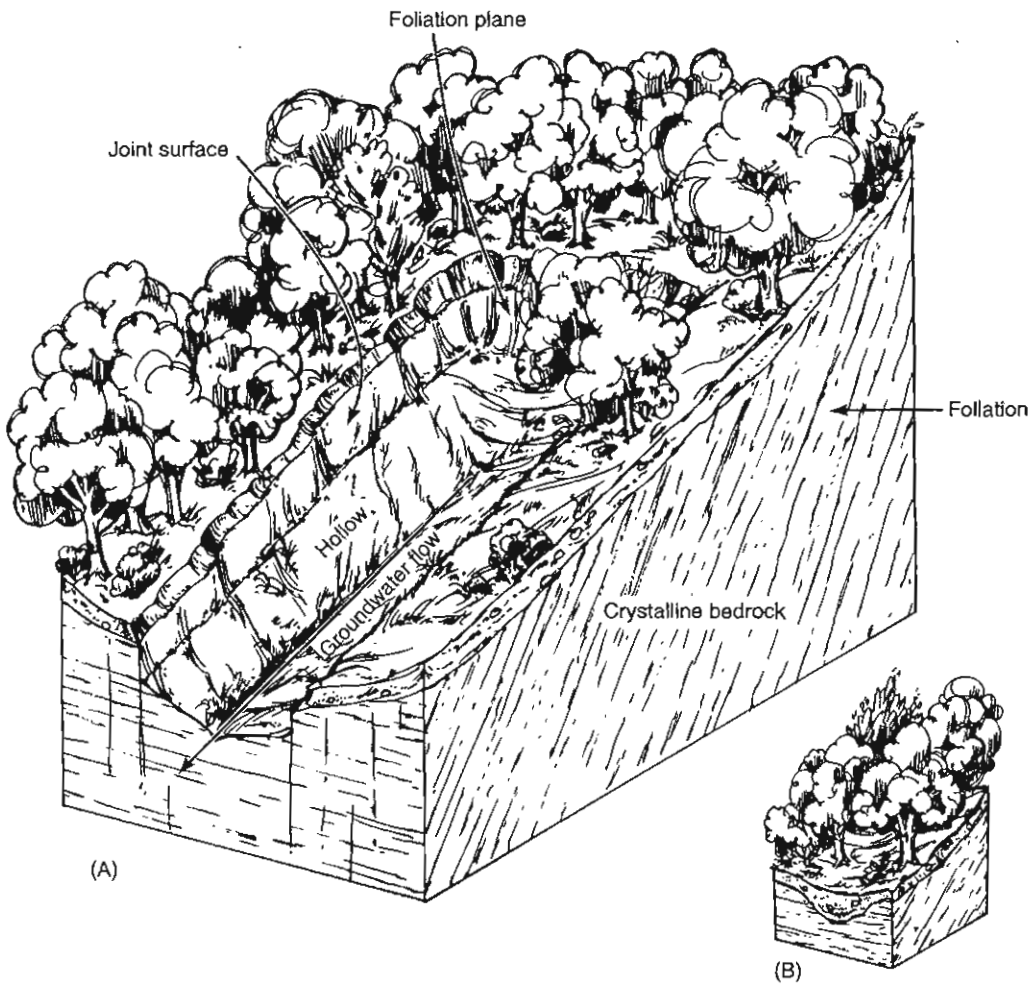


FIGURE 4.40

Schematic model of a colluvium-filled hollow. (A) Hollow excavated to bedrock by a recent debris avalanche/debris flow. (B) Hollow has been refilled with colluvium and slope wash after a few hundred years. The site is now primed for another debris flow event once again.

26

Hoffmeyer AT 12, 2002



↑ Figure 7.
Small initiating landslide.



→ Figure 8.
Scoured transport zone.

↓ Figure 9.
Tangled debris in deposition zone.



of equilibrium, failures can be the result of seemingly minor modifications. In a fundamental sense, modifications that lead to failures can be simply grouped into factors that (a) increase the gravity-driven forces acting downslope and (b) reduce the resisting forces acting to keep the slope in place (Figure 10). Multiple factors may be involved in triggering any given debris flow.

Natural events that can induce failures include high-rainfall storms, rapid snow melt, earthquake shaking, breach of landslide or other natural dams, and volcanic eruptions (Wieczorek, 1996). By far the greatest number of debris flows that have occurred in Oregon (at least in historical times) have been associated with severe rainfall and rain-on-snow storm events.

Severe Rain Storms

High-precipitation storms can trigger slope failures through a number of mechanisms. Water infiltration into zones of weakness can trigger failures by (1) reducing the frictional resistance to sliding, (2) increasing pore pressures within a slope mass, and (3) adding weight (through saturation of the soil mass) (Turner and Schuster, 1996). Typically, all three of these mechanisms combine during long-duration, heavy-precipitation storm events to trigger widespread slope stability problems. During three 1996/97 storm events, for example, thousands of landslides (including many debris flows) were triggered throughout western Oregon (Figure 11).

Given the importance of rainfall events for slope failures, it is not surprising that a number of studies have

27

CORA, 1984

30 m/s are computed (Wigmosta et al. 1981; Janda et al. 1981). This unbelievable average velocity is probably a result of (a) super-acceleration from the lateral blast of the volcanic eruption, or (b) result of poor site selection, or (c) wave splatter setting unrealistically high mud marks. The fundamental validity of velocity values calculated from superelevation, and assumptions therein, remain unverified for use with mud and debris flows (Ikeya and Uehara 1982). Since this method is promising because of its wide applicability, more research is needed on the influences of fluid strength on superelevation.

Earlier it was noted that mudlines on surviving trees in the path of debris and mud flows show runup of the fluid on upstream sides. This runup reflects the point surface velocity of the moving fluid, and for debris flows can probably be assumed nearly equal to the mean velocity at that point. Runup from mudlines on trees, hills, or canyon walls might be used to obtain any number of point mean velocities of flows by substituting the amount of runup into the velocity head equation ($\Delta h = \alpha v^2 / 2g$). Strictly speaking, hydrostatic pressure relationships are not valid for flows with strength. However, no data exist to my knowledge to verify just how well or how poorly runup on trees or other obstructions compares with measured velocities for mud and debris flows. Studies have been made on clear-water streamflow (Wilm and Storey 1944). This method needs further investigation.

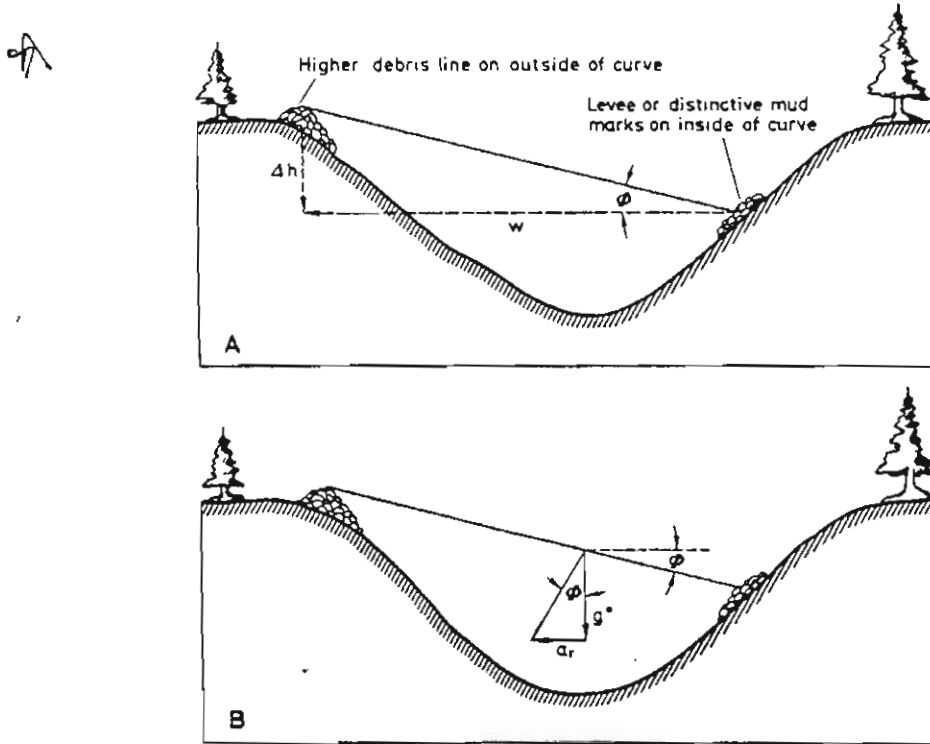


Fig. 14. Technique for estimating average velocity of debris flows from superelevation in curves. (From Johnson 1979)

28

Hightmension PT Ar, 2002



Figure 15. Unchanneled debris flow deposit.

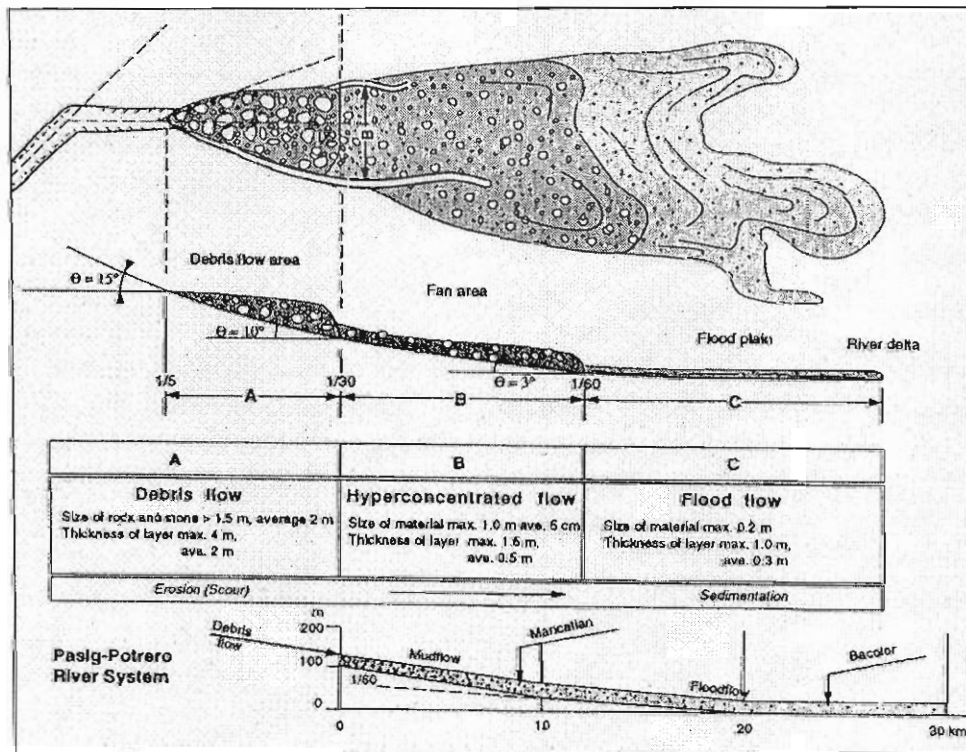


Figure 16. Schematic of transition from debris flow to hyperconcentrated flow to flooding. (From United Nations, 1996)

Huffman et al, 2002

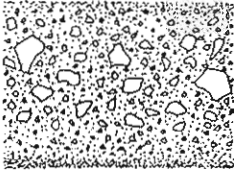
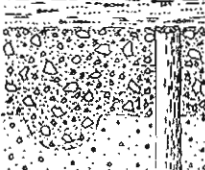
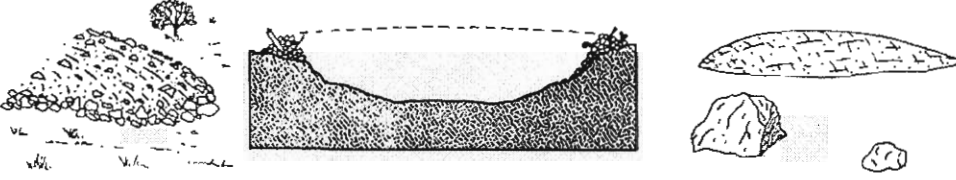
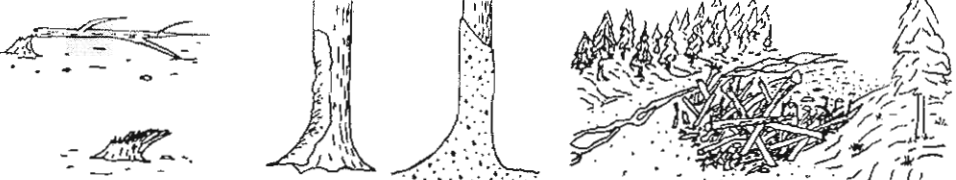
STRATIGRAPHIC	 <p>Nonstratified Normal, reverse grading Sole layer</p>		 <p>Buried trees Buried channels</p>	
SEDIMENTOLOGIC	<p>Closed, interlocking structure Matrix between clasts Vesicles</p>	<p>Coarse grain size < 10 - 15% silt & clay</p>	<p>Extremely poor sorting 3.0 - 6.5Φ (2.0 - 4.0Φ)</p>	<p>Fine skewed distribution</p>
MORPHOLOGIC				
BOTANIC				

Figure 18. Geomorphic features that can aid in the identification of historic debris flows. (Diagram courtesy of Tom Pierson)

Both the Oregon Departments of Geology and Mineral Industries (DOGAMI) and ODF performed these targeted field investigations. Geographically distributed (and geologically diverse) areas were evaluated as shown in Figure 19. In these areas, reconnaissance-level field investigations were conducted. Where geologic evidence clearly defined the extent of historic debris flow deposits, boundaries were mapped. More commonly, the geologic evidence was discontinuous or otherwise inconclusive. In these cases, field investigations focused on a general rating of terrain for high versus low relative debris flow hazard.

Improved GIS Modeling

During and following the initial field mapping, a variety of GIS models that could aid in the hazard mapping effort were evaluated.

Our focus was on identifying a suitable modeling framework to delineate the range of debris flow hazards observed in the field, including initiation, transport, and deposition areas. While numerous models have been developed for evaluating initiation potential, fewer have focused on the transport and deposition hazards—areas that are critical for impact and public safety.

In a general review of modeling approaches and available models, a modeling framework developed by the Earth Systems Institute (ESI) was selected as the starting point. The ESI program uses topographic input data (DEMs) and a suite of rules to model initiation, transport, and deposition zones. In this study, the general three-part framework implemented was as follows:

For initiation, steep slopes are used as the

and stop in place
ow.
n all latitudes, ir-
lication of Black-
ople began to ap-
beaty 1963, 1974).
tional mechanism
15). Probably the
nized for so long
le 3) and the ex-

ely by rainfall fre-
at one time, but a
ooding. Sediment
sorted colluvium
by rates of weath-
is flows.

alluvial fans (e.g.,
ost entirely of de-
Williams and Guy
nents, where con-
small basins under-
nd debris flow for-
n to be infrequent
h (1954) reports a
mean annual pre-
o 483 mm (5-10%
water-laid deposits
tes. This is at vari-
ows were the domi-

ormation of alluvial
v the work of Mills
n are almost exclu-
y reworked, sorted,
at water flows when
1974; Johnson and
ates because of in-
to water-laid sedi-
to be reworked, de-
f the deposits. The
ted by subsequent
ncapable of rework-
ned above are much

osits can vary verti-
ghout the history of

CGA, 1984 285

Table 1. Estimated recurrence intervals of debris flows

Location	Estimated recurrence intervals (years)	Basis of Estimate	Reference
Montgomery Creek, White Mts., California	300 - 500	Geomorphology	Beaty 1974
Mayflower Gulch, Tenmile Range, Colorado	150 - 400	Lichenometry	Curry 1966
Pfaffler-Redwood Creek, Santa Lucia, California	140	Dendrochronology, stratigraphy, radiocarbon	Jackson, 1977
Aleslino, Nassunvage Rivers and Tribbs, Northern Sweden	50 - 400	Historical data, lichenometry, ppt. records, geomorphology	Rapp and Nyberg 1981
Takahara River, Japan	300	Historical data, radiocarbon	Iso, et al. 1980
Volcanic Mountains, Japan	0.2 - 0.4	Historical data	Okuda 1978
Andøya Island, Norway	50 - 60	Historical data	Rapp and Sirömqvist 1976
Torneträsk-Narvik Area, Lappland	8	Ppt. records	Rapp and Sirömqvist 1976
Steel Creek, Yukon	(decades)	Vegetation, historical data	Broscoe and Thomson 1969
Mt. St. Helens, Washington	500 - 3,000	Stratigraphy, radiocarbon	Crandell and Mullineaux 1978
Mt. Shasta, California	600 - 5,000	Stratigraphy, radiocarbon	Miller 1980
	("large" debris flow) 10 - 25		
	("small" debris flow) 3,000 - 6,000		
Davis Creek, Virginia	300	Stratigraphy, radiocarbon	Kochel et al 1982
Blanco Mt., White Mts., California	150	Dendrochronology	La Marche 1968
Mt Baker, Washington	800	Stratigraphy, radiocarbon	Hyde and Crandell 1978
Nisqually River, Mt. Rainier, Washington		Stratigraphy, radiocarbon	Crandell 1971
White River, Mt. Rainier, Washington	600	Stratigraphy, radiocarbon	Crandell 1971
Reshün Stream, Pakistan	> 30 ("large" debris flow) < 10 ("small" debris flow)	Historical data	Wasson, 1978
Portland and Cascade Creeks, Ouray, Colorado	10	Historical data	Simons Li and Associates 1982
Santa Monica Mts., California	75 - 150	Ppt. records	Campbell 1975
Cambria County, Pennsylvania	5,000 - 10,000	Ppt. records	Pomeroy 1980
Rocky Mts., British Columbia	15 - 25	Dendrochronology	Gardner 1982
Fall Creek Tributary, New York	10 - 70	Ppt. records	Renwick 1977

31

Material Transfer Processes in Forested Watersheds

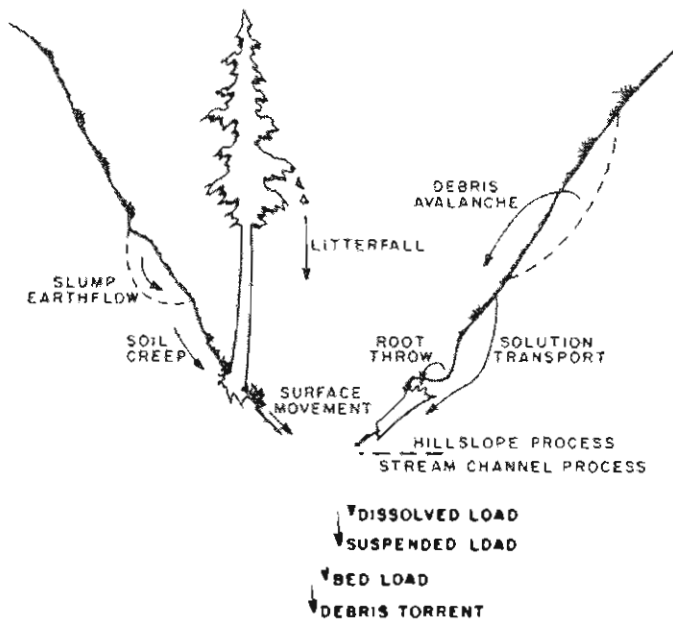


FIGURE 8.1 Processes that transfer organic and inorganic material in a steep forest watershed ecosystem.

or breakage, litterfall to the forest floor or stream. In steep terrain, downhill lean of large trees and canopy closure over small streams result in a net downslope displacement of organic matter.

Surface erosion is the particle-by-particle transfer of material over the ground surface by overland flow, raindrop impact, and ice- and snow-induced particle movement and dry ravel, which occurs during dry periods (Anderson et al. 1959). *Creep* is here considered "continuous" creep (Terzaghi 1950); that is, slow, downslope deformation of soil and weathered bedrock. This is a more restrictive definition than that applied by Leopold et al. (1964) and others who include root throw, needle ice, and other processes as part of creep. *Root throw* occurs as movement of organic and inorganic matter by the uprooting and downhill sliding of trees. *Debris avalanches* are rapid, shallow (generally one- to two-meter soil depth) soil mass movements. *Slump and earthflow* are slow, deep-seated (generally five- to ten-meter depth to failure plane) rotational (slump) and translational (earthflow) displacements of soil, rock, and covering vegetation.

ROOTING PROCESSES

Dietrich ET AL., 1987

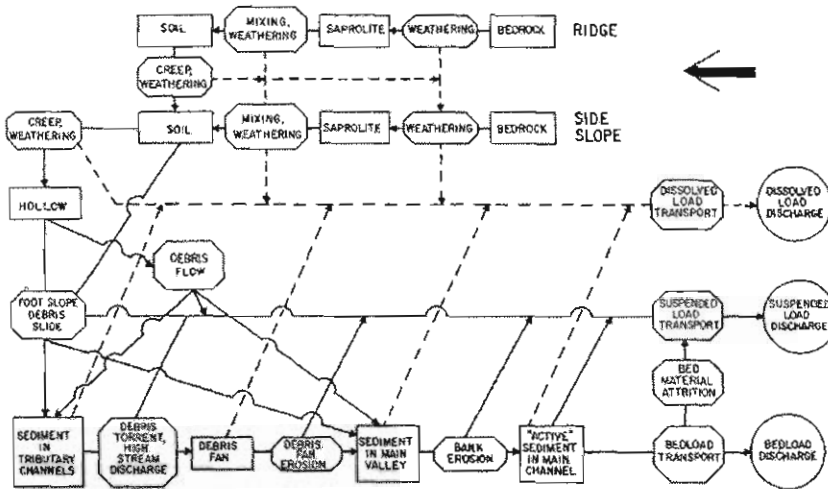


Figure 2—Sediment-budget model for the Rock Creek basin, central coastal Oregon: rectangles, storage sites; octagonals, transfer processes; circles, outputs; solid lines, transfer of sediment; and dotted lines, migration of solutes (from Dietrich and Dunne 1978).

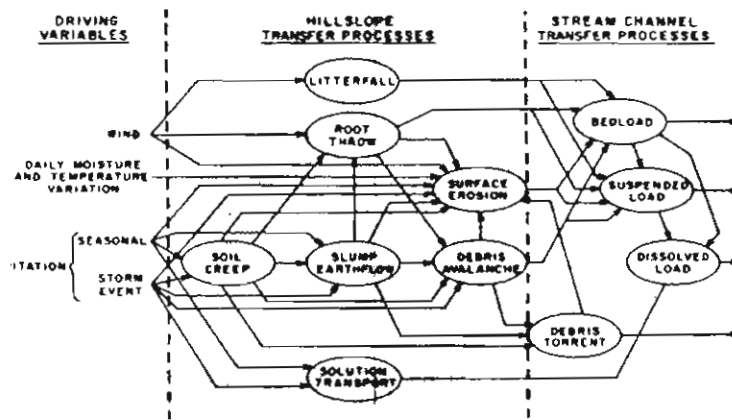


FIGURE 8.2 Relations among mass transfer processes and principal driving variables. Arrows indicate that one process influences another by supplying material for transfer or creating instability that culminates in the occurrence of the second process.

Swanson ET AL., 1982

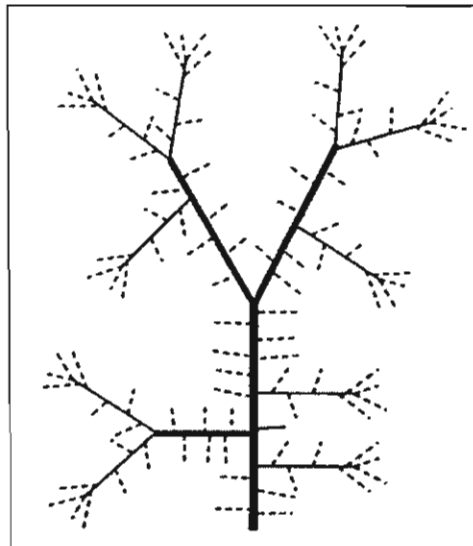
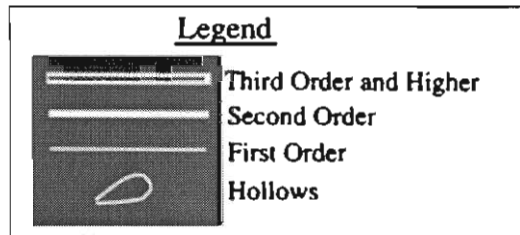
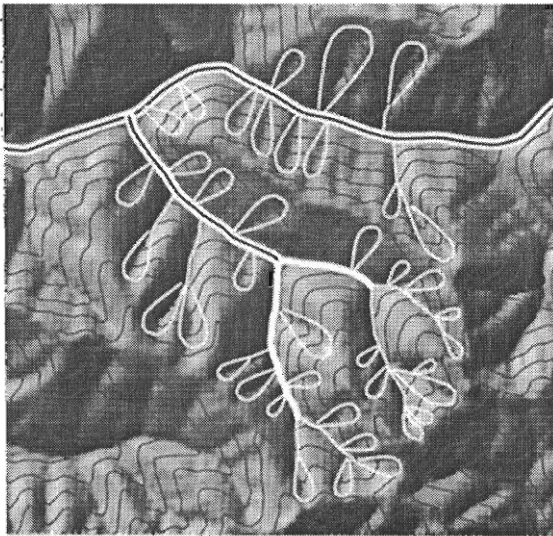


Figure 2. (a) Topographic contours and shaded relief showing the bedrock hollow-channel network structure up to third-order in the central Oregon Coast Range (OCR). Landslides in hollows trigger debris flows in first- and second-order channels, which deliver sediment to third- and higher-order valley floors. In addition, some bedrock hollows are located adjacent to third- and higher-order channels. First- and second-order channels comprise about 90% of all channel length in the region. (b) Schematic diagram of the structure of the hollow-channel network in an average 1-km² area containing a third-order stream (thickest line), three second-order channels (medium lines), 10 first-order channels (finest lines) and 100 hollows (dashed lines).

years B.P.) of colluvial wedges in the upper parts of nine bedrock hollows to indicate a change in the mid-Holocene climate of the OCR that favored landsliding. *Personius et al.* [1993] established an age of 9000–11,000 years B.P. for an alluvial terrace throughout the central OCR, implying a region-wide evacuation of colluvium from bedrock hollows, presumably brought about by climate change during the Pleistocene-Holocene transition. *Benda and Dunne* [1987] interpreted four basal radiocarbon dates (1600–9500 years B.P.) collected at recent landslide scars in the lower parts of hollows to represent the time necessary to refill landslide scars with colluvium to the point of failure in an unchanging climate. This proposal was not meant to deny the possible role of climatic change but only to admit ignorance in the face of sparse data. *Dunne* [1991] suggested a reconciliation of the differing interpretations of colluvium ages from the upper and lower parts of hollows with a simulation model which suggested that under a steady climate colluvium becomes unstable more frequently in the lower portion of a hollow than in the upper part. Evacuation of the latter may require changes of climate and fire regime of the magnitude proposed by *Reneau and Dietrich* [1990] and *Personius et al.* [1993].

3. Climate and Vegetation History

The application of our simulation model to the central OCR is based on the hypothesis that climate of the region has not changed for at least 3000 years. This hypothesis is based on studies of plant pollen assemblages in western Washington State by *Heusser* [1974, 1977], *Barnosky* [1981], *Leopold et al.* [1982], and *Cwynar* [1987], and in western Oregon by *Worona and Whitlock* [1995], indicating that a climate similar to the present one has existed in the OCR for the past 3000–6000 years. *Long's* [1995] study of pollen and charcoal profiles in a small lake in the OCR suggests no change in fire frequency over at least the past 2000 years, even through the Little Ice Age. The principal reason for climatic stability throughout the mid- to late Holocene in the Pacific Northwest is the moderating influence of the Pacific Ocean and the semipermanence of the north Pacific subtropical high and the Aleutian low that largely control the Pacific coast climate [*Johnson*, 1976].

During the mid- to late Holocene, the humid mountain landscape of the central OCR has been forested predominantly by Douglas fir (*Pseudotsuga menziesii*) and western hemlock (*Tsuga heterophylla*) [*Franklin and Dryness*, 1973] under a climate of rainy winters ($\approx 2200 \text{ mm yr}^{-1}$) and dry summers. Wildfires infrequently kill large areas of trees (Figure 3) [*Teensma et al.*, 1991; *Agee*, 1993] and control the distribution of forest ages, which range up to more than 200 years [*Andrews and Cowlin*, 1934].

4. Stochastic Model of Sediment Supply to a Channel Network

This paper describes a stochastic model for interpreting the roles of temporal and spatial factors that control the sediment influx to channel networks through landsliding and debris flow at the scale of a 215-km² watershed over thousands of years. We begin by positing a landscape of bedrock hollows linked to a network of channels (Figure 2); the axes of the hollows have probability distributions of gradients and colluvium depths, which are independent of one another as the model begins. Each year, colluvium accumulates in each hollow at rates

D. G. M. C. A. R., 1982

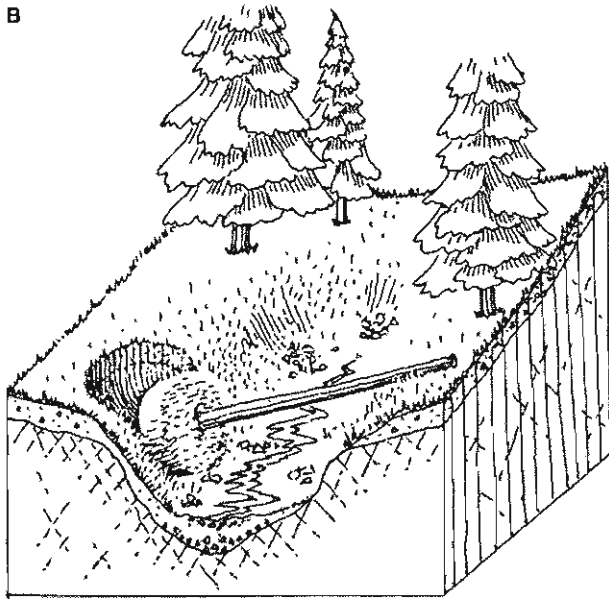
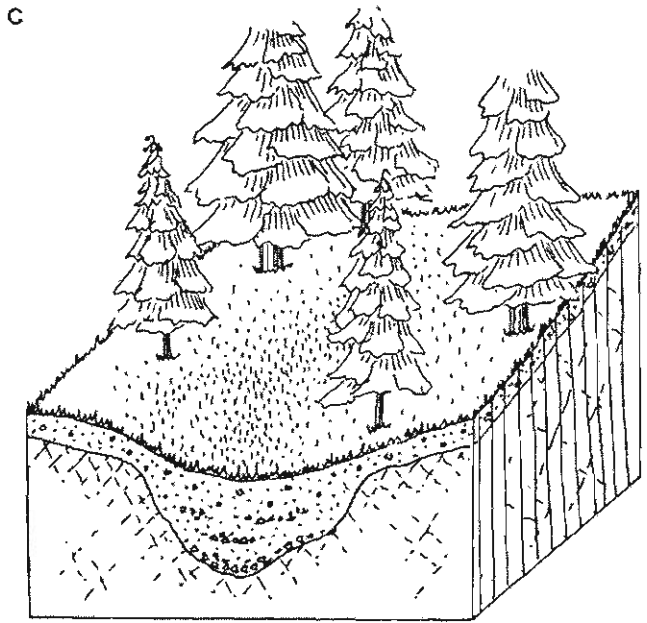
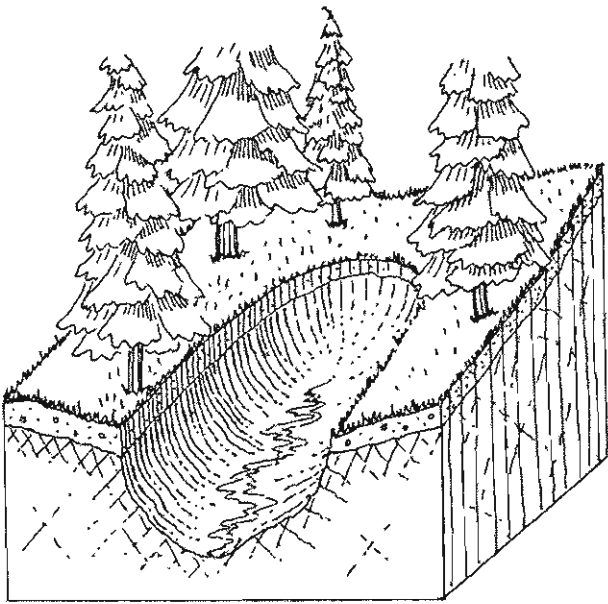


Figure 5—Evolution from a landslide scar in a bedrock depression to a soil wedge. After the landslide, the exposed bedrock surface forms an impermeable horizon shedding rainwater and subsurface discharge into the depression as overland flow. B. Sediment eroded from the over-steepened soil perimeter into the depression is washed of its fine component, leaving a gravel-lag deposit covering the rock surface. C. Continued deposition leads to less frequent saturation overland flow and less surface transport. Eventually, the lack of surface wash causes the soil near the surface of the soil wedge to become similar in texture to surrounding soil from which it is derived.

1997

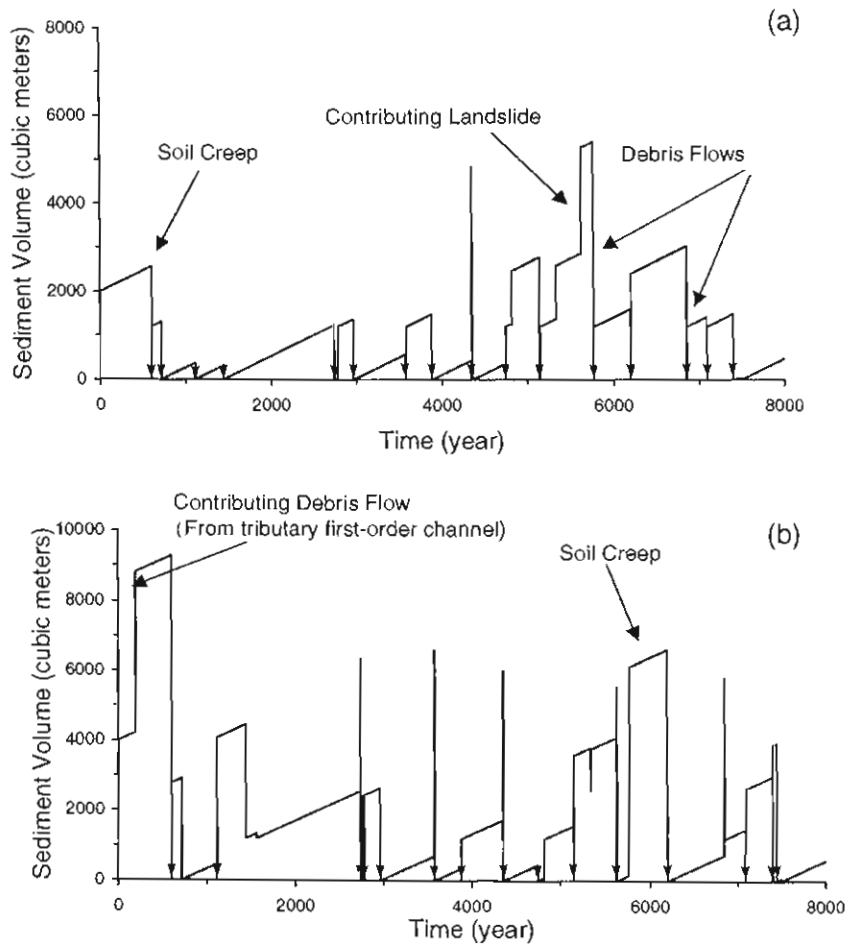


Figure 8. (a) Predicted time series of sediment stored in a typical first-order channel over a period of 8000 years. Instantaneous decreases to zero in sediment storage (downward pointing arrows) represent debris flows triggered by landslides in bedrock hollows (a process controlled by hollow-channel network topology). Gradual increases (sloping lines) in sediment storage are the net result of soil creep and fluvial erosion. Abrupt increases in sediment storage of 1200 m³ are caused by landslides that contribute sediment to the channel. (b) Predicted time series of sediment stored in a typical second-order channel over a period of 8000 years. Processes of debris flow scour, soil creep, and landslides are similar to those in first-order channels (Figure 8a). The larger (>1200 m³) increases in sediment storage in Figure 8b are the result of debris flows that scour sediment from a first-order tributary and deposit it in the second-order channel. Both accumulation of landslide debris and scouring by a debris flow occur in the reach in some years, resulting in sharp spikes in storage or decreases that appear to not go to zero. Not all scouring debris flows are shown; some arrows represent multiple debris flows closely spaced in time, particularly in the second-order channel.

basin of 3 km² the frequency of landsliding increases to about once every 200 years (range: 100–1000 years), and the magnitude of pulses of sliding increases to 1–13 slides per fire episode (Figure 12a). As basin size increases to 25 km², the frequency of landsliding increases to once every 50–100 years (ranging from a few years to a few centuries), and the magnitude of landsliding increases to 5–165 slides per fire episode (Figure 12b). At a drainage area of 215 km² (Figure 12c) the frequency of landsliding in the watershed increases to almost once per decade and the number of landslides during fire episodes increases to 10–550.

Approximately 90% of landslides predicted by the model follow wildfires when root strength is reduced, and hence although slides may be distributed widely after a particularly large storm, they typically clump persistently for some years

within a fire boundary (Figures 3 and 6). Only a small portion of all landslides are triggered by rainstorms alone because the likelihood of creating the necessary thick colluvial wedges (approximately >1.5 m) that would fail under intact forest canopy is small when the average interarrival time of forest-replacing fires is 250 years and the time required to create colluvium thicker than 1.5 m exceeds 2500 years.

The model predictions of frequency and magnitude of landsliding illustrate some relationships between disturbance frequency and size and basin area. In this case the dominant disturbance is stand-replacing fires, and the secondary disturbance is a rainstorm. If the basin area is smaller than or equal to the size of most fires (such as in the case of the 3 km² basin in Figure 12a), then frequency of landslide episodes is similar to the frequency of fires. If the basin is larger than commonly

37

Bewick & Cowog, 1990

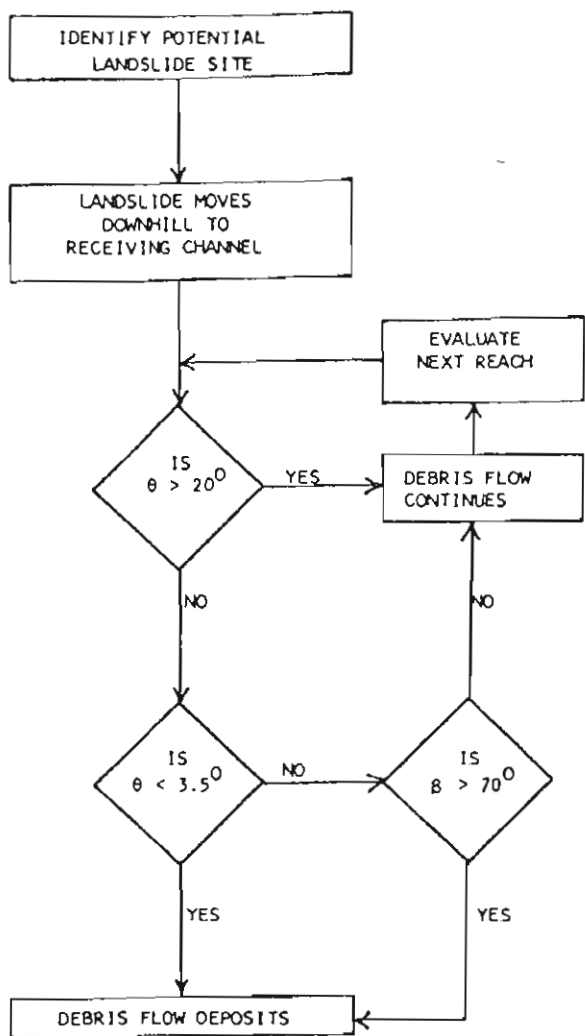


FIG. 6. Flow chart for predicting deposition of debris flows.

is shown in Fig. 5. The data in Fig. 5 include debris flows 1-7 used in the slope analysis and seven other debris flows (8-14, Table 2), which deposited on channel gradients greater than 3.5° at second- to third-order junctions with angles greater than 70°. Therefore, a channel-junction angle of greater than 70° predicted deposition at these sites (Fig. 5). In most cases of deposition at a channel junction, at least part of the deposit extended downstream between 50 and 150 m. The importance of junctions in causing deposition was shown in previous work (Swanson and Lienkaemper 1978).

A flow chart for the empirical model to predict debris-flow deposition is shown in Fig. 6. Analysis begins by identifying the location of a potential landslide site; this is done independently of the debris flow analysis; for example, by the method of Burroughs (1984).

Next, the gradient of the receiving channel is evaluated. In the study area some hollows intersect steep first-order channels at angles greater than 70°. Landslides originating from these hollows may temporarily deposit in the channel; subsequent failure of this material may initiate a debris flow. This form of initiation was not observed in this study; however, it is included in the model for completeness. The minimum slope necessary for failure of landslide debris in a

TABLE 3. Observed and predicted travel distances for debris flows measured on air photos

Debris flow	Approximate travel distance (m)	Predicted travel distance (m)
Knowles Creek		
30	240	240
31	380	380
32	220	220
33	360	360
34	600	600
35	890	890
36	480	480
37	620	620
38	240	240
39	960	960
40	840	840
41	910	910
42	1300	1300
43	1200	1200
44	1000	1000
basalt basins		
B1	360	960
B2	1100	1100
B3	720	720
B4	550	550
B5	840	840
B6	1130	1130
B7	288	288
B8	760	760
B9	1130	1130
B10	760	760
B11	1050	1050
B12	840	840
B13	890	890
B14	290	290
B15	780	780
B16	1080	1080
B17	550	550
B18	430	2300
B19	960	960
B20	920	920
B21	1080	1080
B22	550	550
B23	770	770
B24	1560	1560
B25	840	1320
B26	600	600
B27	550	550
B28	630	630
B29	670	670

channel was estimated from an infinite-slope analysis (Sidle *et al.* 1985). Soil was assumed cohesionless because of the breakup of the soil and its reinforcing network of roots following the initial landslide; saturation was also assumed. Using an effective angle of internal friction of 38° and a saturated unit weight of 1.9 g/cm³ (Schroeder and Alto 1983), we estimated that a slope of 20° caused failure of landslide debris in first-order channels.

Following the evaluation of steep channels ($\theta > 20^\circ$), subsequent reaches are evaluated until either a channel gradient of less than 3.5° or a junction angle of greater than 70° is encountered. When either of these criteria are satisfied, deposition is predicted. When a contour interval contains

DIRECT OF AL., 1982

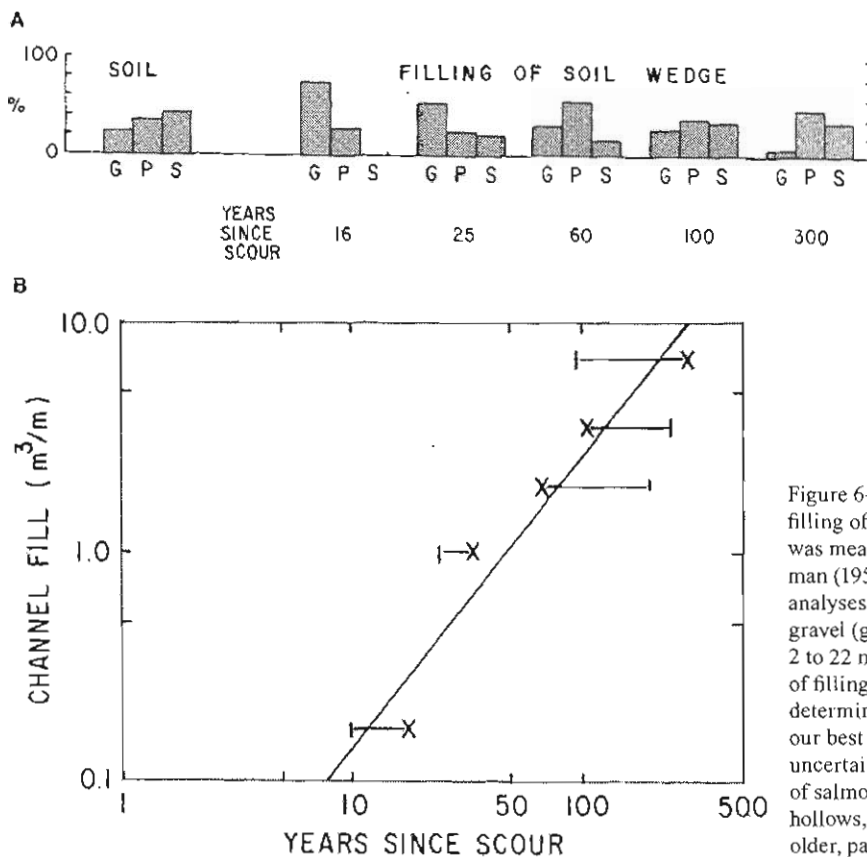


Figure 6—A. Successive fining of material during filling of hollows. The fraction greater than 22 mm was measured by the pebble-count method of Wolman (1954), and the data were combined with sieve analyses of the finer particles. The letters indicate gravel (g) (greater than 22 mm), pebbles (p) (from 2 to 22 mm) and sand (s) (less than 2 mm). B. Rate of filling of scoured hollows. Time of scour was determined by ages of vegetation on fills. (X) is our best estimate, error bar represents the range of uncertainty in our estimate. Vegetation consisted of salmonberry and alder on more recently sourced hollows, and large alder, hemlock, and Douglas-fir on older, partially filled hollows.

the texture of the upper layer of the wedge is similar to that of the surrounding soil. As the scar fills, sediment discharge from the wedge decreases. The scar may fill completely so that no topographic expression remains, or it may fail during a large storm that occurs as it is filling. During accumulation, sediment discharge from the wedge must be less than prefailure levels. When the filling is complete or when an equilibrium depth is reached that balances the influx and discharge of soil, the latter attains its prefailure rate (fig. 7).

The time required to refill a depression can be estimated by computing a creep discharge rate into the slide scar across its exposed perimeter. For example, a creep rate of 3 mm/year in a 50-cm-thick soil will refill a bedrock depression 5 m wide, 20 m long, and 2 m deep in 3,000 years. This estimate represents a minimum because much of the initial soil discharge into the exposed hollow will be washed out. An increase in the frequency of failure because of a climatic change or management activity would accelerate soil movement towards the scar and thin the surrounding soil over periods of hundreds to thousands of years. Debris-slide scars then probably fill between 1,000 and 10,000 years after initial failure. Although transport into the scar will be accelerated by the sloughing of soil and gullyng of exposed soil, the ultimate transport rate into the scar will be limited by the supply of soil and the rate of soil transport toward the location of failure.

On the short time scale for which a quantitative sediment budget might be developed from a monitoring program, debris-slide scars will generally be sources of high sediment discharge. That the period of increased erosion extends for a long time after the slide occurs is well illustrated by Tanaka's (1976) measurements in the Tanzawa Mountains of Japan. His repeated topographic surveys showed rates of sediment discharge from 50-year-old debris scars to be about 100 times greater than the estimated undisturbed rate of sediment discharge from hillslopes. Lundgren (1978) has also reported that in the subhumid mountains of Tanzania, erosion during a 7-year period after formation of landslide scars was as great as the initial loss from the landslides.

If debris slides lead to accelerated weathering of the underlying bedrock during exposure and burial, or if they cause loss of debris from the weathered bedrock in the scar or its surroundings, then a component of their discharge can be defined as a contribution to the sediment budget separate from creep and biogenic transport. Otherwise, debris slides emanating from the soil mantle act more as periodic fluctuations in the rate of discharge of sediment from the hillslope by soil creep and biogenic transport.

1996-1997 Oregon Storm Event

Hoffmeister 15 Ar, 2002

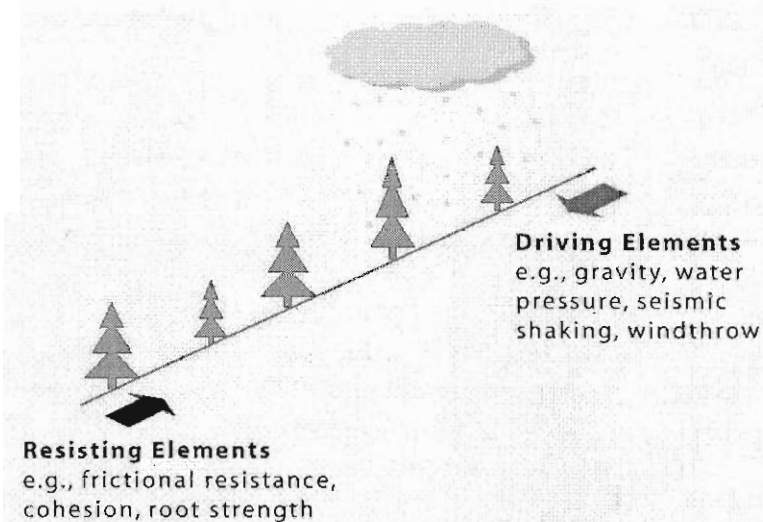


Figure 10. Schematic of a slope, showing driving and resisting elements.

focused on evaluating relationships between storm characteristics and debris flow occurrences (e.g., Campbell, 1975; Crozier and Eyles, 1980; Keefer and others, 1987; Cannon, 1988; Wiczorek and Sarmiento, 1988; Wilson

and Wiczorek, 1995; Wilson, 1997; Wiley, 2000). Several of these studies have focused specifically on identifying rainfall thresholds above which landslides (and particularly debris flows) become significantly more widespread and numerous (Keefer and others, 1987; Wilson and Wiczorek, 1995; Wilson, 1997; Wiley, 2000).

One rainfall threshold study that used storm data specifically from the Pacific Northwest was reported by Wiley (2000). This study included evaluations of climatic data in comparison with landslide occurrences recorded for the period of

February 1996 through January 1997 and indicated that widespread landslide activity in steep terrain throughout western Oregon is likely to be triggered by rainfall intensity/duration combinations of (a) 40

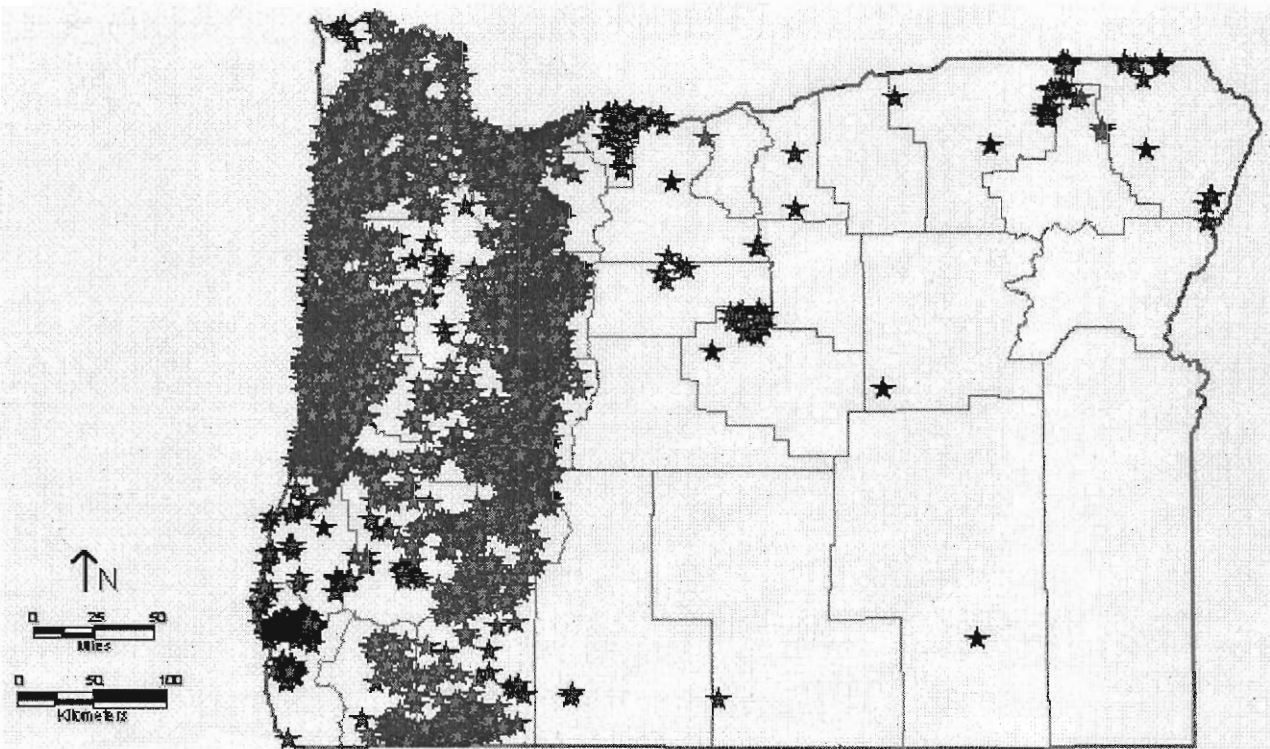


Figure 11. Distribution of the more than 9,500 landslides triggered in Oregon by the storms of 1996-97. (From Hofmeister, 2000)

ROBINSON ET AL., 1999

interval greater than 100 years while the peak flow on the Wilson River (the next major river basin to the south) corresponded with a 25 year recurrence interval flood (Laenen et al., 1997). In the Oregon Cascades, peak flow on the Sandy River near Marmot corresponded with a recurrence interval greater than a 100 year flood while the nearby Hood River experienced a 10-15 year flood (Laenen et al., 1997).

November Storm

The November 1996 storm was a shorter duration and higher intensity rainfall event than the February storm. Since the November 1996 storm occurred early in the season, predominately at lower elevations in Oregon's Willamette Valley and southern Coast Range, it lacked a rain-on-snow component. Since it occurred in the fall it also lacked significant antecedent precipitation. Therefore, soil moisture levels prior to the storm event were relatively low. However, all-time, one-day precipitation records were set at many locations (Table 1).

In addition, the following comments by George Taylor (State Climatologist) characterize the storm:

"Daily and monthly records were set at many sites as well. At Portland Airport, 3.86 inches was recorded between 4 p.m. on the 18th and 4 p.m. on the 19th. This broke the November 24-hour total of 2.82 inches, which was set November 10-11, 1995. Rainfall intensities for some areas in the Willamette Valley and Coast Range were calculated as a 100-year return period. While rainfall amounts were high as were stream flows throughout the Willamette Valley, highest impacts in terms of landslides and debris flows were reported in Douglas and Coos counties."

Table 1. One-day precipitation records for selected stations.

Location	1996 Amount (in.)	Date Records Began	Old Record	Year Old Record Set (in.)
Corvallis	4.45	1889	4.28	1965
North Bend	6.67	1931	5.60	1981
Portland	2.70	1939	2.48	1948
Redmond	2.38	1948	1.81	1969
Roseburg	4.35	1931	3.28	1965

There is tremendous spatial variability in timing and intensity of rainfall events for any given storm. For example, two gages in the Oregon Coast were compared to determine if two gages recorded similar precipitation intensities during the same rainfall events (Surfleet, 1997). The two gages were at a similar elevation, a similar distance from coast and within 10 miles from each other. The two gages recorded markedly different storm intensities during significant rainfall events from 1989-1995. The precipitation timing and intensities were disparate enough to suggest that for the highest storm events at one gage the nearby gage was not experiencing a storm event. For example, 31 of the 33 top storms at one gage were not identifiable as one of the top ten storms at the second gage. The combination of variation in storm characteristics (precipitation and flood levels) and

42

Table 2. Studies of comparative landslide ("L.S.") densities and erosion rates in recently harvested forests versus unharvested mature forests.

Reference	Site	Measurement Type*	Recently Harvested Ratio L.S. Density	Ratio L.S. Erosion	Road Right of Way Ratio L.S. Density	Ratio L.S. Erosion
Amaranthus, et al., 1985	Siskiyou Mtn., Oregon	Air	19.0	6.8	138.0	111.0
Bishop and Stevens, 1964	S.E. Alaska, Maybeso Cr.	Air	19.5	NA	NA	NA
Bush et al., 1997	Oregon Coast Range	Air/Size	2.6	NA	31.6	NA
Chesney, 1982	Oregon Cascades, 1949	Air/Field Visit	0.0	NA	11.1	NA
	Oregon Cascades, 1959	Air/Field Visit	3.7	NA	33.3	NA
	Oregon Cascades, 1967	Air/Field Visit	12.9	NA	208.0	NA
	Oregon Cascades, 1972	Air/Field Visit	21.8	NA	705.0	NA
	Oregon Cascades, 1979	Air/Field Visit	4.7	NA	254.0	NA
Dyness, 1967	Oregon Cascades, H.J. Andrews	Air/Size	9.8	5.0	309.0	60.1
Fiksdal, 1974	Olympic Pen. Washington, Sequaleho Cr.	Air/Field Visit	0.0	0.0	1600.0	224.0
Gresswell et al. 1979	Oregon Coast Range, Mapleton Area	Air/Field Visit	23.5	NA	72.2	NA
Hicks, 1982	Oregon Cascades, Middle Santiam	Air/Field Visit	3.6	3.4	73.7	95.3
Hughes and Edwards, 1978	Oregon Cascades, Umpqua basin	Ground	8.0	10.0	NA	NA
Johnson, 1991	Washington Cascades; S Fk. Canyon Cr.	Mixed	5.3	NA	97.0	NA
Ketcheson and Froehlich, 1978	Oregon Coast Range, Mapleton Area	Ground	2.2	3.4	NA	NA
Lyons, 1982	Oregon Cascades, 1959-67	Air/Field Visit	22.8	29.5	NA	NA
	Oregon Cascades, 1967-72	Air/Field Visit	6.8	10.0	NA	NA
Marion, 1981	Oregon Cascades, Blue River	Air/Field Visit	10.0	9.0	106.0	44.0
McHugh, 1987	S.W. Oregon	Air/Field Visit	7.0	NA	48.0	NA
Morrison, 1975	Oregon Cascades, Alder Creek	Air/Size	13.5	2.6	415.0	343.0

NA = Not available

ROBINSON
5/22/99
1999

42A

Table 2 (Continued). Studies of comparative landslide densities and erosion rates in recently harvested forests versus unharvested mature forests.

Reference	Site	Measure- ment Type*	Recently Harvested		Road Right of Way	
			Ratio L.S. Density	Ratio L.S. Erosion	Ratio L.S. Density	Ratio L.S. Erosion
Robison et al., 1999 (This	Oregon Cascades, near Vida	Ground	1.4	3.2	2.7	40.9
	Oregon Coast Range, Elk Creek	Ground	0.8	0.3	1.0	0.8
	Oregon Coast Range, Mapleton	Ground	1.9	1.5	5.0	13.6
	Oregon Coast Range, Scottsburg	Ground	5.2	2.6	NA	NA
Rood, 1984	British Columbia; Graham and Moresby Island	Air	30.0	31.2	76.7	89.7
Schroeder and Brown, 1984	Oregon Coast Range, Palouse Cr.	Air	9.6	NA	NA	NA
	Oregon Coast Range; Larson Cr.	Air	6.1	NA	NA	NA
Schwab, 1983	British Columbia, Queen Charlotte Islands	Mixed	17.0	5.0	41.0	46.0
Smith, 1996	Oregon Cascades; Weak Rock, Steep Slopes	Air	10.7	NA	NA	NA
Swanson and Dyrness, 1975	Oregon Cascades, H.J. Andrews Unstable	Mixed	3.2	2.8	33.0	30.0
Swanson and Grant, 1982	Oregon Cascades, WNF Mod. Stable	Mixed	3.0	2.5	47.0	37.0
	Oregon Cascades, WNF Unstable	Mixed	7.0	5.0	336.0	250.0
Swanson et al., 1977	Oregon Coast Range, Cedar Cr.	Mixed	1.2	NA	15.0	NA
	Oregon Coast Range, Soil Type 47	Mixed	1.3	4.0	15.5	30.8
Swanson and Swanson, 1976	S.W. British Columbia Coast Range	Air/Size	5.0	2.2	20.0	25.2

*Measurement types: 1. "Air" - A study based on air photos with our without ground verification regarding the size of landslides and whether the feature was a landslide. 2. "Air/Size" - A study based on air-photos with a minimum landslide size used to decrease the chance of bias between old and young stands. 3. "Mixed" - Studies that combine more than one method of detection. For instance, one study used air-photos to detect landslides in clearcuts and a ground-based sample in older forests. 4. "Air/Field Visit" - An air based sample with non-systematic field visits used to get some inclinations that most landslides are being found. 5. "Ground" - studies that detect landslides based on a systematic sampling of landslides using the channel network and/or the slope contours as a search path.

Robison
et al.,
1999

42B

Table 8. General summary of landslides for core area portions of the eight study areas (core study area refers to that subset of each study area surveyed in which all stream channels were systematically checked for delivering landslides).

	Red zone Study Areas								Random Study Areas			
	Elk	Scottsburg	Mapleton	Tillamook	Vida	Vernonia	Dallas	Estacada	All			
Core-study area (sq/mile)	6.5	7.2	8.3	4.5	7.1	3.4	3.1	5.5	45.8			
Landslides												
Active Road	2	5	13	7	6	2	2	0	37			
Old Road	5	6	1	5	0	1	2	0	20			
Non-road	152	78	92	50	53	16	6	2	449			
Total	159	89	106	62	59	19	10	2	506			
Landslide Erosion												
Active Road (yd ³)	1261	11544	4243	31603	14892	1240	167	0	64951			
Old Road (yd ³)	2434	7654	191	8877	0	25	35501	0	54683			
Non-road (yd ³)	49898	43628	17442	34014	14357	868	8516	20	168743			
Total (yd ³)	53593	62826	21876	74495	29249	2133	44184	20	288376			
Landslide Densities												
Total Slides (per sq. mi.)	24.4	12.3	12.8	13.8	8.3	5.5	3.2	0.4	11.1			
#Non-road slides (per sq.mi.)	23.3	10.8	11.1	11.1	7.4	4.7	1.9	0.4	9.8			
Landslide Erosion Rate												
Non-road slides (yd ³ /ac)	12.0	9.5	3.3	11.8	3.1	0.4	4.2	0.01	5.8			
All slides (yd ³ /ac)	12.8	13.6	4.1	25.9	6.4	1.0	22.0	0.01	9.9			

Table 9. Landslides identified outside of the core study areas. Streams were not systematically surveyed for landslides in these areas. This table shows only those landslides that directly influenced channels in the core areas.

Landslide Category	Redzone Study Areas								Random Study Areas				Total
	Elk	Scottsburg	Mapleton	Tillamook	Vida	Vernonia	Dallas	Estacada	All Sites				
Active Road	NA	NA	0	3	18	0	0	NA	21				
Old Road	NA	NA	0	2	1	1	0	NA	4				
Non-road	NA	NA	3	5	14	0	5	NA	27				
Total	NA	NA	3	10	33	1	5	NA	52				

ROBISON ET AL., 1999

42C

2013.500 ET AL., 1999

Table 10. Characteristics of landslides within the core study areas.

Landslide Density	Red zone Study Areas					Ranciom Study Areas				Total All Sites
	Elk	Scotts- burg	Mapleton	Tillamook	Vida	Vernonia	Dallas	Estacada		
# Non-road related Slides	152	78	92	50	53	16	6	2	449	
Area surveyed (sq. mi)	6.52	7.21	8.29	4.49	7.14	3.44	3.14	5.49	45.7	
#Non-road slides (per sq.mi.)	23.3	10.8	11.1	11.1	7.4	4.7	1.9	0.4	9.8*	
Landslide Characteristics										
Average Width (ft)	22.3	29.7	15.1	36.4	18.1	23.0	62.0	13.0	24.0	
Average Length (ft)	34.6	44.6	24.5	30.6	32.2	24.9	44.2	21.5	43.1	
Average Area (acres)	0.020	0.035	0.010	0.046	0.015	0.015	0.076	0.006	0.023	
Average Depth (ft)	1.9	3.3	2.1	2.4	2.7	2.1	2.9	0.6	2.5	
Maximum Depth (ft)	3.5	5.5	3.6	4.5	4.6	3.9	5.0	2.3	4.3	
Landslide Average Volume (yd ³)	58	216	26	274	74	49	340	5	109	
Average Total Volume (including debris flow) (yd ³)	328	559	190	680	271	54	1419	10	376	
Erosion (yd ³ /acre.)	12.0	9.5	3.3	11.8	3.1	0.4	4.2	0.01	5.8	

*Average

1996
Silvery
Erosion

42D

FORSON, ET AL., 1999

1996
storm
events

Table 11. Landslide occurrence by origin of occurrence and by study area geology.

Origin	Slides (No.)	Avg. Slope Blw. L.S. (%)	Depth Avg. (ft)	Landslide Characteristics			
				Initial L.S. Avg. Vol. (cu. yd.)	Initial L.S. Med. Vol. (cu. yd.)	Total L.S.* Avg. Vol. (cu. yd.)	Total L.S.* Med. Vol. (cu. yd.)
Red zone Tye Sandstone Geology Study Areas (Elk Cr., Mapleton Scottsburg)							
Up-slope	239	82	2.5	104	36	446	174
Channel Adj.	82	91	1.9	41	46	55	17
Gully	1	55	0	0	0	4	4
Red zone Igneous Geology Study Areas (Tillamook, Vida)							
Up-slope	50	86	2.9	116	25	702	171
Channel Adj.	51	92	3.2	231	53	253	53
Gully	2	56	0	0	0	163	163
Stratified randomly Selected Study Sites (Dallas, Estacada, Vernonia)							
Up-slope	6	78	2.9	341	82	1434	142
Channel Adj.	18	93	2	44	17	44	17
Gully	0	NA	NA	NA	NA	NA	NA
All Study Sites							
Up-slope	295	83	2.5	111	36	509	171
Channel Adj.	151	92	2.3	105	24	120	25
Gully	3	56	0	0	0	110	61

The channel adjacent landslides occurred on steeper slopes than did the up-slope landslides (92% versus 83% steepness). Steepness is measured as rise (vertical distance) over run (horizontal distance) from the top of the landslide scarp downslope over the "reconstructed" (prior to the landslide) ground surface. Field crews were careful to try to measure slope on the initial landslide surface, based on the landslide depth measurements. Failure to do this can lead to overestimation of the pre-landslide slope steepness (which is a critical parameter for determination of landslide hazard). Note that slope percent and slope degrees are very different. A slope of 100% is equal to 45 degrees. The up-slope landslides originated on average slopes of 82% in the Tye red zone study areas, 86% on the igneous red zone study areas, and 78% on the non red zone study areas; however, there were only six up-slope landslides in the stratified random study areas. Average slope steepness for the channel adjacent landslides was similar across all study zone types (91% to 93%).

Initial median landslide volumes for the Tye and igneous study areas are similar (up-slope volume of 36 yards in the Tye and 25 yards in the igneous, with channel adjacent volume of 46 and 53 cubic yards respectively). However, mean initial volumes are very different. In the Tye study areas, up-slope landslides averaged 104 cubic yards while channel adjacent landslides averaged 41 cubic yards. In the red zone igneous study areas, the channel adjacent landslides were larger than the up-slope landslides (231 cubic yards compared to 116 cubic yards). However, after including debris flow volumes, up-slope

42E

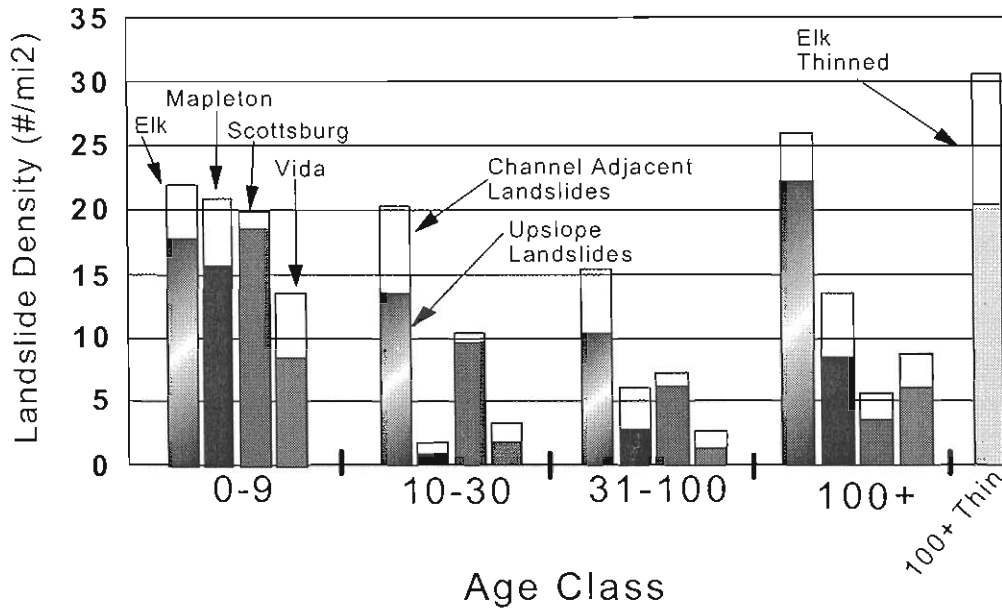


Figure 28. Stacked bar graph of landslide density for upslope and channel adjacent landslides by stand age class for the four red zone study areas.

Landslide erosion volumes are illustrated in Figure 29. In general, this figure indicates there is greater variability in erosion volumes than in landslide densities. Again, the erosion volume is the total volume, including the initial landslide plus the non-channelized debris flow volume. Therefore, the channel adjacent slides (smaller with little or no debris flows) make up only a very small portion of the total landslide erosion.

Landslide erosion volume for the 0 to 9-year class was much more variable than the landslide density, varying between 4 and 17 cubic yards per acre. For the 10 to 30-year age class, it varied between 0.03 and 11 cubic yards per acre, while in the 31 to 100-year class the low value was 0.9 cubic yards per acre and the high value was 6 cubic yards per acre. For the 100-year plus age class, the values ranged between 2 and 18 cubic yards per acre. The aforementioned volumes are for the four red zone sites with good age class distribution (Elk Creek, Scottsburg, Mapleton and Vida). Erosion volumes for the four other sites (Dallas, Vernonia, Estacada and Tillamook) are also compared in Table 14.

percent of mean December rainfall in a 24-hour time period, (b) 25 percent of mean December rainfall in a 12-hour period, or (c) 15 percent of mean December rainfall in a 6-hour period. Figure 12 is a map showing the general magnitude of the 24-hour rainfall thresholds in western Oregon. Storms that produce rainfall in excess of these levels are considered to be particularly prone to triggering dangerous landslides.

Slightly more conservative rainfall-threshold criteria are used by the Oregon Department of Forestry (ODF) for the Oregon Debris Flow Warning System (discussed in the Risk Management Strategies section). Thresholds of 3 in. in 12 hours, 4 in. in 24 hours, 5.5 in. in 36 hours, or 7 in. in 48 hours are used by ODF to issue debris flow advisories for forecast storms. As will be discussed in later sections, a number of important variables affect local debris flow occurrences, and no simple criteria can be used to precisely predict debris flows on a regional scale. Nevertheless, rainfall intensity studies and warning systems are important attempts to save lives by providing advance notice of dangerous storms.

Human Actions

While large storms and other natural

events beyond our control are often the prime triggers of landslides in the Pacific Northwest, human actions resulting in adverse modifications to the natural environment can also be significant factors in causing and/or exacerbating slope instabilities. Many common artificial alterations to topography make slopes more vulnerable to landslides, and it is important to evaluate how human actions affect slope stability over both the short and the long term.

Modifications that alter the internal

DEBRIS-FLOW THRESHOLDS

WESTERN OREGON

- 1-2
- 2-3
- 3-4
- 4-5
- 5-6
- 6-7
- 7-8
- 8-9
- 9-10
- >10

WILEY, 2000

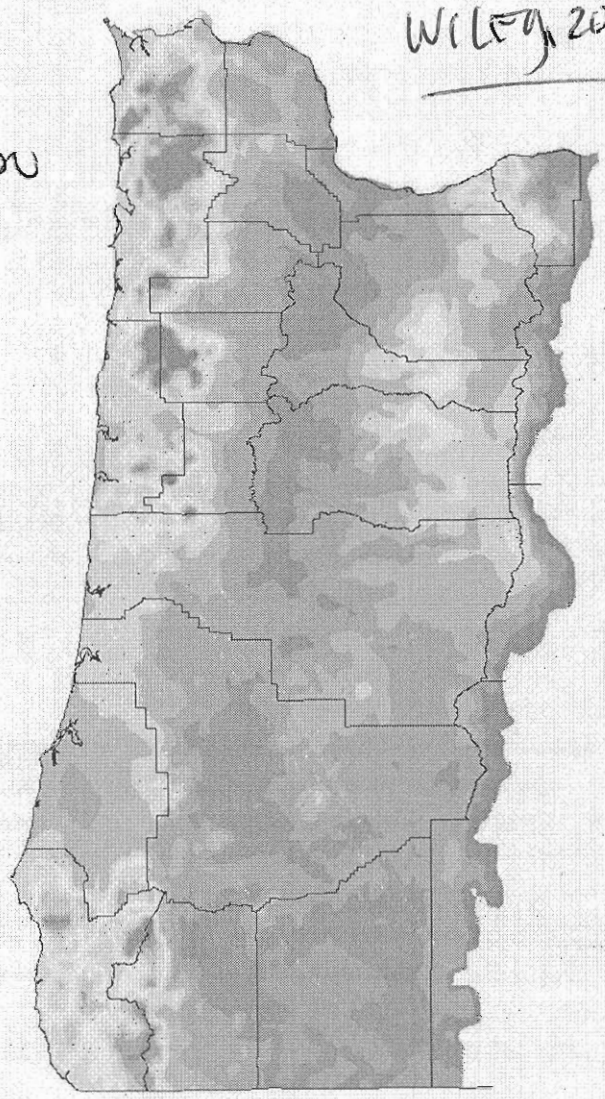


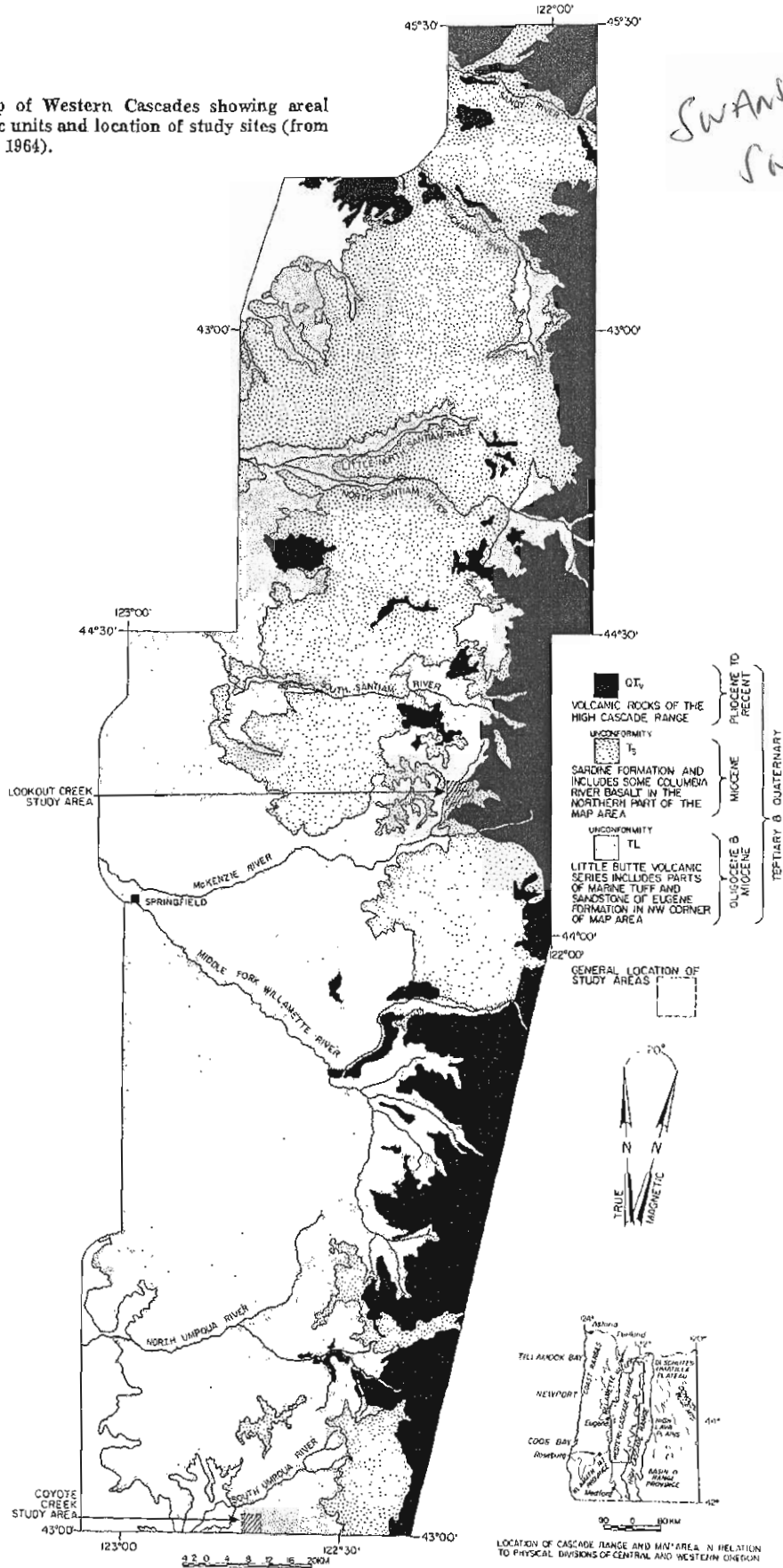
Figure 12. Map of estimated 24-hour rainfall intensity-duration thresholds in western Oregon (measurements in cm). Contours are derived from the Oregon Climate Service data of mean December precipitation. (From Wiley, 2000)

44

Landslide and Debris Flow Occurrence at HJ Andrews

Figure 1. Map of Western Cascades showing areal extent of geologic units and location of study sites (from Peck and others, 1964).

Swanson & Swanson, 1977



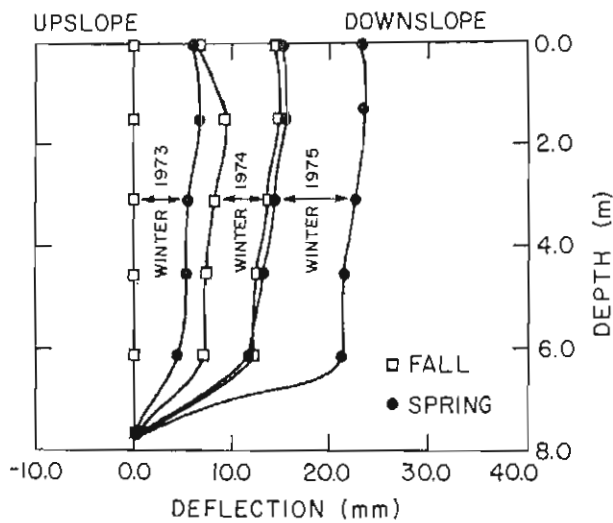


Figure 3. Apparent seasonal deformation along N70°E direction recorded in inclinometer tube installed in complex mass-movement terrain at Coyote Creek. Movement is directly plotted from field data and has not been projected into the plane of maximum deformation (N50°E). Note minor upslope movement of tube during summer of 1974 owing to settlement in hole.

variety of volcanoclastic rocks, but the headwall occurs in an area of capping basalt flows.

The area experiences average annual precipitation of more than 240 cm, falling mainly between October and May. A wet snowpack persists from December through April.

Most of the earthflow terrain is covered with a mixture of old-growth Douglas fir and western red cedar, 300 to 500 yr old, and a stand of the same species that developed following wildfire in the mid-1800s. About 1.5 ha of the forest at the earthflow was clearcut logged in 1968, and an equal area along the lower east side was clearcut in 1961.

The earthflow covers an area of approximately 20 ha on a south-facing valley wall. The flow extends from a rocky headwall at an elevation of 1,010 m downslope 900 m into Lookout Creek at a 790-m elevation (Fig. 4).

Topography on the earthflow surface is very irregular because of earthflow movement and stream erosion processes. Open cracks as much as 1.5 m wide have developed in areas of active tensional or shear deformation. Active crack systems bound major blocks or subunits of the earthflow that are presently undergoing differential movement (Fig. 4). There are also numerous inactive cracks defined by scarps or linear depressions. It appears that differential shear or tensional movement of less than about 1 cm/yr does not produce open, conspicuously active cracks, because litterfall, surface erosion, and growth of vegetation are effective in obscuring fine-scale features of ground breaks.

Drainage patterns on the earthflow are very irregular owing to frequent disruption by earth movement (Fig. 4). In several instances, streams have been channeled along tensional and shear cracks. Discontinued gullies, unusual features in the western Cascades, have developed along restricted stream reaches. Surface-water movement has been altered by the

formation of poorly drained depressions on the uphill side of rotational slump blocks and where drainage has been obscured by fallen trees.

Movement History and Rates

A part of the history of earthflow movement may be learned from geomorphic and dendrochronologic observations, as well as by direct measurement. Various observation methods yield information on the age of the earthflow movement, rate of relative motion between discrete blocks within the earthflow, absolute movement of portions of the earthflow relative to stable reference points, and creep deformation within individual earthflow blocks.

Arrays of 4 to 9 stakes were established on several areas of the earthflow where shear and tensional movement appear to be very active (locations shown in Fig. 4). The stake arrays

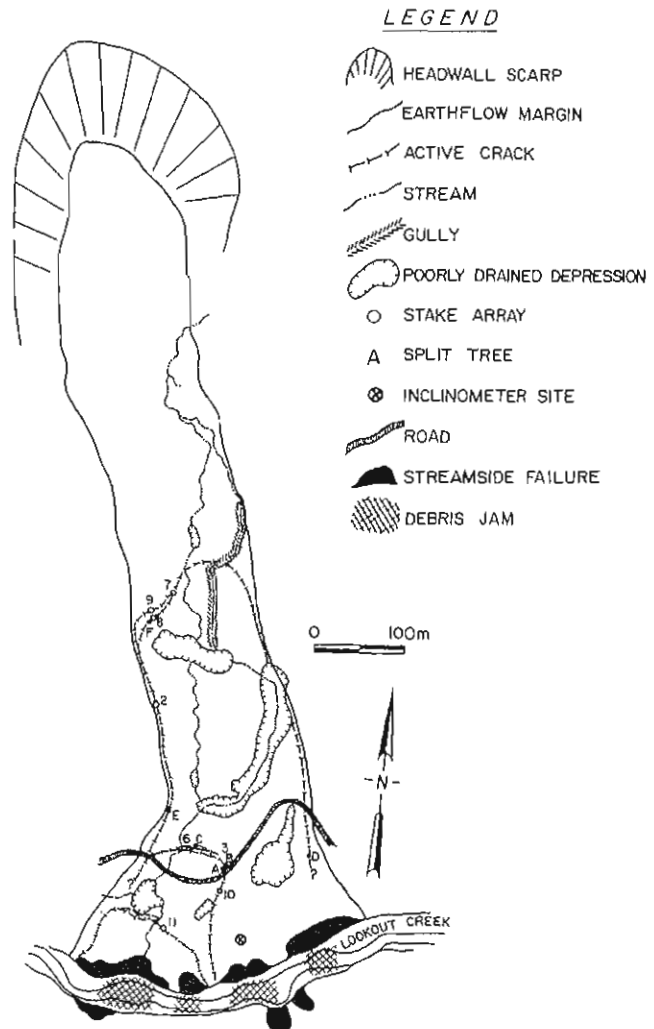


Figure 4. Map of Lookout Creek earthflow. Mapped by G. Lienkaemper using compass and range-finder. See also Tables 2 and 3.

SWANSTON &
Dyrness, 1975

TABLE 1. SUMMARY OF DATA ON SLIDES IN THE H. J. ANDREWS EXPERIMENTAL FOREST, 1950-1974

Land status	Area (X) (km ²)		No. of events	No./km ²	Volume material moved (m ³)	Volume material moved per km (m ³ /km ²)	Slide erosion relative to forested area
<i>Unstable zone (30.8 km²)</i>							
Forest	69.4	21.4	32	1.5	46,600	2,180	x1.0
Clear-cut	25.6	7.9	36	4.6	48,400	6,130	x2.8
Road right-of-way	5.0	1.5	71	47.3	98,200	65,470	x30.0
<i>Stable zone (33.4 km²)</i>							
Forest	85.9	28.7	0	0	0	0	..
Clear-cut	12.3	4.1	0	0	0	0	..
Road right-of-way	1.8	0.6	2	3.3	420	700	..

sidered at comparable levels of development.

We can correct for this difference in road and cutting development by assessing slide erosion on a hypothetical square kilometre of the unstable zone. The data in Table 1 may be used in making this assessment if we assume that the hypothetical area has been entirely clear-cut logged and roaded progressively over the past 25 yr. Assuming that 8 percent of the area was in road right-of-way, there would have been 5,240 m³ of erosion by road-related slides (8 percent of 65,470 m³/km², from Table 1). The 92 percent area that was clear-cut logged would have undergone 5,640 m³ of erosion by slide activity in the clear-cut area (92 percent of 6,130 m³/km²). By these calculations the clear-cut areas would have contributed slightly more than roads to the total erosion by slide activity from the managed site.

The sum of erosion from roads and clear-cuts totals 10,880 m³ over the hypothetical square kilometre of the unstable zone. Assuming that the slide erosion in forested areas (2,180 m³/km², from Table 1) represents the natural background level of slide erosion, management activities result in an increase by 5 times in slide erosion. However, as pointed out in the discussion below, there are several reasons why this assessment cannot be reliably projected to estimate impact of future management activities.

DISCUSSION

Analysis of data collected on the forest reveals an apparent increase in erosion by slides as a result of both logging and road construction. Deforestation of hillslopes

results in a number of changes that may increase the probability of shallow failures of the soil mantle (see general reviews by Gray, 1970, and Swanston, 1970): (1) rooting strength is decreased, lowering the "apparent cohesion" of the soil (Swanston, 1970) and possibly releasing creep-generated stresses in the soil-root complex; (2) transpiration is decreased (Bethlahmy, 1962); and (3) snowmelt runoff may be increased (see, for example, Anderson, 1969; Rothacher and Glacebrook, 1968). These factors have been cited as contributing to a period of increased slide frequency after deforestation, especially between the time of decomposition of root systems of killed trees and establishment of stabilizing roots by incoming vegetation (Bishop and Stevens, 1964; Swanston, 1970; Nakano, 1971, and others). This temporal relationship between deforestation and slide activity has also been observed in the Andrews forest, where most hillslope failures in clear-cut areas occurred in the first 12 yr after cutting.

Since logging began in the unstable zone, the net result of deforestation has been an increase in slide erosion by a factor of 2.8. During the same period, no slides occurred in clear-cut areas in the stable zone. This indicates that on marginally stable sites, the stabilizing effect of vegetation is an important check on erosion but is of little consequence in more stable areas.

Many authors have observed that road construction is a more important factor than deforestation in accelerating erosion (Dyrness, 1967; Fredriksen, 1970; O'Loughlin, 1972, and others). Roads increase potential slope instability through all of the factors imposed by deforestation. However, they also create several additional

critical problems: (1) interruption of surface drainage associated with road surfaces, ditches, and culverts (described by Dyrness, 1967); (2) alteration of subsurface water movement due to redistribution of soil and rock material, especially where road cuts intersect a water table (Parizek, 1971; Megahan, 1972); and (3) change in distribution of mass on a slope surface by cut-and-fill construction. As in the case of deforestation, maximum impact of roads probably occurs during the first few severe storms after disturbance. By 15 to 20 yr after construction, most unstable areas have undoubtedly failed. However, the 25-yr period of observation in this study is too short to reveal a clear attenuation of the impact of roads. In several cases in the forest, reconstruction of roads in problem areas appears to have contributed to failure during subsequent storms due to insufficient control of reconstruction work or inadequate correction of the original cause of failure.

Since road cutting began in 1950, the volume of slide material moved from road right-of-way in the unstable zone has been 65,470 m³/km², which is 30 times the rate of slide activity in undisturbed forested areas and about 10 times that in clear-cut areas. The fact that only two small, road-related slides occurred in the stable zone underscores the contrasting effects of roads in the two terranes.

When road impact is assessed at a level of development comparable to timber cutting, roads contribute about half of the total management impact. The combined impact of roads and clear-cut logging has constituted a fivefold increase in landslide erosion relative to undisturbed forested areas.

48

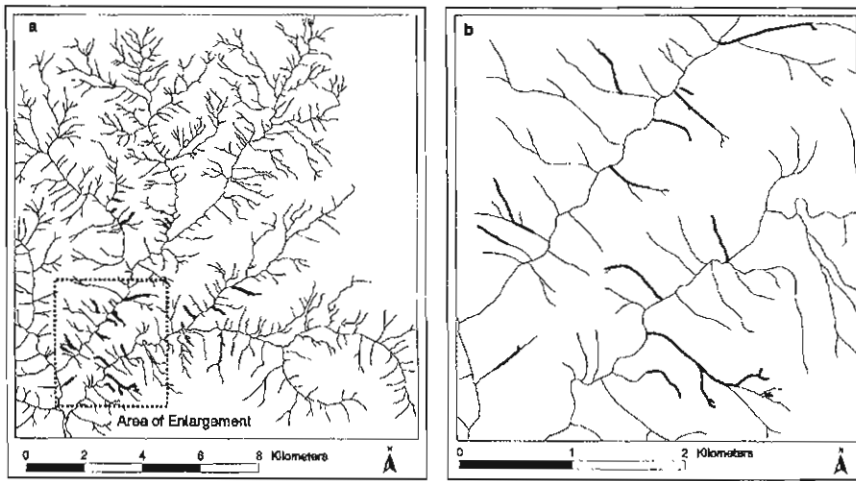


Figure 4. Map of 1996 debris-flow paths in the Blue River area reveals two scales of disturbance patterns. (a) A zone of high-debris flow frequency occurs in the southwest quadrant at lower elevations, where weak rocks and soil, high rates of snowmelt during the storm, relatively high road density, and steep slopes create debris flow-prone areas. (b) Area of enlargement shows that even within the high-debris flow zones, most small tributary networks have some channels that experienced debris flows and others that did not. Thick lines indicate debris-flow paths; thin lines indicate the rest of the stream network.

as levers to increase the water's force until trees topple (Figure 3c).

Phenomena operating at several geographic scales create the complex patterns of disturbance severity observed among steep headwater streams. Some streams may experience high flows but escape major disturbance entirely, whereas other streams and riparian zones are severely scoured by debris flows (Figures 3a and 3b). The disturbance cascade may be interrupted if the debris slides or flows pile up on roads or on the edges of the floodplains, for example, obstructing further flow. In the Blue River watershed, areas of slide-prone soils or high rates of water delivery to soils in the transient-snow zone create predictable geographic zones of high slide and debris flow frequency (Figure 4a; Hack and Goodlett 1960, Swanson and Dyrness 1975). Geographic patterns of debris flows in the 1996 flood were nearly identical to patterns triggered by floods in the 1950–1995 period, indicating that the geography of controls on debris-flow occurrence causes some but not all headwater streams to experience repeated, severe disturbance.

On a finer scale, debris flows commonly affect only parts of the stream networks of small watersheds, even within a landscape with a high inci-

dence of debris flows (Figure 4b). The small tributaries that do not experience debris flows may serve as refuges for organisms that can contribute to the recolonization of channels that were severely affected by debris flows.

Much of the heterogeneity of disturbance severity in larger channels occurs along lateral gradients from the channel axis to the floodplain and from reach to reach along the main channel. Both lateral and along-stream variation in flood disturbance are regulated in part by the width of the valley floor: Narrow valley floors confine flood waters, limiting lateral channel migration and extent of disturbance, whereas wide valley floors have room for both the zone of severe disturbance and areas of more tranquil flow. In wide valley floor areas (unconstrained reaches; *sensu* Swanson and Sparks 1990, Gregory et al. 1991, Grant and Swanson 1995), sections of the main channel experience severe disturbance by complete reworking of the streambed and removal or toppling of riparian vegetation, commonly red alder (*Alnus rubra*), that had established after previous major floods. Flood waters may also inundate areas of riparian forest in which water velocity and the momentum of entrained wood and coarse sediment are not

sufficient to damage standing vegetation. Narrow valley floor areas with steep, rocky stream banks may record fewer effects of flooding simply because they have less floodplain and riparian vegetation, although physical disturbance can be intense.

Biotic response to flooding

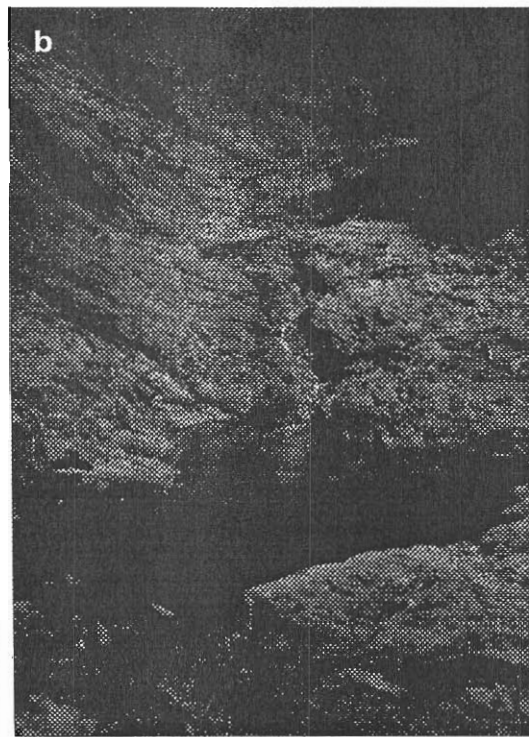
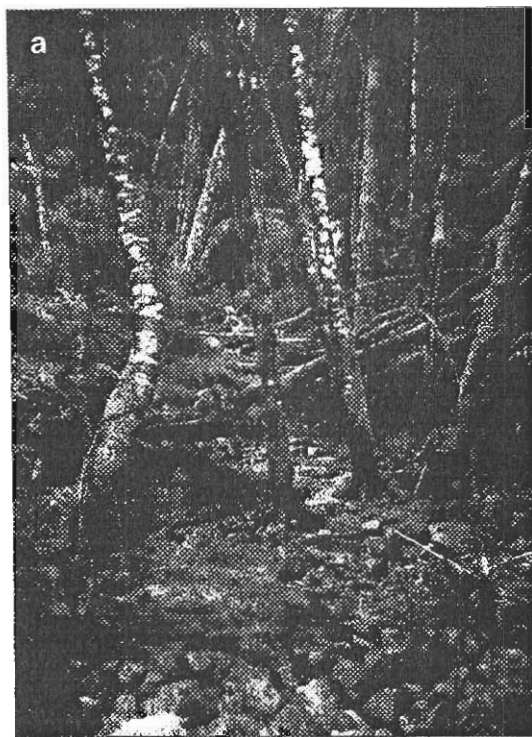
Landforms and geophysical processes establish the physical template within which aquatic and riparian ecosystems operate (Gregory et al. 1991). The disturbance history of the landscape strongly influences patterns of upland, aquatic, and riparian biota in Pacific Northwest landscapes (Schoonmaker and McKee 1988, Morrison and Swanson 1990, Lamberti et al. 1991, Swanson et al. 1992). Floods are the most frequent and intense natural physical disturbances that alter communities of aquatic organisms.

A fundamental ecological question related to flood disturbance is: How do spatial patterns of flood disturbance and refuges in a river network affect the survival and recovery of aquatic and riparian organisms? Species differ greatly in their responses to floods, depending on the type of refuge available to them, their dispersal capabilities, their mode of reproduction, and other life-history traits that affect persistence through floods and subsequent recovery (Table 1). We address the variability of biotic response to floods by examining several types of taxa that represent a range of interactions with floods—riparian vegetation and several groups of aquatic vertebrates.

Riparian vegetation. Natural riparian forests in many Cascade Mountain landscapes are commonly composed of narrow bands of red alder that established after flooding in previous decades. Adjacent to these flood-reset alder stands are taller, older conifer forests that typically established after wildfire (Swanson et al. 1992). Thus, spatial patterns of species and age classes of trees strongly reflect past flooding and other disturbances.

Surveys in major tributaries of the McKenzie River after the 1996 flood revealed heterogeneous patterns of disturbance to riparian forests. Nu-

Figure 3. Flood effects on stream channels and riparian vegetation. (a) A small stream and alder (*Alnus rubra*) riparian zone that experienced the February 1996 flood but no debris flow. Alder trees, even those growing in the channel, survived the flood and created complexity that provided refuge for some species. (b) A small bedrock stream after passage of a debris flow in February 1996. Streambed sediment and riparian vegetation, including alder trees of the stature shown in (a), have been removed. (c) High streamflow rotated a 1.5 m diameter conifer log from left to right, toppling riparian alder trees.



This stream reach, here flowing to the upper right, is viewed from above by a camera suspended below a balloon.



ity. These patterns can be interpreted in terms of downstream variation in physical processes and geographic variation in landscape susceptibility to key processes. Flood waters flow progressively through the stream network, yet physical disturbance processes, a hallmark of flooding in mountain environments, vary in their properties and effects along the gradient from hillslopes, through small streams, to large channels. When considering either physical processes or the biology of mountain stream systems, therefore, it is useful to distinguish steep headwater streams draining 1–100 ha from larger, lower-gradient streams (drainage areas of 1–1000 or more km²) because some key processes (e.g., debris flows or movement of floating logs) and biota are restricted largely to one or the other.

Water, soil, sediment, and woody debris move down hillslopes and stream channels by a cascade of processes, following the gravitational flow path. Moving solid material may have variable disturbance effects. Sediment and wood, for example, may move as individual par-

ticles with little ecological impact or as large mass movements with the force to substantially disturb ecosystems. Soil mass movement by debris slides originating on hillslopes may enter steep headwater channels and change into debris flows. Varying in size from hundreds to thousands of cubic meters, debris flows are water-charged masses of sediment and organic matter that move down headwater channels at velocities of up to 10 m/s or more (Hack and Goodlett 1960, Sidle et al. 1985), scouring channel sediment and riparian veg-

etation (Figures 3a and 3b). Debris flows may enter larger, lower-gradient channels that carry sufficient water to float large logs on the water surface, while gravel and boulders roll audibly along the streambed. Generally, in wet landscapes, an increasing amount of water is available along this flow path to dilute the sediment in transit and to float larger pieces of woody debris. Moving woody debris can become a significant agent of disturbance in larger channels as floating logs ram into or lodge against standing trees, acting

Smyon, 2020

Figure 3. The pattern of debris flow initiation by year, WY 1946 - WY 1996.

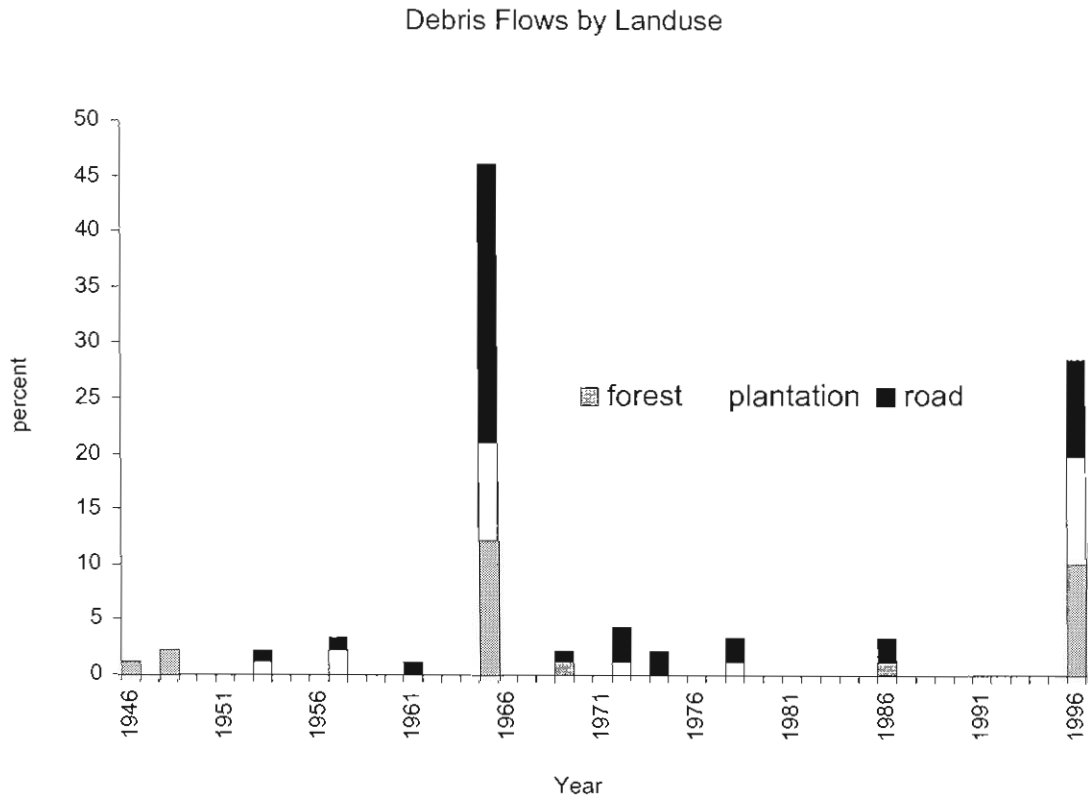


Table 1. An overview of debris flow occurrence WY 1946- WY 1996: cumulative density over the study period, and the number and percentage of events by land use.

Cumulative Density of debris flows										
Geology	All Events				Natural Forest		Plantations		Roads	
	# dfs	%df	ha	#/ha	#	%	#	%	#	%
weak	22	24	1090	0.0202	9	10	3	3	10	11
moderate	56	62	6470	0.0087	11	12	18	20	27	30
strong	13	14	4840	0.0027	6	7	1	1	6	7
					26	29	22	24	43	47
Elevation										
400-699m	40	44	2430	0.0165	10	11	14	15	16	18
700-999m	50	55	4960	0.0101	16	18	8	9	26	29
1000-1699m	1	1	5010	0.0002	0	0	0	0	1	1
					26	29	22	24	43	47
Slope										
0° - 19°	1	1	6060	0.0002	0	0	1	1	0	0
20o +	90	99	6340	0.0142	26	29	21	23	43	47
					26	29	22	24	43	47
Topo. Setting										
channel head	27	30	n/a	n/a	6	7	11	13	10	11
planar hillslope	52	57	n/a	n/a	14	16	10	11	28	32
stream-side	9	10	n/a	n/a	5	6	1	1	3	3
unknown	3	3	n/a	n/a	1	1	0	0	2	2
					26	29	22	24	43	47

In natural forest, 26 debris flows (29% of the total) occurred during the study period (Table 1). Natural forest events occurred in 6 of the 12 debris flow-producing years. Debris flow initiation frequency in weak rock types in natural forest was 5 times greater than in moderate and strong geologic types, on a number per percent-area basis (Table 2). Thirty-five percent were from weak, 42% moderate, and 23% from strong rock types.

Initiation site elevations in natural forest ranged from 605 m to 990 m, with an average of 763 m. Initiation frequency was similar for the 400-699 m and 700-999 m

SNY DEN 2000

located on planar hillslopes in natural forest. At channel heads there were 7% fewer events, while there were 9% more from the stream-side in natural forest than overall.

The number of unknown sites was about the same; there were 1% more unknown sites in natural forest.

Table 2. Debris flow occurrence in natural forest for all years combined, and for all years combined, and for WY 1965 and WY 1996 separately.

Natural Forest										
Geology	All years (1946 area)				WY 1965			WY 1996		
	#	%	%area	#/%area	#	%area	#/%area	#	%area	#/%area
weak	9	35	9	1.02	5	8	0.66	3	8	0.38
mod	11	42	52	0.21	5	52	0.10	2	48	0.04
strong	6	23	39	0.15	1	40	0.02	4	44	0.09
Elevation										
400-699	10	38	20	0.51	4	17	0.24	3	16	0.18
700-999	16	62	40	0.40	7	40	0.18	6	37	0.16
1000-1699	0	0	40	0.00	0	43	0.00	0	46	0.00
Slope										
0° - 19°	0	0	49	0.14	0	0	0.00	0	46	0.00
20° +	26	100	51	0.37	11	53	0.21	9	54	0.17
Topo. Setting										
chan. head	6	23	n/a	n/a	0	n/a	n/a	5	n/a	n/a
hillslope	14	54	n/a	n/a	7	n/a	n/a	3	n/a	n/a
stream-side	5	19	n/a	n/a	3	n/a	n/a	1	n/a	n/a
unknown	1	4	n/a	n/a	1	n/a	n/a	0	n/a	n/a

In WY 1965, 19% of the debris flows initiated from plantations, while 26% initiated from natural forest. Plantation-associated initiation in WY 1996 accounted for 35% of the debris flows, the same percentage as natural forest in that water year (Table 3, Figure 4). However, the frequency of debris flow initiation was 7 times greater in

53

5 My Oct, 2020

Table 3. Debris flow initiation WY 1965 and WY 1996. The number of events, percentage of each year's total, and density (#/km²) are represented for geology, elevation, slope, and topographic position.

	water year 1965									water year 1996								
	forest			plantation			road			forest			plantation			road		
Geology	#	%	#/km ²	#	%	#/km ²	#	%	#/km ²	#	%	#/km ²	#	%	#/km ²	#	%	#/km ²
soft	5	12	0.60	1	2.4	0.59	7	17	7.78	3	12	0.44	0	0	0.00	3	12	3.00
mod	5	12	0.09	6	14	1.02	13	31	5.65	2	7.7	0.18	9	35	0.48	3	12	0.73
hard	1	2.4	0.02	1	2.4	0.29	3	7.1	2.73	4	15	0.40	0	0	0.00	2	7.7	1.00
Total:	11	26	0.10	8	19	0.73	23	55	5.35	9	35	0.10	9	35	0.30	8	31	1.13
Elevation																		
400-699	4	10	0.22	4	10	0.98	12	29	6.32	3	12	0.21	8	31	0.98	2	8	1.00
700-999	7	17	0.16	4	10	0.89	11	26	0.06	6	23	0.18	1	4	0.07	6	23	1.94
1000-1699	0	0	0.00	0	0	0.00	0	0	0.00	0	0	0.00	0	0	0.00	0	0	0.00
Total:	11	26	0.10	8	19	0.73	23	55	5.35	9	35	0.10	9	35	0.30	8	31	1.13
Slope																		
0° - 19°	5	12	0.10	2	4.8	0.33	9	21	2.65	0	0	0.00	2	7.7	0.13	4	15	0.74
20° +	6	14	0.10	6	14	1.20	14	33	15.56	9	35	0.19	7	27	0.48	4	15	2.35
Total:	11	26	0.10	8	19	0.73	23	55	5.35	9	35	0.10	9	35	0.30	8	31	1.13
Topo. Position																		
channel head	0	0	n/a	5	13	n/a	5	13	n/a	5	19	n/a	4	15	n/a	2	7.7	n/a
hillslope	7	18	n/a	3	7.5	n/a	17	43	n/a	3	12	n/a	4	15	n/a	6	23	n/a
streamside	3	7.5	n/a	0	0	n/a	0	0	n/a	1	3.8	n/a	1	3.8	n/a	0	0	n/a
unknown	1	1	n/a	0	0	n/a	1	0	n/a	0	0	n/a	0	0	n/a	0	0	n/a
Total:	11	26	0.10	8	19	0.73	23	55	5.35	9	35	0.10	9	35	0.30	8	31	1.13

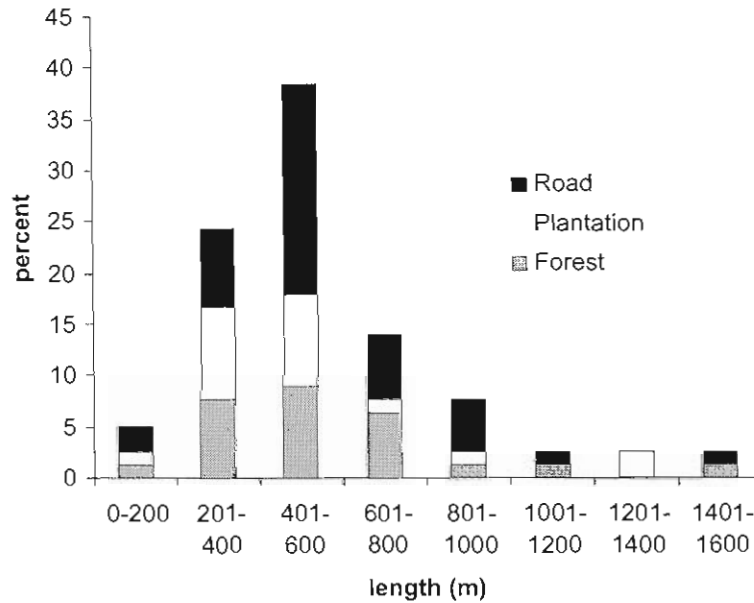
Debris flows from plantations originated at lower elevations, on average, than from natural forest ($p=0.002$, $df=2$, $F=6.5$, ANOVA). The mean elevation of the initiation site for debris flows in plantations was 90 m lower than natural forest. There was no evidence that debris flows originated on more gentle slopes in plantations, on average, than in natural forest ($p=0.52$, ANOVA).

On a percentage basis, debris flows initiated from channel head topographic settings in plantations at nearly twice the rate of natural forest, although the number of observations was small ($n=14$). The rate of initiation from planar hillslopes was similar for plantations (13%) and natural forest (16%).

54

SNY 002, 2000

Figure 6. Debris flow track length, based on longest single channel length, by land use.



4.3 Termination

A total of 78 debris flow termination sites were inventoried. Twenty-eight percent (22 sites) terminated at a mainstem stream tributary, 24% (19 sites) terminated in a first-through third-order channel, 28% (22 sites) terminated at a road, and 10% (8 sites) terminated on a floodplain, terrace, or a fan. The termination setting of 9% (7 sites) was indeterminable.

Nineteen percent of the debris flow termination sites (15 sites) resulted from events that initiated, transported, and terminated in natural forest. Of these, the majority (7 events) terminated at a mainstem stream, 4 events terminated in a first- to third-order

55

ARE WE HAVING FUN YET??

TABLE 8.1 *Material transfer process characteristics for watershed 10 in old-growth forest condition.*

Process	Downslope movement rate [*]	Frequency	Watershed area influenced	Landforms
<i>Hillslope processes</i>				
Solution		continuous	total	
Litterfall		continuous, seasonal	total	
Surface erosion	1	continuous	total	small terraces
Creep	2	seasonal	total	
Root throw	3	~ 1/yr	0.10% [*]	pit & mound topography
Debris avalanche	4	~ 1/370 yr	1 to 2% [*]	shallow, linear down-slope depressions
Slump/earthflow	5 [†]	seasonal [†]	5 to 8%	scraps, benches
<i>Channel processes</i>				
Solution	3	continuous	~ 1%	
Suspension	3	continuous, storm	~ 1%	
Bedload	3	storm	~ 1%	channel bedforms
Debris torrent	4	~ 1/580 yr	~ 1%	incised, U-shaped channel cross section

*1 = cm to m/yr, 2 = mm/yr, 3 = m/s, 4 = 10 m/s, 5 = mm to cm/yr.

^{*}Area influenced by one event.

[†]Inactive in past century in watershed 10.

Channel Processes

Solution transport is movement of material dissolved in stream water. *Suspended sediment transport* is movement of material in colloidal to sand size carried in suspension in flowing water. *Bedload transport* is movement of material approximately coarse sand size and larger by tractive forces imparted by streamflow. *Debris torrent* is the rapid, turbulent movement down stream channels of masses that may exceed 10,000 m³ of soil, alluvium, and living and dead organic matter. Whole trees may be included. *Streambank erosion* occurs as lateral cutting by a stream as it entrains material such as older alluvium or colluvium moved to the streamside area by creep, surface erosion, or other processes.

Relations Among Processes

The movement of a single particle of material through a watershed is accomplished by a series of steps involving numerous material transfer process-

Debris Flow and Stream-Channel Impacts: Oregon Coast Range

2503

sediment storage capacity of the channel, large wood buffers the sedimentation impacts on downstream reaches when pulses of sediment enter headwater streams (Swanson and Lienkaemper, 1978; Lancaster *et al.*, 2001).

Debris flows transport sediment and wood stored in low-order channels and leave behind an erosional zone that is typically scoured to bedrock (Swanson and Lienkaemper, 1978; May, 2002). The erosion of the channel to bedrock provides a unique opportunity to calculate the rate of wood and sediment accumulation, and to gain insight into the processes that refill the channel with sediment and wood in the interval between debris flows. In low-order streams, the size of wood is typically large in relation to the size of the channel (Bilby and Ward, 1989; Bilby and Bisson, 1998), and it can be assumed that fluvial processes transport very few pieces of wood in the interval between debris flows. Conversely, the sediment transport capacity of the channel may be high immediately following a debris flow because bedrock channels are typically straight, steep, and have a high hydraulic radius and low roughness. Therefore, immobile pieces of wood can form a physical obstruction to sediment transport that may be critical for sediment accumulation in this portion of the drainage network.

The goal of this study was to investigate changes in sediment and wood storage volumes, and associated changes in channel morphology, in low-order streams that are prone to erosion by debris flows. We used a space-for-time substitution approach to align spatially separated states along a temporal sequence (Welch, 1970). Specific objectives were to: (1) quantify the rate of wood and sediment accumulation in second-order streams that are prone to erosion by debris flows; (2) identify the mechanisms for storing sediment in high-gradient, low-roughness channels; and (3) assess the relative importance of debris-flow-prone tributaries as storage reservoirs for sediment in the drainage basins.

STUDY AREA

Two third-order basins with a minimal history of timber harvest and road construction were selected for this study (Figure 1; Table I). Sediment production and transport processes in the basins were considered typical of debris flow terrain in the central Coast Range of Oregon. Skate Creek has a drainage area of 2.5 km² and

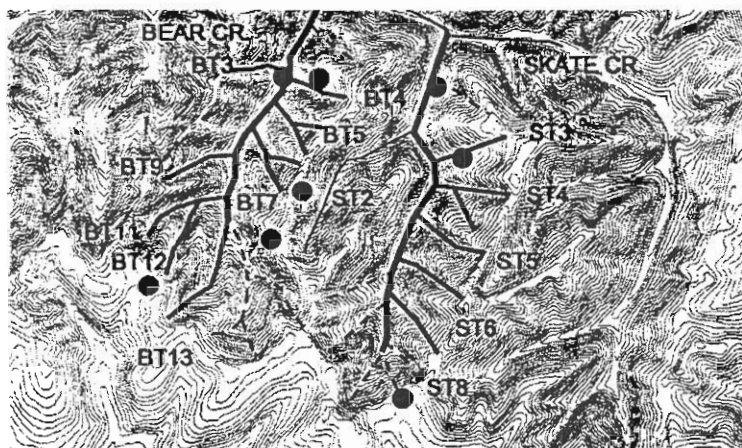


Figure 1. Site map of Skate and Bear Creeks, Siuslaw River drainage in the central Oregon Coast Range. Dark solid lines represent channels investigated for wood and sediment storage. Dashed lines represent colluvial tributaries impacted by timber harvest and not investigated. Thin solid line (ST2) is only tributary with no evidence of delivering debris flows to the mainstem. Numerous first-order channels throughout the network are not highlighted and are not well represented on low-resolution topographic data. Solid circles represent sample sites for the dendrochronology-based fire history reconstruction. Contour interval = 10 m

59

Tributary

- Skate T3
- Skate T4
- Skate T5
- Skate T6
- Skate T8
- Bear T3
- Bear T4
- Bear T5
- Bear T7
- Bear T9
- Bear T11
- Bear T12
- Bear T13

Bear Cree and small timber ha

The stu The Tye mudstone order stre have a toy drained at

The do (Tsuga he These sta Red alder most corr spectabili tum), sals landslide

Second-on deposition differentia All of the empirical

The ert high likel in this are scoured b flows. Th channels v bedrock v at the upp defined b

MAY 8 GROSSMAN 2003

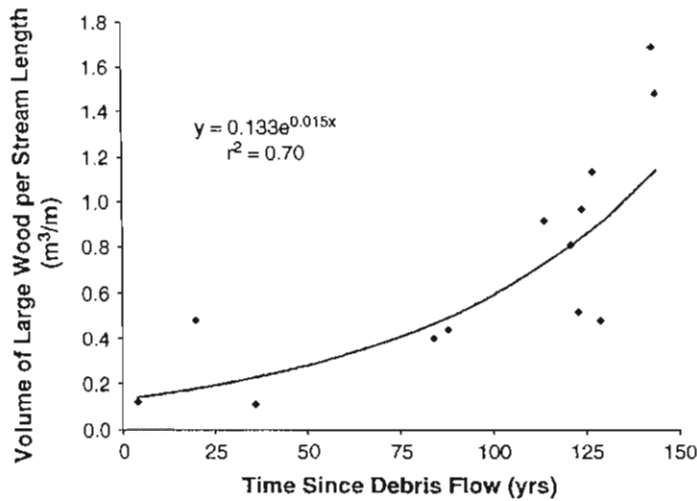


Figure 2. Volume of large wood in the study streams based on the time since the previous debris flow as estimated by dendrochronology

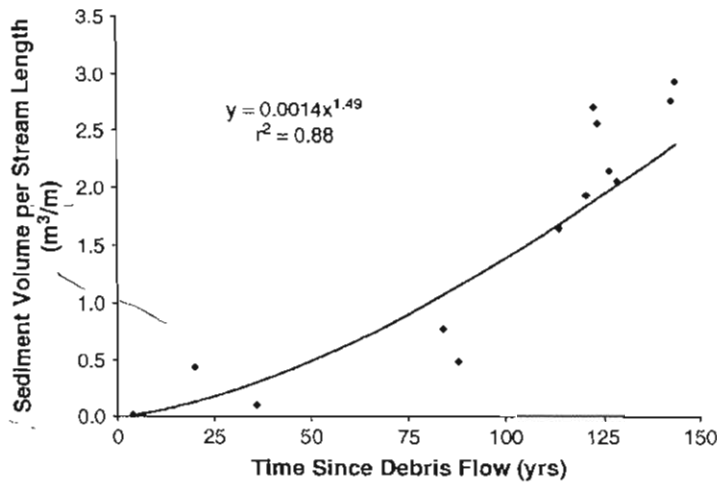


Figure 3. Sediment accumulation in the study streams based on the time since the previous debris flow as estimated by dendrochronology

predicted to have an almost continuous covered of sediment, with very little exposed bedrock. The decrease in the proportion of the channel with exposed bedrock, and the average length of bedrock reaches with increased age, depicts how these discontinuous patches of sediment coalesced through time (Table II).

Landslides from bedrock hollows and on planar sideslopes appeared to be an important source of sediment to the channels we investigated. Unfortunately, it was not possible to quantify the long-term contribution of sediment delivered from landslides because landslide scars were rapidly vegetated, and only failures that occurred in the last decade could be detected. Where landslide scars could be detected, the scar was measured, and this volume accounted for an average of 19 per cent of the sediment stored in the channels.

The observed volume of sediment stored in the channel was contrasted with a predicted input rate (Table III; Figure 7) calculated from the maximum bedrock lowering rate ($1.1 \times 10^{-4} \text{ m a}^{-1}$) and a soil to bedrock bulk density ratio of 0.5 estimated by Reneau and Dietrich (1991). The observed volume of sediment stored in the

length reaches (m)

pes were hillslopes (± one maximum average standard on valley 46 cm of before, the

ment and tion rates per cent of ite, and a a power e ratio of exponent nterval = to time. mulation he ability am wood d linearly

y can be flow the 50 years e channel i was still atches of would be

60

MAY & GRESSWELL, 2003

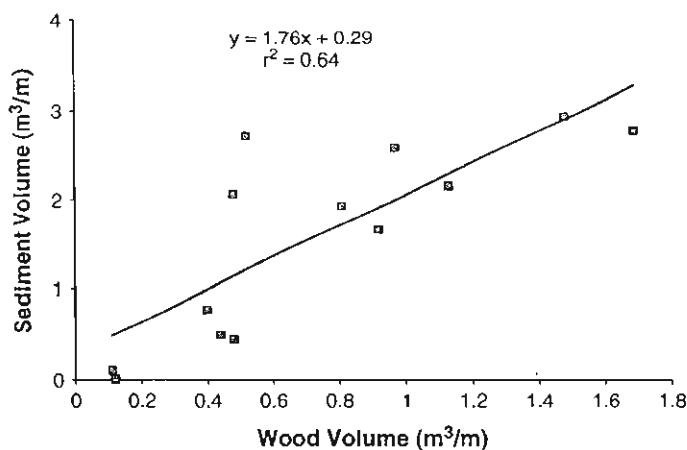


Figure 4. The association between wood and sediment storage volumes in debris-flow-prone channels

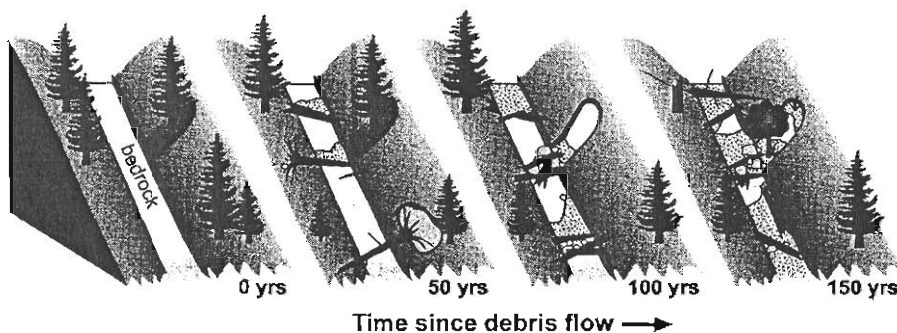


Figure 5. Conceptual illustration of the changes in channel morphology based on the time since the previous debris flow

Figure 6.

channel was less than predicted from the bedrock lowering rate. The area between the curves can be used for a rough approximation of the amount of sediment exported by fluvial transport. Immediately following a debris flow the majority of sediment entering the channel is likely to be transported downstream. As the time since the previous debris flow increases, the proportion of sediment exported appears to decrease.

Basin-scale sediment storage

The quantity of sediment stored in debris flow runout paths was contrasted with the volume of sediment stored in the mainstem channel and valley floor landforms of Skate Creek. Wood provided a physical obstruction to sediment transport, and 73 per cent of the sediment in tributaries that are prone to debris flows was stored directly behind wood (Figure 8). Large wood stored 59 per cent of this sediment, and small wood (pieces <2 m in length and <20 cm average diameter) stored 14 per cent. A total of 389 pieces of wood was measured in debris-flow-prone tributaries to Skate Creek, and 37 per cent of these pieces stored sediment. Wood >15 m in length accounted for only 22 per cent of the number of pieces, but accounted for 78 per cent of the total volume of wood. Despite this inconsistency, the number of pieces explained 60 per cent (r^2) of the observed variance in the volume of wood in the channels.

Large wood was also a major component of sediment storage in the mainstem of Skate Creek (Figure 8); however, <0.5 per cent of the sediment in the mainstem was stored by small wood. In contrast to the

tributary
absence

Wood
of wood
relatively
spanning
inundate
located
30 years
of the b

Copyright

61

MAY 8 GREENWICH, 2003

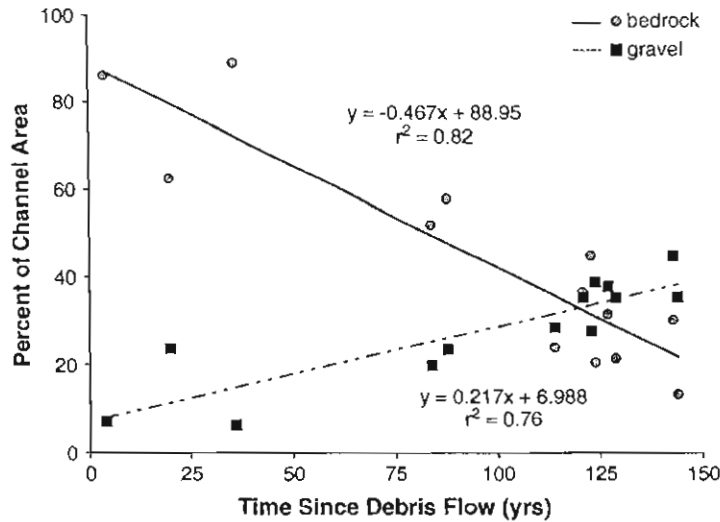


Figure 6. Changes in the proportion of the channel length with exposed bedrock and gravel, based on the time since the previous debris flow

Table III. Measured sediment storage volumes and predicted sediment input volumes estimated from a long-term average bedrock lowering rate (Reneau and Dietrich, 1991)

Tributary	Time since debris flow (years)	Erosional zone sediment volume (m ³)	Sediment volume predicted from bedrock lowering (m ³)
Skate T3	123	939	1005
Skate T4	121	1110	1012
Skate T5	84	223	503
Skate T6	36	27	180
Skate T8	143	800	947
Bear T3	129	443	443
Bear T4	127	546	582
Bear T5	114	394	529
Bear T7	144	1138	737
Bear T9	124	1183	611
Bear T11	20	106	165
Bear T12	88	208	544
Bear T13	4	27	44

tributaries, the mainstem had low-gradient reaches (1–5 per cent slope) where sediment was stored in the absence of wood or boulders.

Wood influenced channel morphology on multiple spatial scales. Individual pieces, or small accumulations of wood, functioned to store sediment at small spatial scales (10⁰–10¹ m). These individual pieces were relatively abundant and broadly distributed spatially throughout the channel network. In contrast, large, valley-spanning wood dams formed by debris flows stored sediment on larger spatial scales (10¹–10² m) and inundated entire stream reaches and valley floor surfaces. These large dams were infrequent and were discretely located near tributary junctions. Two large, valley-spanning wood dams formed by debris flows in the last 30 years were located in the mainstem of Skate Creek. These debris flows originated in the upper portion of the basin where timber was harvested in the mid-1970s. The channel was actively incising the wedge of

flow

1 be used
llowing a
s the time

sediment
1 obstruc-
flows was
all wood
wood was
sediment.
8 per cent
nt (r^2) of

Figure 8);
ast to the

62

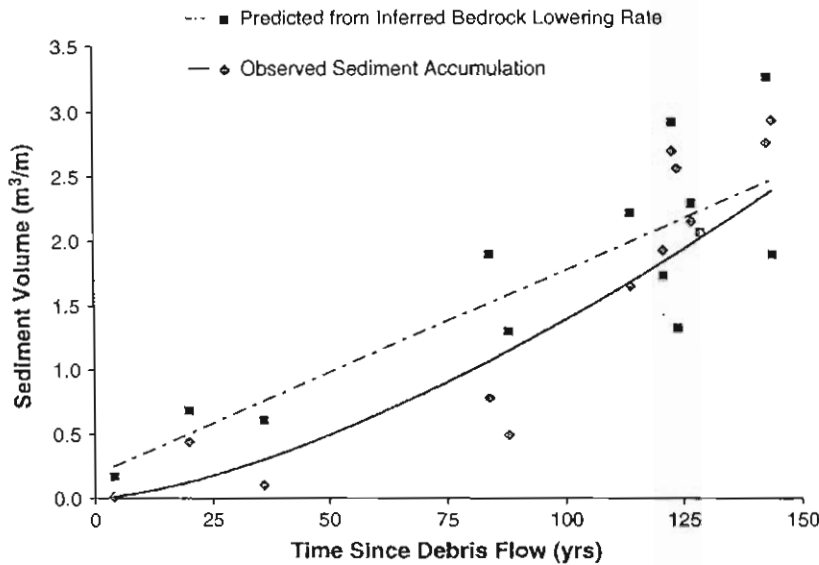


Figure 7. Measured sediment accumulation compared to a predicted sediment input volume from an inferred bedrock lowering rate (Reneau and Dietrich, 1991). The observed sediment accumulation rate was based on field measurements from our study streams, solid line regression equation $y = 0.0014x^{1.49}$, $r^2 = 0.88$. Predicted sediment input from an inferred bedrock lowering rate was $1.1 \times 10^{-4} \text{ m a}^{-1}$ multiplied by the drainage area and a soil to bulk density ratio of 0.5, dashed line regression equation $y = 0.016x + 0.168$, $r^2 = 0.70$. The area between the curves represents the proportion of sediment presumably exported by fluvial transport

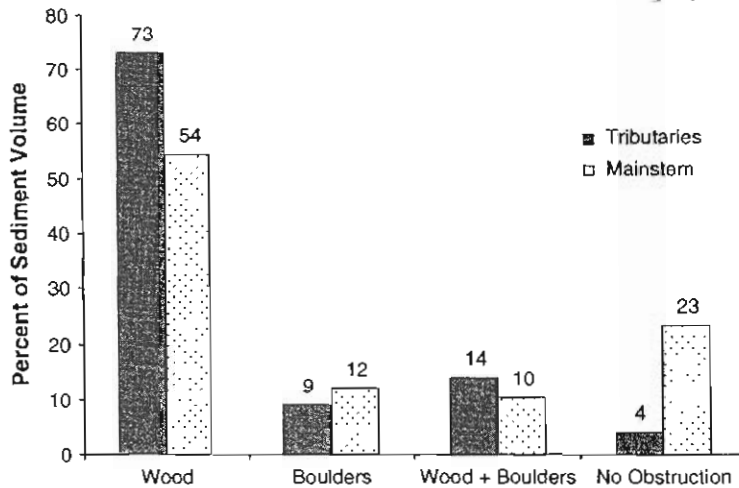


Figure 8. Sediment stored by obstructions in the channel network of Skate Creek. Numbers represent the percentage of stored sediment

sediment upstream of the debris dam, resulting in the formation of continuous terraces along the channel. These large dams stored 32 per cent of the sediment in the mainstem, and individual pieces of wood and small accumulations accounted for 22 per cent.

A total channel length of 6860 m was surveyed in Skate Creek, and a total volume of 21 950 m³ of sediment in storage was estimated in this portion of the channel network. Numerous first-order channels throughout the network were not investigated; therefore, the proportion of the network in low-order colluvial channels was substantially under-represented. The majority of sediment in the network was stored in tributaries (Figure 9),

which al
was 210
an avera
sedimen
In ad
the mair
debris fl
along th
time for
1978). T
soil pro
ratio of

Sedimen

The a
structure
space-fc
assumpt
attempt
work w
channel
pared w
that the

The a
first ass
There is
field ob
in 1996
uncomm
cent we
assump
debris f
no infor

For r
still pre
time be
capacity

Copyright

63

Forest Road Processes at HJ Andrews

FOREST ROAD IMPACTS

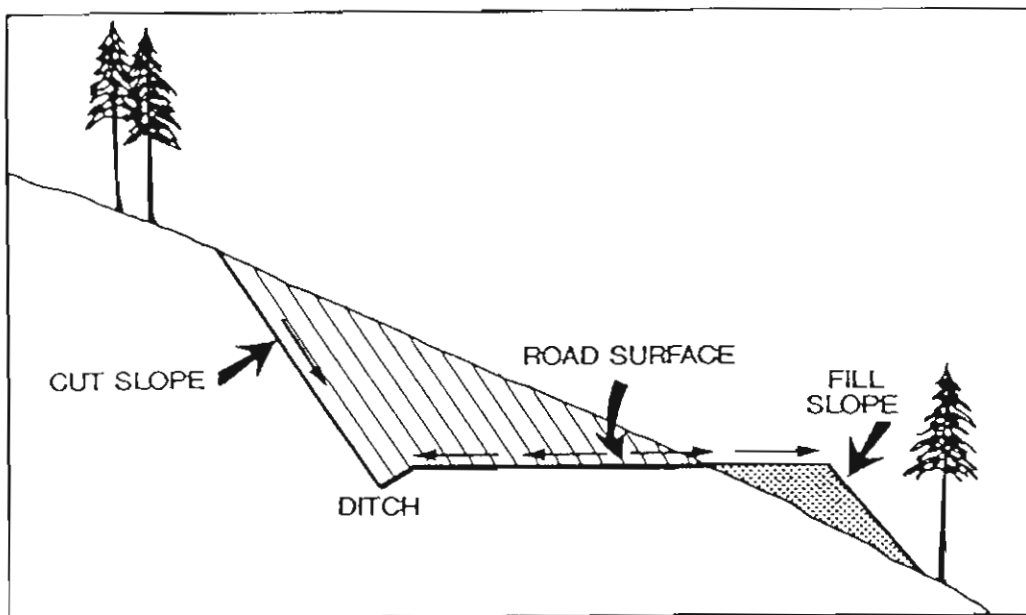


Figure 1. Road/hillslope cross-section schematic

Current forest practice regulations prohibit sidesteading to the extent that landslides and channel damage are likely. A technique known as end-hauling is used to transport excess excavated materials to more stable waste area locations. Using steeper grades to keep roads on ridgetops is a far less expensive road system design alternative than end hauling, and is also effective at landslide prevention. However, where these practices are not possible, end hauling may be an effective, albeit expensive, technique for reducing landslides (Sessions et al., 1987). Forest practice regulations for end-hauling have been in place since 1983. However, most existing forest roads in western Oregon were constructed prior to 1983, when sidesteading was the common construction practice.

A road damage inventory conducted in Washington found that roads constructed in the last 15 years survived a landslide inducing storm with minimal damage, while roads constructed earlier had very high damage rates (Toth, 1991). Department of Forestry landslide monitoring has made similar findings (Mills, 1991). Although most surface erosion tends to occur in the first few years after construction or during periods of heavy traffic use, landslides can occur many decades after original construction.

ODF monitoring has also found that road drainage is associated with about one-third of the investigated road-related landslides (Mills, 1991). Culverts were associated with 29 percent of the damage sites in the Deschutes River (Washington State) study (Toth, 1991). Concentration of road drainage can also be associated with interactions between road systems and channels in steep terrain, sometimes resulting in landslides (Montgomery, 1994).

Stream crossings with culverts, and to a lesser extent under-designed bridges, are subject to plugging and/or the capacity being exceeded by high flows. If water backs up and flows over

65

is defined as the sum of stream length (LS) over the basin area

$$D_d = \frac{\sum L_S}{A} \quad (3)$$

We propose that roads modify drainage density by extending the total length of effective surface flow-paths in a basin, expressed as

$$D'_d = \frac{\sum(L_S + L_{Rc} + L_{Rg} + L_G)}{A} \quad (4)$$

where $\sum L_{Rc}$ represents the length of road segments discharging runoff directly to stream channels, $\sum L_{Rg}$ represents the length of road segments discharging runoff to hillslopes where channelized surface flow occurs in newly-eroded gullies, and $\sum L_G$ represents the length of those gullies connecting roads to streams on previously unchanneled hillslopes (Figure 2). We define gullies in this study as surface flowpaths evident at road culverts created either by

chronic channel incision on hillslopes or episodic scour by landslides.

In this study, we focused on assessing road effects at the drainage-basin scale. We examined drainage network length in two basins and the extent to which roads modify drainage density by extending the channel network.

METHODS

Approach

The study included three components: (1) determination of the increase in drainage density attributable to road-stream connectivity in the Lookout Creek and Blue River basins; (2) examination of factors contributing to road-stream connectivity, particularly the formation of gullies; and (3) comparison of the timing and spatial distribution of road construction in Lookout vs. Blue River to evaluate whether road-stream

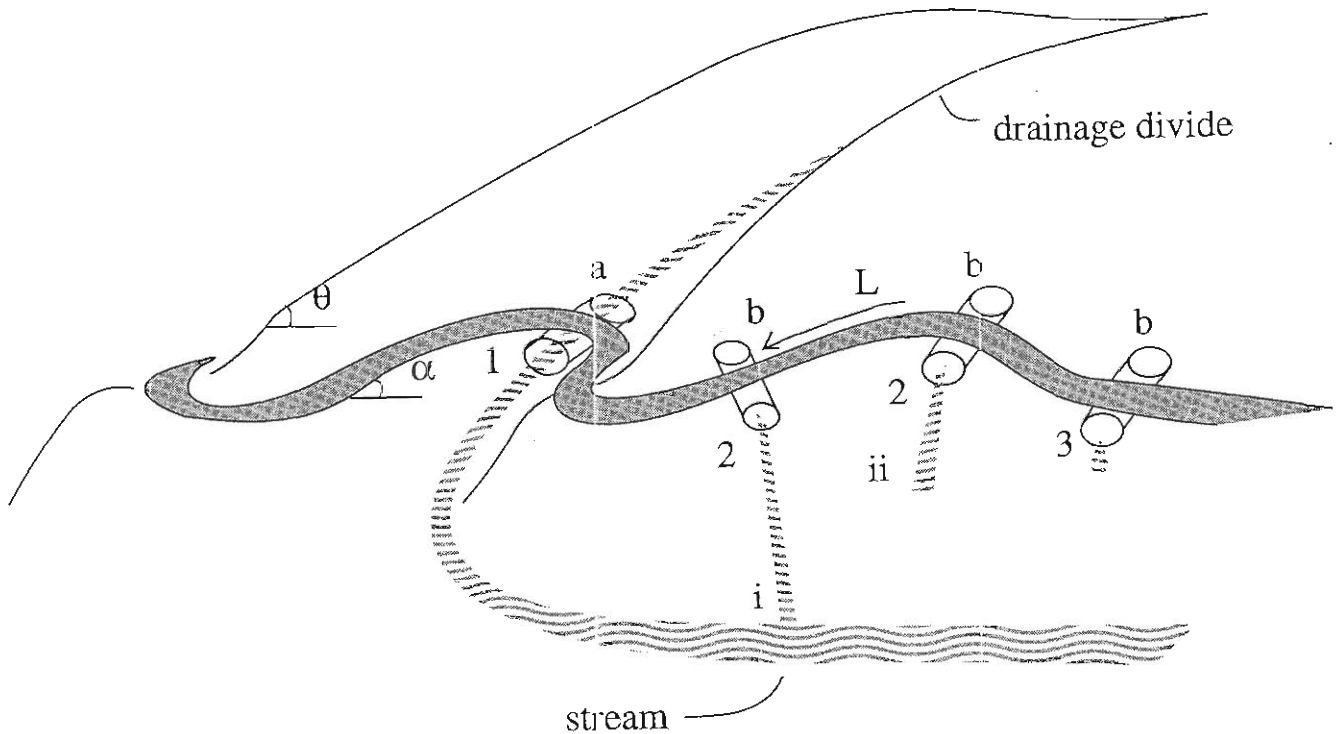


Figure 2. Road Drainage Structures on Forest Roads. Stream-crossing culverts which route a stream below a road (a) and ditch-relief culverts (b) were classified according to whether they discharged directly to a stream channel (1), onto hillslopes below roads where gully incision occurs (2), or where water reinfilters into the hillslope soil (3). Gully incision may provide a continuous flowpath to streams (i) or may function as a discontinuous channel segment (ii). The length of the road segment draining to the culvert (L), the road grade (α), and the hillslope angle (θ) were used to test predictions of the occurrence of gullies.

WEMPLE ET AL., 1996

(Harr *et al.*, 1975; Harr *et al.*, 1979; Jones and Grant, 1996), but not in an experiment in California (Ziemer, 1981; Wright *et al.*, 1990). Studies of large (> 50 km²) forested basins subjected to dispersed harvesting and road construction over several decades found increased peak flows associated with the proportion of basin area in roads and clearcuts in some cases (Anderson and Hobba, 1959; Christner and Harr, 1982; Jones and Grant, 1996), but not in others (Duncan, 1986).

Previous watershed studies have not examined the mechanisms by which roads influence changes in peak flow hydrology. This study was initiated to explore mechanisms by which roads may alter routing efficiency in a basin. Specifically, we examined the type and extent of hydrologic flow paths linking road segments to stream channels in two adjacent basins in the western Cascades of Oregon.

CONCEPTUAL MODEL

We propose a conceptual model to describe the hydrologic function of roads based on two effects: (1) a volumetric effect, increasing the volume of water available for quickflow; and (2) a timing effect, altering flow routing efficiency through extensions to the drainage network (Figure 1).

The volumetric effect of roads operates at the hillslope scale (Figure 1). Precipitation on hillslopes is partitioned to slow subsurface drainage contributing to baseflow (Q_{base}) and rapid surface and subsurface runoff contributing to quickflow (Q_{quick}). The hydrograph represents the summation over time of the volumes contributed by these two components, expressed as

$$Q(t) = Q_{base} + Q_{quick} \tag{1}$$

Roads increase the total volume of water available for quickflow in two ways. Overland flow is generated by the interception of precipitation on compacted road surfaces with low infiltration capacities (Reid and Dunne, 1984; Luce and Cundy, 1994). In addition, shallow subsurface flow may be intercepted at road cutbanks and converted to rapid surface runoff (Megahan, 1972; Sullivan and Duncan, 1981). This effect of increasing total quickflow volume may be expressed as

$$\Delta Q_{quick} = Q_{intercepted} + Q_{subsurface \rightarrow surface} \tag{2}$$

The timing effect of roads operates at the basin scale (Figure 1). The length and arrangement of stream channels determines the flow-routing efficiency of the basin (Leopold *et al.*, 1964). Drainage density, often used as an index of drainage efficiency,

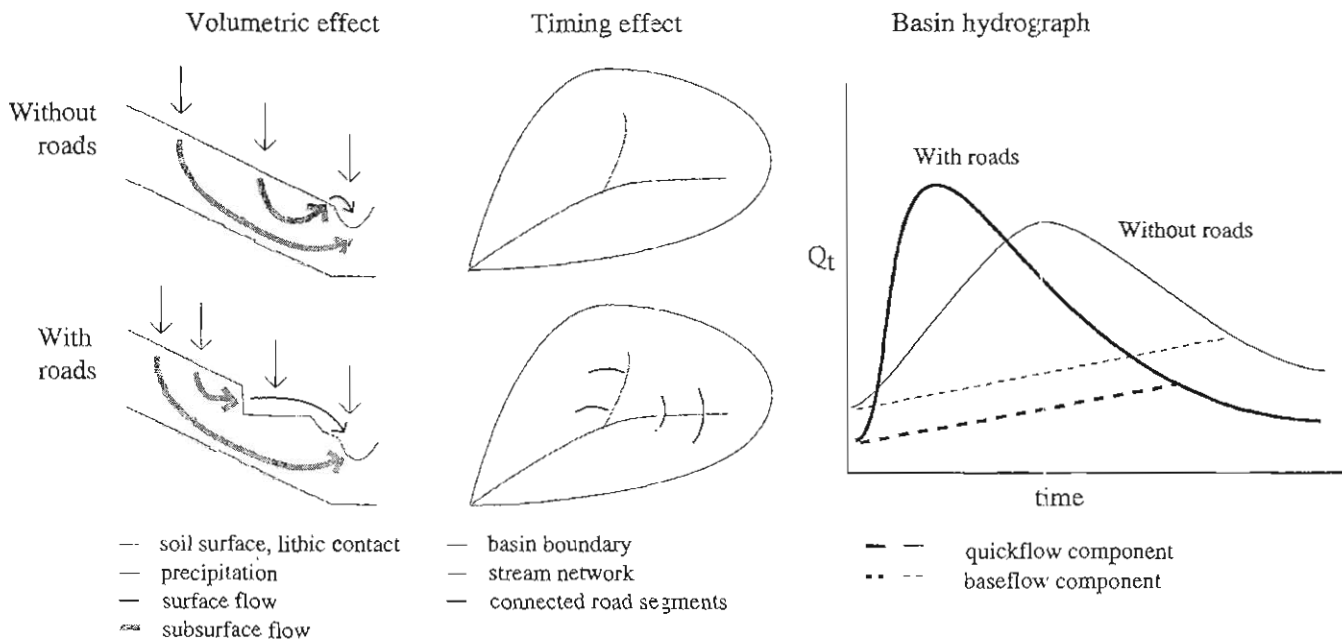


Figure 1. A Conceptual Model of the Hydrologic Function of Roads Based on Two Effects: (1) a volumetric effect, increasing the total volume of water available for quickflow; and (2) a timing effect, altering the flow routing efficiency through extensions to the drainage network (see text).

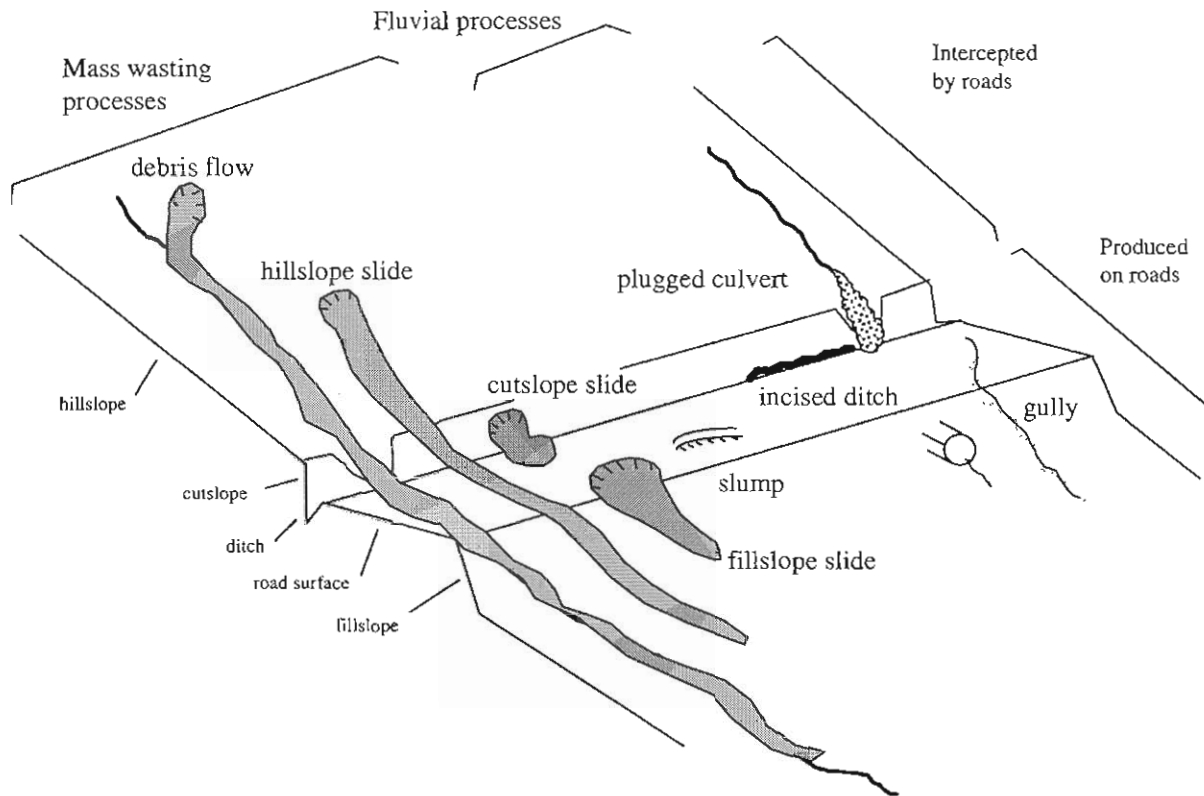


Figure 1. Typology of erosional and depositional features produced by mass-wasting and fluvial processes and associated with forest roads

The February 1996 storm

A sequence of events typical of major floods in western Oregon (Harr, 1981) led up to the February 1996 storm. Following a period of below-average precipitation, prodigious snowfall in late January brought snowpack levels to 112 per cent of the long-term average in the region (Swanson *et al.*, 1998). On the afternoon of 5 February, a strong subtropical jet stream moved into the Pacific Northwest, bringing warm rains from the central Pacific Ocean. Rainfall for the period 5–9 February exceeded 290 mm. Rain and associated snowmelt triggered flood flows with return periods of 30 to 100 years, with profound and diverse geomorphic and ecological impacts (Swanson *et al.*, 1998; Johnson *et al.*, in press).

As is typical of rain-on-snow events in these basins (Perkins, 1997), the relative timing of peak precipitation and snowpack melting differed by elevation during the February 1996 storm. At low elevations (400 to 800 m), rain-saturated snowmelt coincided with peak precipitation intensity, whereas at middle elevations (800–1200 m), maximum snowmelt occurred roughly 24 hours after peak precipitation, and upper elevations (>1200 m) experienced little snowmelt during the event (Dyrness *et al.*, 1996).

Inventory methods and mapped features

In the first few months after the storm, the entire road network in the study area was surveyed by vehicle or on foot. All erosional and depositional features within the road prism (cutslope, ditch, road surface and fillslope) were identified (Figure 1). Locations of features were mapped on 7.5 minute topographic maps and subsequently digitized into a geographic information system (GIS).

Eight types of features were identified, involving erosion and deposition by mass-wasting and fluvial

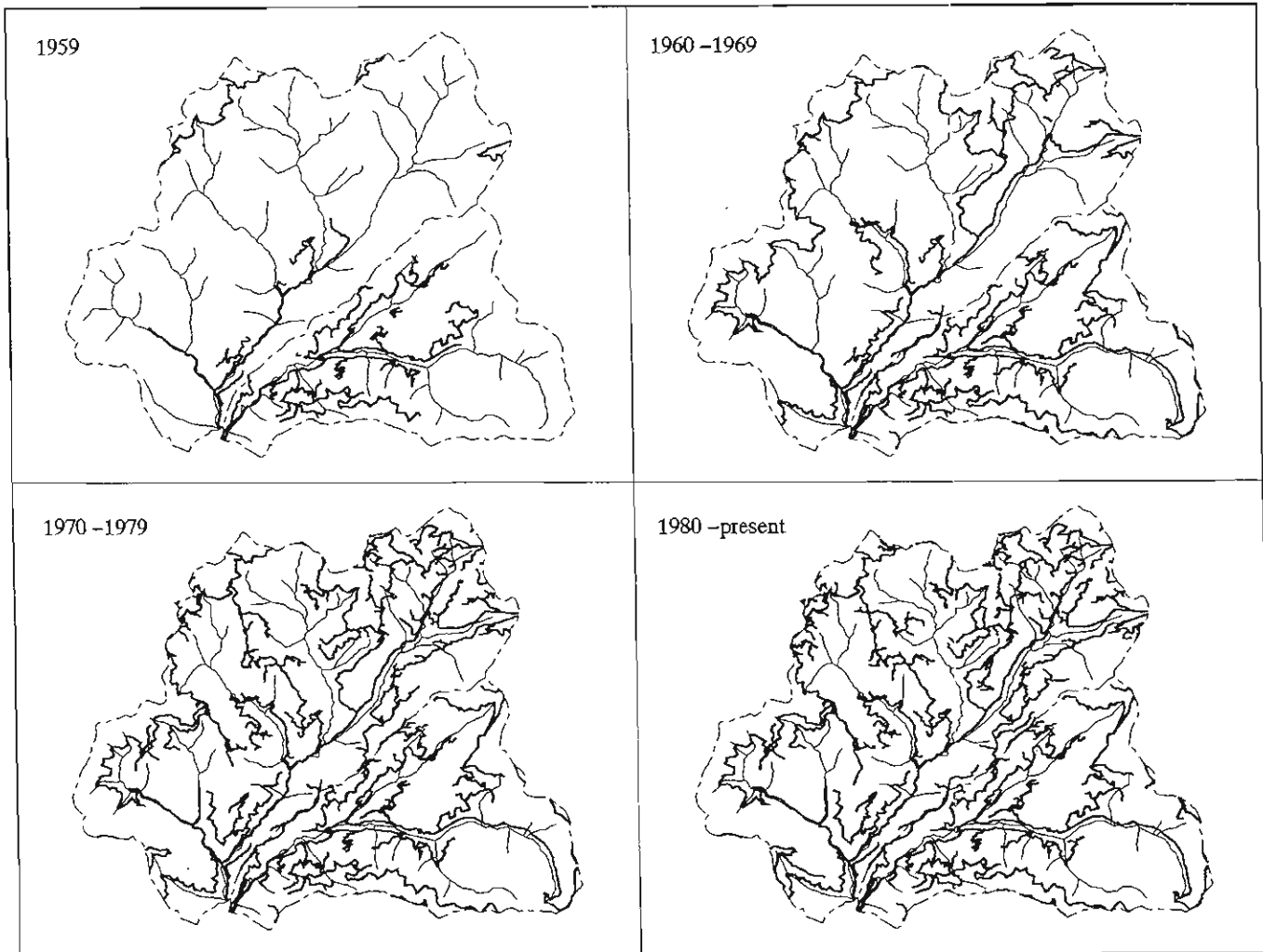


Figure 4. Pattern of Road Network Construction in Lookout Creek and Blue River During Four Decades.

were selected from roads constructed in valley bottom, ridgetop and midslope hillslope positions in each decade between 1950 and 1990 (Figure 3). The starting point for each transect was randomly selected at road junctions or road ends that could be located both in the field and on maps.

Each transect was subdivided into segments demarcated by culverts (Figure 2). For each sampled road segment the following data were recorded: length of road draining to each culvert (L), road grade or average slope of the road draining to each culvert (α), average hillslope gradient for the road segment (θ), and the routing of water below the culvert outlet as defined below. The length of each segment was estimated to the nearest 0.01 mile (0.02 km) based on readings from an automobile odometer calibrated

with a distance meter with a resolution of 0.01 km. Road grade was measured with a clinometer. Due to difficulties in measuring hillslope gradients under forest cover and distinguishing cut-and-fill slopes from the average hillslope gradient, hillslope gradient was assigned as a categorical variable to each road segment, based on a GIS classification of slopes greater than or less than 40 percent.

Each culvert outlet was classified into one of three categories based on whether its outlet delivered water: (1) directly to a natural stream channel, (2) into a gully incised below the culvert outlet, or (3) onto a hillslope where the water reinfilted (Figure 2). Road segments were assigned to category 1 if the culvert was a stream-crossing culvert (which transmits stream water below a road crossing), where

WEMPLE ET AL., 1996

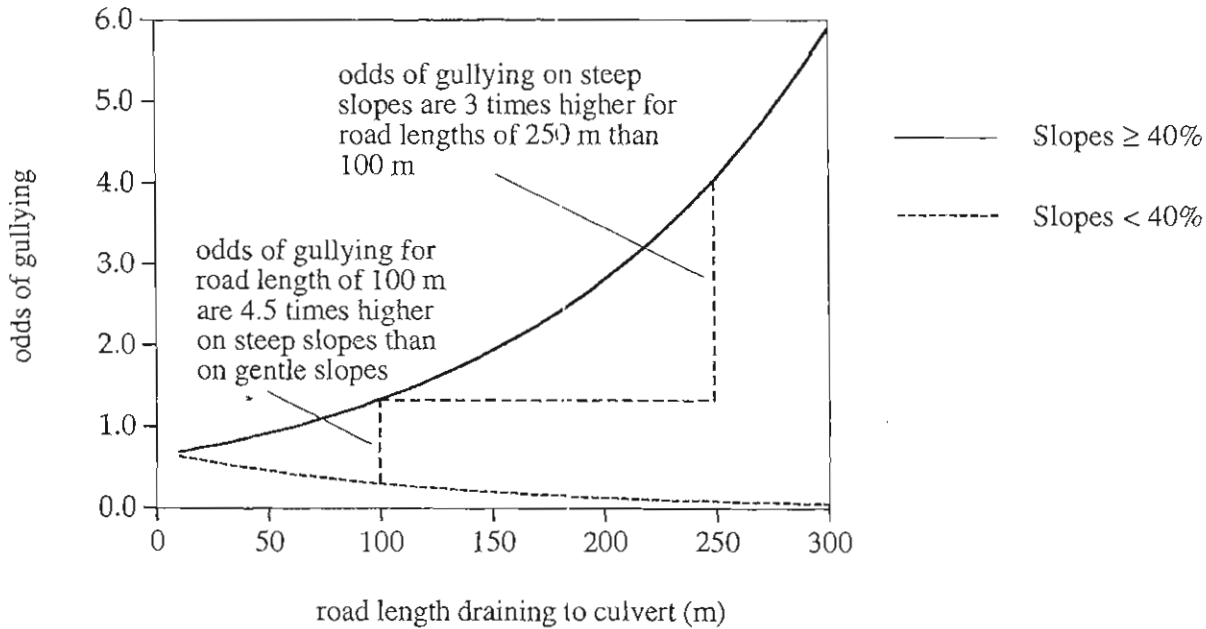


Figure 6. Relationship Between the Odds for the Occurrence of a Gully Below Ditch Relief Culverts Against Road Length. The logistic regression equation for the relation between the occurrence of gullying and road length (in meters), hillslope gradient (1 for slopes < 40 percent, 0 for slopes \geq 40 percent), and the interaction of these two variables is given by $\text{odds} = \exp[-0.4522 + (0.0074 \times \text{length}) + (0.0810 \times \text{slope}) - (0.0156 \times \text{length} \times \text{slope})]$ (Hosmer and Lemeshow, 1989). At a road length (e.g., culvert spacing) of 100 meters, gullies are 4.5 times more likely to occur on steep (\geq 40 percent) than on gentle (< 40 percent) slopes (odds ratio for steep vs. gentle slopes at 100 meters = $1.34/0.30$). Steep slopes show increased odds of gullying with increasing road length, for example gullies are roughly three times as likely to occur on steep slopes as road length increases from 100 to 250 meters (odds ratio for 250 m vs. 100 m road length on steep slopes = $4.07/1.34$).

Conversion of Subsurface Drainage to Quickflow

Following our conceptual model (Figure 1), the hydrologic impact of roads depends upon the extent to which roads contribute to the volume of rapid surface runoff in a basin. We observed several road segments carrying unit area discharges as high as those of the larger basins to which they contribute. A discharge of 1.18 L/s was measured from an estimated 2-ha drainage area on a Lookout Creek road ditch during a storm on March 19, 1993, representing only 20 percent of the basin-wide unit area discharge for Lookout Creek on this date (3.21 L/s/ha). However, on June 9, 1993, a discharge of 7.3 L/s was measured from an estimated 10-ha drainage area on a Blue River road ditch, representing roughly 100 percent of the unit-area basin discharge on this date (0.652 L/s/ha).

We expect that hillslope position affects a road segment's ability to convert subsurface water to surface runoff. Connected ditch segments along midslope roads are more likely than those along ridgetop or valley bottom roads to intercept significant amounts of subsurface flow and convert it to surface runoff

(e.g., Megahan, 1972). Ridgetop roads may lower the threshold for channel initiation (Montgomery, 1994), but road segments along ridgetop roads may not intercept subsurface flow because of their small contributing drainage areas. Valley bottom roads frequently have culverts discharging directly to streams but are relatively ineffective at diverting subsurface water to surface runoff (Wright *et al.*, 1990). Differences in the effectiveness of roads in capturing subsurface water and the routing of water via surface flowpaths associated with roads may explain some of the variability in results of small-basin experiments investigating road effects on basin hydrology.

Generalization of Study Results Using GIS

This study made extensive use of a geographic information system to select sites for sampling and to generalize results to the basins studied. GIS layers were overlaid to develop the sampling design for the field survey of roads. Algorithms provided in the GIS software were coupled with field observations to generate a map of the extended stream network that

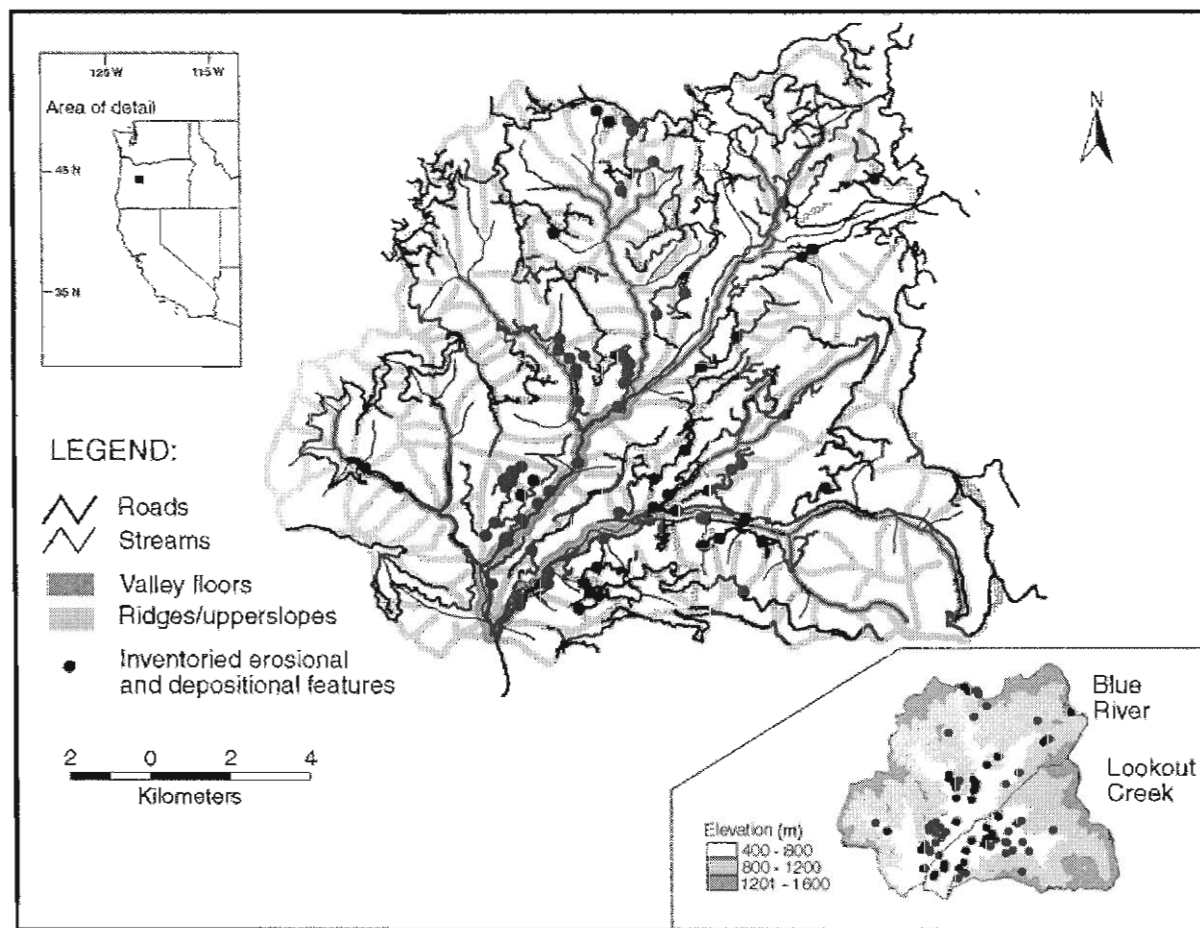


Figure 2. Location map of the Lookout Creek and Blue River basins in the western Oregon Cascades, USA, showing location of roads and stream network, hillslope position classes and erosional and depositional features mapped in this study. Locations of mapped features relative to elevation classes are shown on inset map at lower right

Table I. Summary of characteristics of study basins

	Lookout Creek basin	Blue River basin
Harvested area (%)	22	25
Drainage area (km ²)	62	119
Drainage density (km km ⁻²)*	3.0	2.9
Road length, total (km)	118	230
Upper slope (km)	27	75
Midslope (km)	73	132
Valley floor (km)	18	23
Road density (km km ⁻²)	1.9	1.9
Area of basin in roads (%)†	3.1	3.1

* Estimated winter baseflow drainage density (see Wemple *et al.*, 1996)

† Computed using an average width of road cut, surface, and fill of 16 m from Silen and Gratkowski (1953)

Table II. Numbers and frequencies (numbers per kilometre of road length) of inventoried features in the Lookout Creek and Blue River basins

	Lookout Creek basin		Blue River basin		Total	
	No.	No./km	No.	No./km	No.	No./km
<i>Mass movements</i>						
Debris flows	9	0.08	7	0.03	16	0.05
Hillslope slides	4	0.03	1	0.004	5	0.01
Cutslope slides	1	0.01	11	0.05	12	0.03
Fillslope slides	18	0.15	13	0.06	31	0.09
Slumps	1	0.01	12	0.05	13	0.04
Total	33	0.28	44	0.19	77	0.22
<i>Fluvial features</i>						
Plugged culverts	3	0.03	10	0.04	13	0.04
Incised ditches	1	0.01	2	0.01	3	0.01
Gullies	5	0.04	5	0.02	10	0.03
Total	9	0.08	17	0.07	26	0.07
Grand total	42	0.36	61	0.27	103	0.30

RESULTS

Numbers, frequencies, volumes and interactions among features

A diverse suite of geomorphic processes occurred during the February 1996 flood event, producing 103 mapped features associated with roads in the Lookout Creek and Blue River basins (Table II). The vast majority of these features occurred in the southern portion of the study area at low elevation sites (Figure 2). Mass movements were more numerous than fluvial features, and sediment production exceeded sediment storage by roads. Three-quarters of the inventoried features were mass movements, and one-quarter were fluvial features. Two-thirds of the features involved sediment production from roads, in the form of cutslope slides, fillslope slides, incised ditches and gullies, while one-third involved sediment capture, in which roads intercepted debris flows, hillslope slides and bedload (Table II).

Fillslope slides were the most numerous and frequent type of feature. They accounted for 30 per cent of all mapped features and 40 per cent of mass movements, with approximately one occurrence for every 10 km of road length in the two basins (Table II). Together, cutslope slides and slumps accounted for one-quarter of all inventoried features and one-third of mass movements, with average frequencies of three (cutslope slides) or four (slumps) for every 100 km of road. Hillslope slides and debris flows that were intercepted by roads accounted for the remaining mass movements inventoried.

Stream-crossing culverts plugged by bedload accounted for half of the fluvial features that were inventoried, while gullying of road surfaces and fillslopes also was relatively common. Plugged culverts and gullies together accounted for almost one-quarter of the features inventoried and nearly all (90 per cent) of the fluvial features, with average frequencies of three (gullies) or four (plugged culverts) for every 100 km of road.

Roads intercepted, stored and produced sediment, but overall were a net source of sediment to hillslopes and channels in the two basins (Table III). Roads intercepted almost 26 000 m³ of sediment contributed from hillslopes and channels and stored over 19 000 m³ of sediment. However, more than 32 000 m³ of sediment were mobilized within the road prism, so roads were a net source of more than 13 000 m³ of sediment in these two basins during this event. Debris flows accounted for two-thirds of the sediment intercepted by roads, and hillslope slides and bedload trapped at stream-crossing culverts accounted for the remaining one-third. Fillslope slides accounted for four-fifths of sediment mobilized within road prisms, while cutslope slides accounted for most of the remaining one-fifth; ditch incision and gullying accounted for less than 5 per cent of the total sediment volume eroded from roads. Most of the sediment stored on roads was from debris flows, but

Table III. Sediment budget for road-associated features inventoried after the February 1986 storm in the Lookout Creek and Blue River basins. Sediment volumes (m^3) are shown as basin totals and by hillslope position (see text). Net storage (ΔS) = $H - (H_t + R_t)$

	Debris flows	Hillslope slides	Cutslope slides	Fillslope slides	Plugged culverts	Incised ditches	Gullies	Total	Net storage (ΔS)
<i>Upper slope roads</i>									
From hillslopes, streams (H)	0	0	0	0	0	0	0	0	0
From road prism (R)	0	0	0	5450	0	0	0	5450	0
Stored on roads ($H_s + R_s$)	0	0	0	0	0	0	0	0	0
Exported ($H_t + R_t$)	0	0	0	5450	0	0	0	5450	-5450
<i>Mid-slope roads</i>									
From hillslopes, streams (H)	4700	6985	0	0	790	0	0	12475	0
From road prism (R)	530	5	4255	19110	0	480	185	24565	0
Stored on roads ($H_s + R_s$)	3120	1880	4120	0	790	0	0	9910	0
Exported ($H_t + R_t$)	2110	5110	135	19110	0	480	185	27130	-14 655
<i>Valley-floor roads</i>									
From hillslopes, streams (H)	12410	575	0	0	175	0	0	13160	0
From road prism (R)	565	0	145	1095	0	160	305	2270	0
Stored on roads ($H_s + R_s$)	8450	535	135	0	175	0	0	9295	0
Exported ($H_t + R_t$)	4525	40	10	1095	0	160	305	6135	+7025
<i>All roads (basin total)</i>									
From hillslopes, streams (H)	17110	7560	0	0	965	0	0	25635	0
From road prism (R)	1095	5	4400	25655	0	640	490	32285	0
Stored on roads ($H_s + R_s$)	11570	2415	4255	0	965	0	0	19205	0
Exported ($H_t + R_t$)	6635	5150	145	25655	0	640	490	38715	-13 080

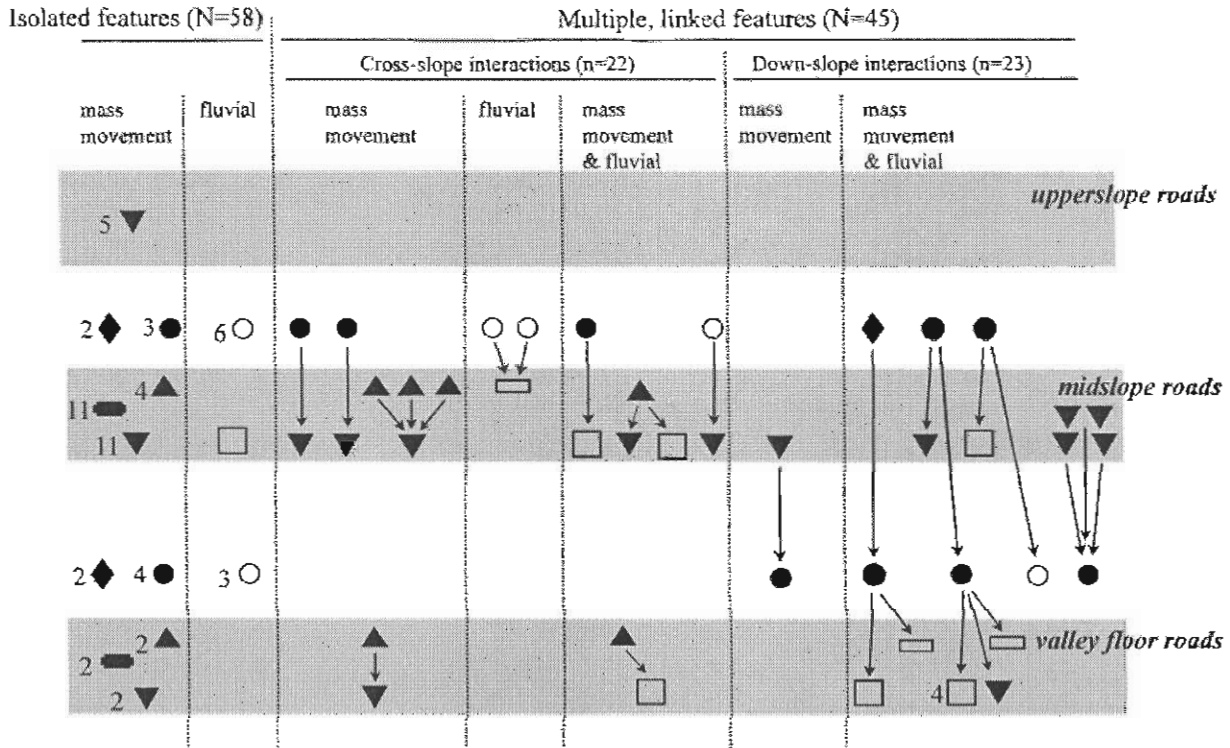


Figure 4. Schematic representation of the distribution and spatial complexity of features inventoried in this study. Closed symbols represent mass movements (●, debris flows; ◆, hillslope slides; ▲, cutslope slides; ▼, fillslope slides; ■, slumps). Open symbols represent fluvial features (○, plugged culverts; □, incised ditches; □, gullies). Features are positioned relative to point of origin, on hillslopes above roads or within the road zone (represented by grey bars). Arrows indicate features that triggered an associated feature, and show impacts to multiple tiers of roads where applicable. Numbers beside symbols indicate number of inventoried features of that type

cutslope slides, hillslope slides and bedload (i.e. in plugged culverts) contributed small fractions of the sediment stored on roads. Fillslope slides accounted for two-thirds of the net sediment exported from roads, but debris flows and hillslope slides accounted for most of the remaining one-third (Table III).

Slightly more than half (56 per cent) of the erosional and depositional features associated with roads occurred as solitary events, unconnected with other inventoried features (Figure 4). All of the inventoried slumps occurred as solitary events, apparently unaffected by diverted surface runoff or other documented mechanisms. Most (nine of 13) plugged culverts occurred as solitary events, and apparently did not lead to gullying or fill failure. Most (four of five) hillslope slides deposited sediment on roads without triggering additional erosion within the road prism.

Two types of complex, interacting sets of inventoried features were observed on roads, involving almost half (44 per cent) of all mapped features: (1) hillslope slides, cutslope slides or bedload in ditches or culverts led to diversions of surface runoff and triggered fillslope slides, gullying or ditch incision; and (2) fillslope slides entered stream channels and became debris flows (Figure 4). One-quarter of the 22 fillslope slides on mid-slope roads were apparently connected to debris flows intercepted by roads (three cases), cutslope slides in the road prism (two cases) or plugged culverts (one case). Seven of ten instances of gullying were connected to debris flows, and two were connected to cutslope slides in the road prism. Ditch incision was also connected to debris flows (two of three cases) or plugged culverts (one case). One-quarter of the fillslope slides on midslope roads entered channels and became debris flows (five cases).

TABLE 2. DIVISIONS OF THE QUATERNARY AND THEIR BOUNDARY DATES AS USED IN THIS VOLUME*

		Present
	Holocene (Oxygen-isotope stage 1)	
Late Pleistocene	Late Wisconsin (Oxygen-isotope stage 2)	10 to 12 ka
	Middle Wisconsin of Richmond and Fullerton (1986) (O-isotope stages 3 and 4)	~28 ka
	Late Sangamon (Early Wisconsin and Eowisconsin of Richmond and Fullerton, 1986; O-isotope stages 5a-5d)	~71 ka
	Sangamon of Richmond and Fullerton (1986) (O-isotope stage 5e)	~115 ka
Middle Pleistocene	Late-Middle Pleistocene (Illinoian of Richmond and Fullerton, 1986; O-isotope stages 6-8)	~128 ka [†]
	Middle-Middle Pleistocene of Richmond and Fullerton (1986) (O-isotope stages 9-15)	~300 ka
	Early-Middle Pleistocene (Richmond and Fullerton, 1986) (O-isotope stages 16-19)	620 ka [§]
	(Matuyama-Brunhes Chronozone boundary)	750-775 ka ^{**}
	Early Pleistocene	
	Upper boundary of Olduvai Subchron	1.65 Ma
	or Gauss-Matuyama Chron boundary	2.48 Ma
	Pliocene	
		5.0-5.5 Ma [‡]
	Miocene	

25



GEOLOGICAL SOCIETY OF AMERICA

DECADE OF NORTH AMERICAN GEOLOGY GEOLOGIC TIME SCALE

DMAG



CENOZOIC				MESOZOIC				PALEOZOIC				PRECAMBRIAN			
AGE (Ma)	PERIOD	EPOCH	AGE (Ma)	PERIOD	EPOCH	AGE (Ma)	PERIOD	EPOCH	AGE (Ma)	PERIOD	EPOCH	AGE (Ma)	EON	ERA	RDY AGES (Ma)
65-66.4	PALEOCENE	L	DANIAN	TRIASSIC	EARLY	SCYTHIAN	TRIASSIC	EARLY	245	CAMBRIAN	EARLY	570	ARCHEAN	EARLY	3800?
63.6			ANISIAN			240			22			560			
60-63.6	L	L	UNNAMED	MIDDLE	MIDDLE	LADINIAN	MIDDLE	MIDDLE	540	LATE	MIDDLE	3500	ARCHEAN	MIDDLE	3400
57.8			THANETIAN			230			22			540			
55-57.8	E	E	YPRSIAN	LATE	LATE	NORIAN	LATE	LATE	505	ORDOVICIAN	EARLY	3250	ARCHEAN	MIDDLE	3000
52.0			500			18									
45-52.0	E	E	LUTETIAN	EARLY	EARLY	SINEMURIAN	EARLY	EARLY	498	SILURIAN	EARLY	2500	ARCHEAN	LATE	2500
43.6						480			16						
40-43.6	L	L	PRIABONIAN	MIDDLE	MIDDLE	BATHONIAN	MIDDLE	MIDDLE	448	DEVONIAN	EARLY	1750	PROTEROZOIC	LATE	1600
40.0			440			12									
35-40.0	E	E	RUPELIAN	LATE	LATE	VALANGINIAN	LATE	LATE	380	MISSISSIPPIAN	EARLY	1500	PROTEROZOIC	MIDDLE	900
36.6						380			15						
30-36.6	E	E	CHATTIAN	LATE	LATE	BERRIASIAN	LATE	LATE	352	CARBONIFEROUS	EARLY	1250	PROTEROZOIC	EARLY	750
30.0						360			8						
25-30.0	E	E	ADULTIAN	LATE	LATE	TITHONIAN	LATE	LATE	320	PERMIAN	LATE	750	PROTEROZOIC	LATE	570
23.7						320			12						
21.8	E	E	BURDIGALIAN	LATE	LATE	BARREMIAN	LATE	LATE	315	PERMIAN	EARLY	750	PROTEROZOIC	LATE	570
18.6						315			12						
15-18.6	M	M	LANGHIAN	EARLY	EARLY	HAUTERIVIAN	EARLY	EARLY	300	PERMIAN	EARLY	750	PROTEROZOIC	LATE	570
15.1						300			12						
11.2	M	M	SERRAVALLIAN	EARLY	EARLY	APTIAN	EARLY	EARLY	286	PERMIAN	EARLY	750	PROTEROZOIC	LATE	570
11.2						286			12						
10-11.2	L	L	TORTONIAN	LATE	LATE	ALBIAN	LATE	LATE	280	PERMIAN	EARLY	750	PROTEROZOIC	LATE	570
8.5						280			12						
8-8.5	L	L	MESSINIAN	LATE	LATE	CENOMANIAN	LATE	LATE	280	PERMIAN	EARLY	750	PROTEROZOIC	LATE	570
6.5						280			12						
5-6.5	L	L	ZANCLEAN	LATE	LATE	NEOCOMIAN	LATE	LATE	280	PERMIAN	EARLY	750	PROTEROZOIC	LATE	570
5.3						280			12						
3-5.3	L	L	PIACENZIAN	LATE	LATE	BAJOCIAN	LATE	LATE	280	PERMIAN	EARLY	750	PROTEROZOIC	LATE	570
3.4						280			12						
1.8-3.4	L	L	CALABRIAN	LATE	LATE	MAASTRICHTIAN	LATE	LATE	280	PERMIAN	EARLY	750	PROTEROZOIC	LATE	570
0.01						280			12						

92

References Cited – This Document

- Benda, L.E., and Cundy, T.W., 1990, Predicting deposition of debris flows in mountain channels: *Canadian Geotechnical Journal*, v. 27, no. 4, p. 409-417.
- Benda, L.E., and Dunne, T., 1997, Stochastic forcing of sediment supply to channel networks from landsliding and debris flow: *Water Resources Research*, v. 33, no. 12, p. 2849-2863.
- Benda, L.E., Veldhuisen, C., Miller, D.J., and Rodgers-Miller, L., 2000, Slope instability and forest land managers: A primer and field guide: Seattle, Wash., Earth Systems Institute, 74 p.
- Costa, J.E. 1984. Physical geomorphology of debris flows: in Costa, J. E., and Fleisher, P. J., eds., *Developments and Applications of Geomorphology*, Berlin, Springer-Verlag, p. 268-317.
- Dietrich, W.E., Dunne, T., Humphrey, N.F., and Reid, L.M., 1982, Construction of sediment budgets for drainage basins, in Swanson, F.J., Janda, R.J., Dunne, T., and Swanson, D.N., eds., *Sediment budgets and routing in forested drainage basins*: Portland, U.S. Forest Service, Pacific Northwest Forest and Range Experiment Station General Technical Report PNW-141, p. 5-23.
- Hack, J.T., Goodlett, J.C., 1960. Geomorphology and forest ecology of a mountain region in the central Appalachians. U.S. Geological Survey Professional Paper 347, 66.
- Hoffmeister, R.J., Miller, D.J., Mills, K.A., Hinkle, J.C., Beier, A.E., 2002, Text to Accompany GIS Overview Map of Potential Rapidly Moving Landslide Hazards in Western Oregon: Oregon Department of Geology and Mineral Industries Interpretive Map Series IMS-22.
- May, C.L., and Gresswell, R.E., 2003, Processes and rates of sediment and wood accumulation in headwater streams of the Oregon Coast Range, USA : *Earth Surface Processes and Landforms*, Vol. 28, Issue 4, pp.409-424.
- Pierson, T.C., and Costa, J.E., 1987, A rheologic classification of subaerial sediment-water flows, in *Debris flows, avalanches: Process, recognition, and mitigation*, Costa, J.E., and Wieczorek, G.F., eds., Geological Society of America, *Reviews in Engineering Geology*, v. 7, p. 1-12.
- Ritter, D.F., Kochel, R.C., and Miller, J.R., 2002, *Process Geomorphology* 4th Ed.: W.C. Brown Publishers, Dubuque, IA, 539 pp.
- Robison, E.G., Mills, K., Paul, J., Dent, L., Skaugset, A., 1999, Storm impacts and landslides of 1996. Final Report: Oregon Department of Forestry Forest Practices Technical Report 4, 145 p.
- Snyder, K.U., 2000, Debris flows and flood disturbance in small, mountain watersheds: Unpublished M.S. Thesis, Oregon State University, Corvallis, Oregon, 53 p.
- Swanson, F.J., and Dyrness, C.T., 1975, Impact of clearcutting and road construction on soil erosion by landslides in the western Cascade Range, Oregon: *Geology*, v. 3, p. 393-396.

Swanson, F. J., Fredriksen, R. L., and McCorison, F. M., 1982a, Material transfer in a western Oregon forested watershed, in Edmonds, Robert L., ed., Analysis of coniferous forest ecosystems in the western United States: US/IBP Synthesis Series 14. Stroudsburg, PA, Hutchinson Ross Publishing Company, p. 233-266.

Swanson, F.J., Johnson, S.L., Gregory, S.V., and Acker, S.A., 1998, Flood disturbance in a forested mountain landscape: Bioscience, v. 48, no. 9, p. 681-689.

Swanson, F.J. and Swanston, D.N., 1977, Complex mass-movement terrains in the western Cascade Range, Oregon: Reviews of Engineering Geology, v. 3, p. 113-124.

Taylor, S.B. and Kite, J.S., 2006, Comparative geomorphic analysis of surficial deposits at three central Appalachian watersheds: Implications for controls on sediment-transport efficiency: Geomorphology, v. 78, p. 22-43.

Varnes, D.J., 1978, Landslides: Analysis and Control, in Transportation Research Board Special Reports, 176: Landslides, Transportation Research Board, National Research Council, Washington, D.C.

Wemple, B.C., Jones J.A., Grant G.E., 1996, Channel network extension by logging roads in two basins, western Cascades, Oregon. Water Resources Bulletin, v. 32, p. 1195-1207.

Wemple, B.C., Swanson, F.J., and Jones, J.A., 2001, Forest Roads And Geomorphic Process Interactions, Cascade Range, Oregon: Earth Surface Processes and Landforms, v. 26, 191-204.

Wiley, T.J., 2000, Relationship between rainfall and debris flows in western Oregon: Oregon Geology, v. 62, no. 2, p. 27-43.

Debris Flow Process – Literature Review
(Steve Taylor - Updated January 9, 2002)

- Addison, K., 1987, Debris flow during intense rainfall in Snowdonia, North Wales, a preliminary study: *Earth Surface processes and Landforms*, v. 12, p. 561-566.
- Alger, C.S., and Ellen, S.D., 1987, Zero-order basins shaped by debris flows, Sunol, California, USA: in *Erosion and Sedimentation in the Pacific Rim*, Proceedings of the Corvallis Symposium, International Association of Hydrological Sciences, Publication 165, p. 111-119.
- Alger, C.S., Mark, R.K., and Wiczorek, G.F., 1985, Hydraulic monitoring at a debris flow site: *EOS*, v. 66, p. 911.
- Apman, R.P., 1973, Estimating discharge from super-elevation in bends, *American Society of Civil Engineers, Hydraulics Division Journal*, v. 99, No. HY1, p. 65-79.
- Bagnold, R.A., 1954, Experiments on a gravity-free dispersion of large solid spheres in a Newtonian fluid under shear: *Proceedings of the Royal Society of London, Series A*, v. 225, p. 49-63.
- Bathurst, J.C., Burton, A., and Ward, T.J., 1997, Debris flow run-out and landslide sediment delivery model tests: *Journal of Hydraulic Engineering, American Society of Civil Engineers*, v. 123, p. 410-419.
- Beaty, C.B., 1990, Anatomy of a White Mountains debris-flow: The making of an alluvial fan, in Rachocki, A.H., and Church, M., eds., *Alluvial Fans: A Field Approach*: Wiley, New York, p. 69-89.
- Benda, L., 1990, The influence of debris flows on channels and valley floors in the Oregon Coast Range, U.S.A.: *Earth Surface Processes and Landforms*, v. 15, p. 457-466.
- Benda, L., and Dunne, T., 1987, Sediment routing by debris flow, in *Erosion and Sedimentation in the Pacific Rim*, Proceedings of the Corvallis Symposium, International Association of Hydrological Sciences, Publication 165, p. 213-223.
- Benda, L., and Dunne, T., 1997, Stochastic forcing of sediment supply to channel networks from landsliding and debris flow: *Water Resources Research*, v. 33, no. 12, p. 2849-2863.
- Beverage, J.P., and Culbertson, J.K., 1964, Hyperconcentrations of suspended sediment: *Journal of the Hydraulics Division, American Society of Civil Engineers*, v. 90, HY6, p. 117-126.
- Blackwelder, E., 1928, Mudflow as a geologic agent in semiarid mountains: *Geological Society of America Bulletin*, v. 39, p. 465-484.

- Blijenberg, H.M., Degraff, P.J., Hendriks, M.R., Deruiter, J.F., and Vantetering A.A., 1996, Investigation of infiltration characteristics and debris flow initiation conditions in debris flow source areas using a rainfall simulator: *Hydrological Processes*, v. 10, p. 1527-1543.
- Blong, R.J., 1973, A numerical classification of selected landslides of the debris slide-avalanche-flow type: *Engineering Geology*, v. 7, p. 999-114.
- Bovis, M.J., and Dagg, B.R., 1988, A model for debris accumulation and mobilization in steep mountain streams: *Hydrological Sciences Journal*, v. 33, p. 589-604.
- Buchanon, P., Savigny, K.W., and DeVries, J., 1990, A method for modeling water tables at debris avalanche headscarps: *Journal of Hydrology*, v. 113, p. 61-88.
- Caine, N., 1980, The rainfall intensity-duration control of shallow landslides and debris flows: *Geografiska Annaler*, v. 62A, p. 23-27.
- Campbell, R.H., 1975, Soil slips, debris flows, and rainstorms in the Santa Monica Mountains, southern California: U.S. Geological Survey Professional Paper 851, 53 p.
- Church, M., and Miles, M.J., 1987, Meteorological antecedents to debris flows in southwestern British Columbia; some case studies, in Costa, J.E., and Wieczorek, G.F., *Debris flows/avalanches: Process, Recognition, and Mitigation: Geological Society of America Reviews in Engineering Geology*, 7, p. 63-79.
- Costa, J.E. 1984. Physical geomorphology of debris flows: in Costa, J. E., and Fleisher, P. J., eds., *Developments and Applications of Geomorphology*, Berlin, Springer-Verlag, p. 268-317.
- Costa, J.E., 1997, Hydraulic modeling for lahar hazards at Cascades volcanoes: *Environmental and Engineering Geoscience*: v. 3, p. 21-30.
- Costa, J.E., and Jarrett, R.D., 1981, Debris flows in small mountain stream channels of Colorado and their hydrologic implications: *Association of Engineering Geologists Bulletin*, v. 18, p. 309-322.
- Costa, J.E. and Wieczorek, G.F., eds., *Debris Flows/Avalanches: Process, Recognition and Mitigation: Geol. Soc. of America Reviews in Engineering Geology Vol VII*, 240 p.
- Costa, J.E., and Williams, G.P., 1984, *Debris flow dynamics (videotape)*: U.S. Geological Survey Open-File Report 84-606, 22.5 min.
- Coussot, P., and Meunier, M., 1996, Recognition, classification and mechanical description of debris flows: *Earth Science Reviews*, v. 40, p. 209-227.
- DeGraff, J.V., 1994, The geomorphology of some debris flows in the southern Sierra Nevada, California: *Geomorphology*, v. 10, p. 231-252.

- Dott, R.H., 1963, Dynamics of subaqueous gravity depositional processes: American Association of Petroleum Geologists Bulletin, v. 47, p. 104-129.
- Enos, P., 1977, Flow regimes in debris flows: Sedimentology, v. 24, p. 133-142.
- Fisher, R.V., 1966, Mechanism of deposition from pyroclastic flows: American Journal of Science, v. 264, p. 350-363.
- Fisher, R.V., 1971, Features of coarse-grained, high concentrations fluids and their deposits: Journal of Sedimentary Petrology, v. 41, p. 916-927.
- Gottesfeld, A.S., Mathewes, R.W., and Gottesfeld, L.M.J., 1991, Holocene debris flows and environmental history, Hazelton area, British Columbia: Canadian Journal of Earth Sciences, v. 28, p. 1583-1593.
- Hampton, M.A., 1975, The competence of fine-grained debris flows: Journal of Sedimentary Petrology, v. 45, p. 834-844.
- Hampton, M.A., 1979, Buouancy in debris flows: Journal of Sedimentary Petrology, v. 49, p. 753-758.
- Han, G.Q, and Wang, D.G., 1996, Numerical modeling of Anhui debris flow: Journal of Hydraulic Engineering, American Society of Civil Engineers, v. 122, p. 262-265.
- Hogg, S.E., 1982, Sheetfloods, sheetwash, sheetflow, or ...?: Earth Science Reviews, v. 18, p. 59-76.
- Hutter, K., Svendsen, B., and Rickenmann, D., 1996, Debris flow modeling - A review: Continuum Mechanics and Thermodynamics, v. 8, p. 1-35.
- Innes, J.L., 1983, Debris flows: Process in Physical Geography, v. 7, p. 469-501.
- Innes, J.L., 1985, Magnitude-frequency relations of debris flows in northwest Europe: Geografiska Annaler, v. 67A, p. 23-32.
- Iverson, R.M., 1985, A constitutive equation for mass-movement behavior: Journal of Geology, v. 93, p. 143-160.
- Iverson, Richard M et al, 1998 Objective delineation of lahar-inundation hazard zones, in Geological Society of America Bulletin v.110, no. 8; p. 972-984.
- Iverson, R.M., 1997, Stream flows, debris flows and grain flows: Crucial effects of convective accelerations: EOS Transactions of the American Geophysical Union, v. 78, no. 46, Fall Meeting Supplement, p. F 257.

- Iverson, R.M., 1997, The physics of debris flows: *Reviews of Geophysics*, v. 35, p. 245-296.
- Iverson, R.M., Costa, J.E., and LaHusen, R.G., 1992, Debris-flow flume at H.J. Andrews Experimental Forest, Oregon: U.S. Geological Survey Open-File Report 920483, 2 p.
- Iverson, R.M., and Denlinger, R.P., 1987, The physics of debris flows - a conceptual assessment, in *Erosion and Sedimentation in the Pacific Rim*, Proceedings of the Corvallis Symposium, International Association of Hydrological Sciences, Publication 165, p. 155-165.
- Iverson, R.M., LaHusen, R.G., Major, J.J., and Zimmerman, C.L., 1994, Debris flow against obstacles and bends: dynamics and deposits: *EOS, Transactions of the American Geophysical Union*, v. 75, p. 274.
- Iverson, R.M., and Major, J.J., 1986, Groundwater seepage vectors and the potential for hillslope failure and debris flow mobilization: *Water Resources Research*, v. 22, p. 1543-1548.
- Iverson, R.M., Reid, M.E., and LaHusen, R.G., 1997, Debris-flow mobilization from landslides: *Annual Review of Earth and Planetary Sciences*, v. 25, p. 85-138.
- Jackson, L.E., Kostaschuk, R.A., and MacDonald, G.M., 1987, Identification of debris flow hazard on alluvial fans in the Canadian Rocky Mountains, in Costa, J. E., and Wieczorek, G.F., eds., *Debris Flows/Avalanches: Process, Recognition, and Mitigation*, *Reviews in Engineering Geology Volume VII*, Boulder, Colorado, Geological Society of America, p.115-124.
- Johnson, A.M., 1970, *Physical Processes in Geology*: Freeman, Cooper, San Francisco, 577 p.
- Johnson, A.M., 1984, Debris Flow, in Brunsden, D., and Prior, D.B., eds., *Slope Instability*, p. 257-361.
- Johnson, A.M., and Rahn, P.H., 1970, Mobilization of debris flows: *Zeitschrift für Geomorphologie Supplementband*, v. 9, p. 168-186.
- Johnson, A.M., and Rodine, J.R., 1984, Debris flow, in Brunsden, D., and Prior, D.B., *Slope Instability*: New York, John Wiley, p. 257-361.
- Larsson, S., 1982, Geomorphological effects on the slopes of Longyear Valley, Spitsbergen, after a heavy rainstorm in July 1972: *Geografiska Annaler*, v. 67, p. 105-125.
- Lawson, D.E., 1982, Mobilisation, movement and deposition of active subaerial sediment flows, Matanuska glacier, Alaska: *Alaskan Journal of Geology*, v. 90, p. 279-300.
- Liu, X., 1996, Size of a debris flow deposition: Model experiment approach: *Environmental Geology*, v. 28, p. 70-77.

- Lu, Z.Y., and Cruden, D.M., 1996, Two debris flow modes on Mount Cayley, British Columbia, Canadian Geotechnical Journal, v. 33, p. 123-139.
- Major, J.J., 1997, Depositional processes in large-scale debris-flow experiments: Journal of Geology, v. 105, p. 345-366.
- Major, J.J., and Pierson, T.C., 1992, Debris flow rheology: Experimental analysis of fine-grained slurries: Water Resources Research, v. 28, p. 841-857.
- Manville, V. et al., 2000, Dynamic interactions between lahars and stream flows: A case study from Ruapehu volcano, New Zealand: Discussion and reply discussion, in Geological Society of America Bulletin v.112, no. 7; p. 1149-1152
- Mathewson, C.C., and Keaton, J.R., 1986, Role of bedrock groundwater in the initiation of debris flow [abstract]: Association of Engineering Geologists, 29th annual Meeting, p. 56.
- Mills, H.H., 1984, Clast orientation in Mount St. Helens debris-flow deposits, North Fork Toutle River, Washinton: Journal of Sedimentary Petrology, v. 54, p. 626-634.
- Mizuyama, T., Yazawa, A., and Ido, K., 1987, Computer simulation of debris flow depositional processes: International Association of Hydrological Sciences, Publication No. 165, p. 179-190.
- Nordin, C.F., 1964, Study of channel erosion and sediment transport: Journal of the Hydraulics Division, American Society of Civil Engineers, v. 90, p. 173-192.
- Okuda, S., Suwa, H., Okunishi, K., Yokoyama, K., and Nakano, M., 1980, Observations on the motion of a debris flow and its geomorphological effects: Zeitschrift fur Geomorphologie Supplementband 35, p. 142-163.
- Pareschi, M.T., et al., 2000, May 5, 1998, debris flows in circum-vesuvian areas (southern Italy): Insights for hazard assessment, in Geology v. 28; no 7 p. 639-642.
- Parrett, C., 1987, Fire-related debris flows in the Beaver Creek drainage, Lewis and Clark County, Montana: U.S. Geological Survey, Water-Supply Paper 2330, p. 57-67.
- Phillips, C.J., and Davies, T.R., 1991, Determining rheological parameters of debris flow material: Geomorphology, v. 4, p. 101-110.
- Pierson, T.C., 1980, Erosion and deposition by debris flows at Mt. Thomas, North Canterbury, New Zealand: Earth Surface Processes, Vol. 5, p. 227-247.
- Pierson, T.C., 1980, Debris Flows - an important process in high country gully erosion: Journal of the Tussock Grasslands and Mountain Lands Institute, Review 39, p. 3-14.

- Pierson, T.C., 1981, Dominant particle support mechanisms in debris flows at Mt. Thomas, New Zealand, and implications for flow mobility: *Sedimentology*, v. 28, p. 49-60.
- Pierson, T.C., 1986, Flow behavior of channelized debris flows, Mount St. Helens, Washington, in Abrahams, A.D., *Hillslope Processes*: Winchester, MA, Allen & Unwin, Papers from the 16th Annual Binghamton Symposium, p. 269-296.
- Pierson, T.C., and Costa, J.E., 1987, A rheologic classification of subaerial sediment-water flows, in *Debris flows, avalanches: Process, recognition, and mitigation*, Costa, J.E., and Wieczorek, G.F., eds., Geological Society of America, *Reviews in Engineering Geology*, v. 7, p. 1-12.
- Pierson, T.C., and Scott, K.M., 1985, Downstream dilution of a lahar: Transition from debris flow to hyperconcentrated streamflow: *Water Resources Research*, v. 21, p. 1511-1524.
- Rapp, A., and Nyberg, R., 1981, Alpine debris flows in northern Scandinavia: *Geografiska Annaler*, v. 67, p. 183-196.
- Reneau, S.L., and Dietrich, W.E., 1987, The importance of hollows in debris flow studies; Examples from Marin County, California, in Costa, J.E., and Wieczorek, G.F., *Debris flows/avalanches: Process, Recognition, and Mitigation: Geological Society of America Reviews in Engineering Geology*, v. 7, p. 63-79.
- Rickenmann, D., and Zimmermann, M., 1993, The 1987 debris flows in Switzerland: documentation and analysis: *Geomorphology*, v. 8, p. 175-189.
- Rodine, J.R., and Johnson, A.M., 1976, The ability of debris, heavily freighted with coarse clastic materials to flow on gentle slopes: *Sedimentology*, v. 23, p. 213-234.
- Rodine, J.R., 1974, Analysis of mobilization of debris flows: Unpublished Ph.D. Dissertation, Stanford University, Palo Alto, California, 226 p.
- Scott, K.M., 1988, Origins, behavior, and sedimentology of lahars and lahar-runout flows in the Toutle-Cowlitz River system: U.S. Geological Survey, Professional Paper 1447-A, 74 p.
- Southard, J.B., 1971, Lift forces on suspended sediment particles in laminar flow: Experiments and sedimentological interpretation: *Journal of Sedimentary Petrology*, v. 41, p. 320-324.
- Stock, J., and Dietrich, W.E., Valley incision by debris flows: evidence of topographic signature, in *Water Resources Research*, v. 39, no. 4, p. 1-24.
- Suwa, H., and Okuda, S., 1980, Dissection of valleys by debris flow: *Zeitschrift fur Geomorphologie Supplementband*, v. 35, p. 164-182
- Takahashi, T., 1978, Mechanical characteristics of debris flow: American Society of Civil Engineers, *Journal of the Hydraulics Division*, v. 104, p. 1153-1169.

- Takahashi, T., 1981, Debris flow: Annual Reviews of Fluid Mechanics, v. 13, p. 57-77.
- Takahashi, T., 1991, Debris flow: rotterdam, Balkema, 165 p.
- Takahashi, T., Ashida, K., and Sawai, K., 1981, Delineation of debris flow hazard areas: in Erosion and sediment transport in Pacific rim steeplands, International Association of Hydrological Scientists Publication 132, p. 589-603.
- Terranova, T., and Kochel, R.C., 1987, Multivariate analysis of factors related to debris avalanching in Nelson County, central Virginia: Geological Society of America Abstracts with Programs 9, no. 7, p. 866.
- VanDine, D.F., 1985, Debris flows and debris torrents in the southern Canadian Cordillera: Canadian Geotechnical Journal, v. 22, p. 44-68.
- Vanoni, V.A., and Nomicos, G.N., 1960, Resistance properties of sediment-laden streams: Transactions of the American Society of Civil Engineers, v. 125, pt. I, p. 1140-1175.
- Vansteijn, H., 1996, Debris-flow magnitude-frequency relationships for mountainous regions of central and northwest Europe: Geomorphology, v. 15, p. 259-273.
- Whipple, K.X., 1997, Open-channel flow of Bingham fluids: Applications in debris-flow research: Journal of Geology, v.105, p. 243-262.
- Whipple, K.X., and Dunne, T., 1992, The influence of debris flow rheology on fan morphology, Owens Valley, California: Geological Society of America Bulletin, v. 104, p. 887-900.
- Wieczorek, G.F., 1987, Effect of rainfall intensity and duration on debris flows in central Santa Cruz Mountains, California, in: Debris flows, avalanches: Process, recognition, and mitigation, Costa, J.E., and Wieczorek, G.F., eds., Geological Society of America, Reviews in Engineering Geology, v. 7, p. 93-104.
- Wohl, E.E., and Pearthree, P.P., 1991, Debris flows as geomorphic agents in the Huachuca Mountains of Southeastern Arizona: Geomorphology, Vol. 4, p. 273-292.
- Wood, S.H., and Meyer, G.A., 1997, High-velocity river-crossing debris flow triggered by Jan. 1, 1997 warm rains on heavy snowpack in the Payette River drainage of the southwestern Idaho mountains: EOS Transactions of the American Geophysical Union, v. 78, no. 46, Fall Meeting Supplement, p. F 219.

